TECHNISCHE UNIVERSITÄT MÜNCHEN

Klinik für Orthopädie und Sportorthopädie

Klinikum rechts der Isar

(Direktor: Univ.-Prof. Dr. R. von Eisenhart-Rothe)

Decellularized whole organs as vascularized bioscaffolds for bone tissue engineering

Alexandru-Cristian Tron

Vollständiger Abdruck der von der Fakultät für Medizin der Technischen Universität München zur Erlangung des akademischen Grades eines

Doktors der Zahnheilkunde

genehmigten Dissertation.

Vorsitzender: Univ.-Prof. Dr. E. J. Rummeny

Prüfer der Dissertation:

1. Priv.-Doz. Dr. R. H. H. Burgkart
2. Univ.-Prof. Dr. Dr. K.-D. Wolff

Die Dissertation wurde am 29.10.2015 bei der Technischen Universität eingereicht und durch die Fakultät für Medizin am 15.06.2016 angenommen.

TABLE OF CONTENTS

Table of abbreviations

3D	Three-dimensional
ALP	Alkaline phosphatase
BCIP	5-Bromo-4-chloro-3-indolyl phosphate
BSA	Bovine serum albumin
cDNA	Complementary DNA
CHAPS	3-[(3-Cholamidopropyl)dimethylammonio]-1-propanesulfonate
dH_2O	Distilled water
DMEM	Dulbecco's minimum essential medium
DNA	Deoxyribonucleic acid
dNTP	Deoxyribonucleotide
(D)PBS	(Dulbecco's) Phosphate buffered saline
dsDNA	Double stranded DNA
ECM	Extracellular matrix
EDTA	Ethylenediaminetetraacetic acid
ELISA	Enzyme-linked immunosorbent assay
FBS	Fetal bovine serum
FFPE	Formalin-fixed paraffin-embedded
GAG	Glycosaminoglycan
H&E	Hematoxylin and eosin
HEPES	4-(2-hydroxyethyl)-1-piperazineethanesulfonic acid
ICC	Immunocytochemistry
Ig G	Immunoglobulin G
IHC	Immunohistochemistry
ISTN	*In situ* nick translation
LOD	Limit of detection
MRI	Klinikum rechts der Isar der TU München
MV	Matrix vesicles
NBT	Nitro blue tetrazolium
NTIRE	Non Thermal Irreversible Electroporation

OCT-compound	Optimal cutting temperature compound
Pen-Strep	Penicillin-streptomycin
(q)PCR	(quantitative or real-time) polymerase chain reaction
RNA	Ribonucleic acid
rpm	Rotations per minute
SDS	Sodium dodecyl sulphate
TBS	Tris buffered saline

1 Motivation

In the late 1980s a new branch of science caused attention of the scientific community around the world. The term of "Tissue engineering" was first mentioned in 1987 at a meeting of the National Science Foundation of USA (Nerem 1991). Here, it was introduced to name a new area of regenerative medicine. A proper definition was given in 1988, at the first tissue engineering meeting held at Lake Tahoe, California (Skalak and Fox 1988):

"Tissue engineering is the application of the principles and methods of engineering and the life sciences toward the fundamental understanding of structure-function relationships in normal and pathological mammalian tissues and the development of biological substitutes to restore, maintain, or improve functions."

Through tissue engineering it is tried to create a source of artificial or semi-artificial organs, readily available for transplantation, and tailored to the patients' specific needs.

The idea of tissue engineering is not by any means new. Since early times, the replacement of organs or tissues was regarded as an option for the healing of various illnesses or defects. In the beginning of the 20th century the idea of "organ culture" had already started to spread. Alexis Carrel is one of those that performed pioneering work on cell culture and later on organ culture and transplantation. While working at the Laboratories of the Rockefeller Institute for Medical Research in New York he published a number of research articles regarding his concept of *in vitro* cell and organ culture (Carrel and Burrows 1911; Carrel 1912). His ideas were then continued and developed by Charles Lindbergh. Together they developed a working method of long-time organ perfusion (Carrel and Lindbergh 1935; Lindbergh 1935), while maintaining the morphology and function of the organs.

Since then, a lot of work was invested in this area, and this had led to scientific breakthroughs like cold organ storage and transplantation. Since the first successful organ transplantation, techniques were continuously improved. Nowadays, organ transplantation allows treatment of diseases, which once were considered incurable. But being available to more and more patients has also a downside. Finding an

organ for each patient has soon become impossible, and the waiting list for a donor organ, is becoming longer and longer. Therefore, there is an urgent need for finding replacement organs for transplantation purposes that are also more compatible to the receiving patients.

Bone is the one of the most implanted tissues in the body, second only to blood transfusions (Wahl and Czernuszka 2006). Annually, there are about 500000 to 600000 bone grafting operations in the USA alone, of which 10% are involving synthetic bone substitutes (Bucholz 2002). There was a 2.5 fold increase in the number of musculoskeletal tissue donors in the USA from 9443 in the year 1994 to 25157 in 2007 (Forum 2010), but nevertheless this data indicates that there is a clear shortage of donor tissue used for reconstructive operations. The usage of synthetic materials to make up for this shortage has stimulated a large increase in the market of bone replacement materials, which has tripled since 2001 to reach $1.5 billion in 2009 (Forum 2010).

Considering also that half of the 3 million musculoskeletal procedures performed annually in the USA and 2.2 million around the world require bone grafting or substitution (Jahangir AA 2008), it can be realized that there is a clear need of a different approach to developing these materials. In future, tissue engineered bone graft substitutes may hold the solution to the currently limited availability of autografts and allografts to orthopedic regenerative therapies.

2 Background

2.1 Bone

Bone is a type of connective tissue that is specialized for performing three main functions: support for locomotion, protection of the internal organs and nervous system and regulation of the mineral metabolism. It is formed by a combination of organic and inorganic substances, water and bone cells. The osteoblasts produce an extracellular matrix that has the capacity to be mineralized and be remodeled by the osteoblasts. This gives bone the unique properties needed to withstand various types of mechanical forces, but at the same time, the capacity to regenerate itself. The bone is, therefore, the passive component of the locomotion system, but is also providing protection for the central nervous system and a part of the internal organs.

2.1.1 Classification

The human skeleton comprises more than 200 bones, which can be classified according to different criteria (Safadi, Barbe et al. 2009):

1. Shape

    - Short bones – e.g. the bones of the hand, the carpal and the tarsal bones
    - Long bones, or tubular bones – e.g. the tibia, the femur
    - Flat bones – e.g. the skull
    - Irregular bones – e.g. the scapula
    - Sesamoid bones – e.g. the patella

2. Collagen fiber orientation
    - Woven bone
    - Lamellar bone

3. Density
    - Compact bone
    - Trabecular bone

2.1.2 The morphology of the long bone

One typical long bone comprises of multiple parts, including diaphysis, physis, epiphysis, and medullary cavity (Tortora and Derrickson 2012).

The diaphysis, or shaft, is the longest part of the bone and has the cylindrical shape of a tube, giving these bones the name of tubular bones. The diaphysis has a thick cortical bone and in the middle the medullary cavity with trabecular bone.

The medullary cavity houses the bone marrow, comprising of hematopoietic marrow, adipose tissue and trabecular bone. It is supplied by a well-developed network of blood vessels and nerves. The proportion of adipose tissue in the bone marrow increases as the individual progresses in age.

The physis or epiphyseal plate is situated between diaphysis and epiphysis. It exists only during the growth of bones in children. Damages to this region of the bone during their growth can affect the shape and dimensions of the bone.

Figure 1. Diagram of a long bone. The typical long bone of the human skeleton grossly comprises of diaphysis, physis, and epiphysis. The inner compartment contains the bone marrow. From (Kulkarni, Bakker et al. 2012).

The epiphysis is found between the physis and the articular cartilage at both ends of the diaphysis. It is a widened portion of the bone and consists mainly of spongy bone, covered by a thin layer of compact bone and hyaline cartilage. The cartilage has the role of protecting the epiphyseal surface from the stress of articular friction and mechanical shocks.

The surface of the bone is covered by a thick fibrous membrane named periosteum. It is made up of an outer layer which contains blood vessels and nerves, and an inner layer containing osteoprogenitor cells. The periosteum contributes to the bone nutrition, fracture repair and serves as insertion point for tendons and ligaments. The endosteum covers the surface of the medullary cavity and it is formed of only one layer of bone lining cells.

2.1.3 The structure of the bone tissue

Bone is not a solid tissue but is porous, having small spaces in its extracellular matrix. These spaces house the cells of bone or the vascular and nervous system. Two types of tissue can be found in all bones depending on porosity: compact or cortical bone and trabecular or cancellous bone.

2.1.3.1 Cortical bone

The cortical bone is the strongest form of bone, adapted to withstand strong forces generated by movements and the weight of the body. It is found on the exterior of bones, under the periosteum, it has variable thickness and it is smooth and compact.

The structural unit of the compact bone is a tubular formation named osteon, or Haversian system. Each osteon is formed by concentric circular lamellae, which are thin sheets of mineralized extracellular matrix, situated around a central canal, the Haversian canal. Because in a long bone the long axis of an osteon is parallel with the long axis of the bone, the osteons play an important role in the mechanical properties of bone. Through the Haversian canal pass blood vessels, lymphatics and nerves. Between the lamellae there are spaces called lacunae which contain osteocytes. The lacunae are connected to each other by small canals called canaliculi. The canaliculi contain extracellular fluid and processes of osteocytes. In the spaces that remain between osteons there are lamellae called interstitial lamellae, which are remnants of osteons which have been restructured due to bone remodeling. The connection between the Haversian system and the blood vessels, lymphatics and nerves in the periosteum or marrow is accomplished through transverse Volkmann canals, also called perforating canals. Next to the periosteum

and the endosteum, around the entire inner and outer circumference of the bone, there is another type of lamellae, the circumferential lamellae. The outer circumferential lamellae are connected to the periosteum by the Sharpey fibers.

2.1.3.2 Trabecular bone

The trabecular bone is located within the bone, always covered by a layer of compact bone which provides protection. It is the main type of bone of short, flat sesamoid and irregular bones, whereas in long bones it is only found in the epiphyses and in the medullary cavity. It consists of a network of trabeculae, that are small plates or columns formed of a small number of bone lamellae. The lamellae are concentrically arranged, have lacunae with osteocytes interconnected through canaliculi. The arrangement of the trabeculae is not random. The forces to which the bones are subjected have an important role in deciding the direction in which the trabeculae are modelled. In the spaces between the trabeculae is the hematopoietic bone marrow or adipose tissue, supplied with blood by numerous blood vessels.

2.1.4 The bone cells

Bone contains cell populations responsible for the continuous formation and remodeling of the tissue. The chondrocytes, osteoblasts, osteocytes and bone lining cells develop from the mesenchymal stem cell population of the bone marrow and they are responsible for formation of new bone tissue (Harada and Rodan 2003; Kronenberg 2003). The osteoclasts originate in the hematopoietic stem cells in the bone marrow, therefore closely related to the macrophage-monocyte family, and are responsible for the resorption of the mineralized bone matrix (Blair, Robinson et al. 2005).

The chondrocytes play a central role in formation of long bones through endochondral bone formation. They produce a primary cartilage matrix containing mostly collagen type II and X. After the chondrocytes stop proliferating and enter apoptosis, the matrix is invaded by blood vessels and populated by osteoblasts that transform it into primary cancellous bone (Kronenberg 2003).

The osteoblasts are mostly found in active bone-forming areas of the bone. They originate from a population of osteoprogenitor cells in the non-hematopoietic bone marrow (Kassem, Abdallah et al. 2008). Their differentiation towards osteoblasts is highly regulated by the transcription factors Runx2 and Osterix (OSX) (Komori 2003; Fu, Doll et al. 2007). The main function of the osteoblasts is to secrete bone extracellular matrix (ECM) components and to induce its mineralization by crystals of hydroxyapatite. The non-mineralized ECM, named osteoid, contains mostly collagen type I, but also non-collagenous proteins (osteocalcin, osteopontin, osteonectin, fibronectin), proteoglycans, and glycosaminoglycans (Shekaran and Garcia 2011). Osteoblasts are also involved in modulating the function of the osteoclast population, thus the bone resorption (Phan, Xu et al. 2004).
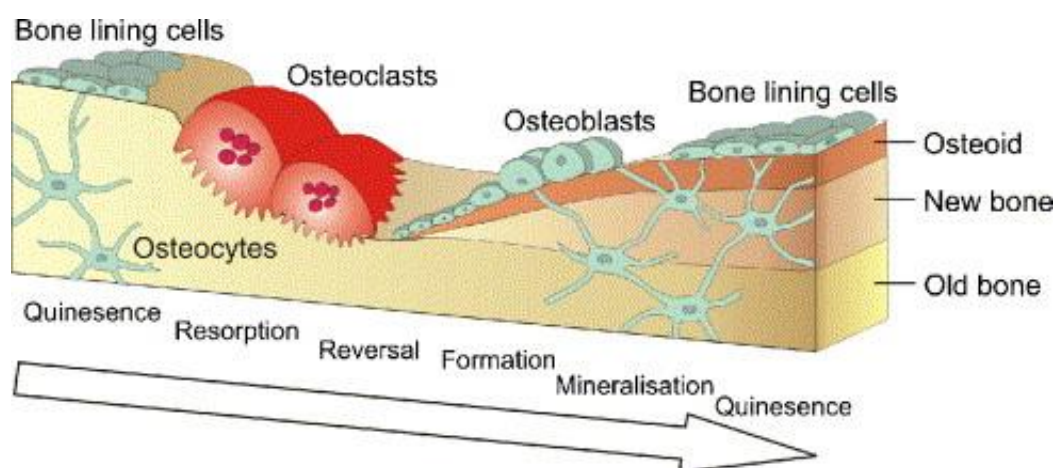
Figure 1. Bone remodeling takes place continuously throughout the bone. There is a constant process of bone resorption performed by the osteoclasts. At the same time osteoblasts are building new osteoid and remain entrapped in the mineralized tissue as osteocytes. The balance between the bone resorption and deposition prevents inadequate loss or gain of bone mass. From Spencer et al (Spencer, McGrath et al. 2007).

2.1.5 Chemical composition of bone

From a chemical point of view, bone is made up of organic and inorganic substances. The organic part is the osteoid and constitutes about 20% of bone, while the inorganic part represents 60-70% of bone (Boivin and Meunier 2003). Of the bone minerals, hydroxyapatite $[Ca_{10}(PO_4)_6(OH)_2]$ is the most abundant, which is formed from the combination of calcium phosphate $[Ca_3(PO4)_2]$ and calcium hydroxide $[Ca(OH)_2]$. The hydroxyapatite combines with other minerals present in

bone, such as fluoride, magnesium or potassium. During calcification, it accumulates in the extracellular matrix induced by osteoblasts (Tortora and Derrickson 2012).

2.1.6 Bone defects

Bone defects can occur in different situations: trauma, surgical interventions, infections, or congenital anomalies (Slater, Kwan et al. 2008). Bone defects can vary greatly in size, from just a fragment to large portions of a bone. They can be cortical, cancellous or cortico-cancellous and can be characterized according to their localization or dimensions. Although there is no universally recognized classification of bone loss, the defects resulting from fractures were classified by Winquist and Hansen (Winquist and Hansen 1980), modified by Robinson et al (Robinson, McLauchlan et al. 1995).

2.1.7 Bone fracture repair

In case of an injury the process of bone repair is started. In contrast to other tissues, bone injuries can heal without leaving any scars. The remaining lesion is often hardly noticeable on control radiographs.

Fracture healing can be of two types, namely primary and secondary. The primary fracture healing happens when the non-displaced bone fragments can be rigidly fixed and stabilized. In this case the bone heals without any cartilaginous intermediates, with reestablishment of the Haversian systems. The secondary fracture healing is the type of healing that occurs in the majority of fractures. It involves the formation of a callus between the bone segments, due to the lack of absolute immobilization of the fracture site. First, a cartilaginous tissue is formed, the callus, which will gradually be replaced by bone.

The repair of bone fractures by secondary fracture healing is considered to comprise of four stages: inflammation, soft callus formation, hard callus formation, and the remodeling stage.

In other situations, the defect of the bone is too extensive and the repair mechanisms of the body are insufficient. These defects that cannot be spontaneously repaired when left untreated are named "critical size defects". This

situation can be seen in atrophic nonunion, after extensive traumas or infections. These are special situations in orthopedic, oral and maxillofacial surgery that require extensive reconstructive surgery.

There are a number of possibilities to treat these lesions. The aim is to create new bone tissue or provide support for the mechanism of self-repair. The general name of these treatment options is "bone grafting".

2.1.8 Bone grafts

Bone grafting is the procedure which is used in certain conditions to accelerate or promote bone healing, when this does not happen or is delayed, and to provide structural support. The current gold standard of bone grafting therapies is the autograft. It possesses all the required characteristics of the ideal bone grafts, which are osteoinduction, osteoconduction and osteogenity (Janicki and Schmidmaier 2011). Osteoinduction is the process of inducing osteogenesis, by stimulating the adult stem cells to become preosteoblasts, bone-forming cells (Albrektsson and Johansson 2001). Osteoconduction refers to a property of a material that permits bone apposition on its surface and enhance bone formation. Osteogenity denotes that the bone graft contains living and viable osteogenic cells, necessary for the bone formation and graft integration.

As mentioned above, autografting is considered the ideal graft type. It involves harvesting the bone from one anatomical region to another on the same individual. Regions where usually bone harvesting is performed are the iliac crest, ribs, ulna or fibula. The limitation of the autograft is the donor site morbidity caused by hematoma, pain, and risk of infections following the supplementary surgery. An additional limitation comes from the quantity of the bone that can be harvested. This under certain circumstances does not suffice for the repair of the defect.

Allografting is an alternative to autografting. It involves transplantation of bone from one individual to another. This procedure surpasses the disadvantages of the autograft, but carries a high risk of disease transmission or graft rejection. To avoid this, comprehensive screening of donor must be performed. Tissues can additionally

undergo procedures of sterilization, such as irradiation, physical debridement and ultrasonic washing.

An alternative to both autografts and allografts are the natural or synthetic bone-like materials. In the last decade these became more and more available on the market and today they are used by surgeons all over the world. Some examples can be the use of ceramics, coral, calcium phosphates, or demineralized bone matrix, with or without the presence of bone-inductive cytokines. Although they show great potential of defect healing, the synthetic grafts lack remodeling capacity and have an inferior healing rate compared to other types of grafts (Salgado, Coutinho et al. 2004). An improvement to the synthetic grafts was the addition of growth factors which can promote bone regeneration by mobilizing host cells to the implantation site (Kimelman, Pelled et al. 2007). However, this approach has limited applicability due to the short half-life of the growth factors and - in certain cases of extensive trauma, disease, or metabolic disorders - due to the limited number of endogenous cells that can be mobilized (Bruder and Fox 1999; Service 2000).

Another approach is bone tissue engineering. This could avoid the disadvantages enumerated above. It is based on combining cells with a biocompatible scaffold, thus the term "cell based bone tissue engineering" (Meijer, de Bruijn et al. 2007).

2.1.9 Cell-based bone tissue engineering

The repair of bone fractures is highly dependent of mesenchymal stem cells and their progeny, the osteoblasts and chondroblasts, to form the fracture callus (Carter, Beaupre et al. 1998; Yoo and Johnstone 1998). Based on this assumption, the development of biocompatible bone grafts has taken a revolutionary turn with the introduction of cell-based tissue engineering, by combining biocompatible bone substitutes with cells. Early studies on animal subjects have shown that mesenchymal stem cells can have a regenerative effect on cartilage lesions when implanted *in vivo* in a collagen type-I gel carrier (Wakitani, Goto et al. 1994) and investigations in the field of bone regeneration have subsequently shown the potential of these cells together with ceramic scaffolds to repair bony defects (Bruder, Kraus et al. 1998; Bruder, Kurth et al. 1998).

It was postulated that four prerequisites are necessary for the success of bone tissue engineering in clinical applications: a sufficient number of cells that show osteogenic properties, a suitable scaffold onto which the cells will be seeded, osteogenic differentiation stimulating factors, and vascular perfusion (Caplan 1991). In what concerns the applicability in humans, bone tissue engineering is not yet regarded as a success (Meijer, de Bruijn et al. 2007). Of the above mentioned four requirements, the insufficient vascular supply especially in the middle of the graft and consequently the lack of nutrients and onset of hypoxia in the profound layers are considered the number one cause of engineered graft failure (Tsigkou, Pomerantseva et al. 2010). Without a vascular network, diffusion is the mechanism by which the cells inside the scaffold can be provided with oxygen and nutrients until the construct is vascularized and remodeled (Valentin, Freytes et al. 2009).

To avoid this setback, there are a number of alternatives tissue engineers have developed, all with the purpose of improving the circulation of fluids through the bio-engineered scaffold.

One of the main approaches is the use of three-dimensional porous scaffolds seeded with mesenchymal stem cells that would allow the passing of fluids through the network of interconnected pores inside and the cells' migration (Zimmermann and Moghaddam 2011). It has been determined that an optimal pore diameter would be 565 µm (Gauthier, Bouler et al. 1999).

Another reported approach involves applying angiogenic growth factors onto the artificial scaffold. Here, these factors are assumed to stimulate endogenous endothelial cells for blood vessel growth into the scaffold and therewith establish a circulatory network within the scaffold (Levenberg, Rouwkema et al. 2005).

2.2 The rat kidney

The kidneys are a pair organ, situated in the retroperitoneal space of the abdominal cavity, on both sides of the spinal column. The main functions of the kidney are to filter waste products of the metabolism from the blood and to regulate the water homeostasis. Aside from these, the kidney plays important roles in calcium and phosphate metabolism, blood pressure regulation and erythropoiesis. It is also the production site for different hormones, such as erythropoietin, renin and angiotensin II.

2.2.1 General anatomical features

The rat kidney has a bean-like shape, similar to other mammals. Its weight can vary between 0.8 g and 1.4 g, has an average length of 10 mm, width of 6 mm and thickness of 4 mm. Thus, it is approximately 10 times smaller than an average human kidney.

The kidneys are covered by a fibrous non-adherent capsule. They have a hilum on the concave side, through which the vessels and nerves enter the organ. The kidney is irrigated by the renal artery, renal vein and lymphatics.

Seen in cross-section (Figure 2), the kidney presents two regions: an outer region, named cortex, and an inner region, named medulla. The cortex can be further subdivided into the cortical labyrinth and the medullary rays, and the medulla into the outer medulla and the inner medulla.

Unlike the human or pig kidney, where the medulla is subdivided into 8-18 renal pyramids, the medulla of the rat kidney possesses a single renal
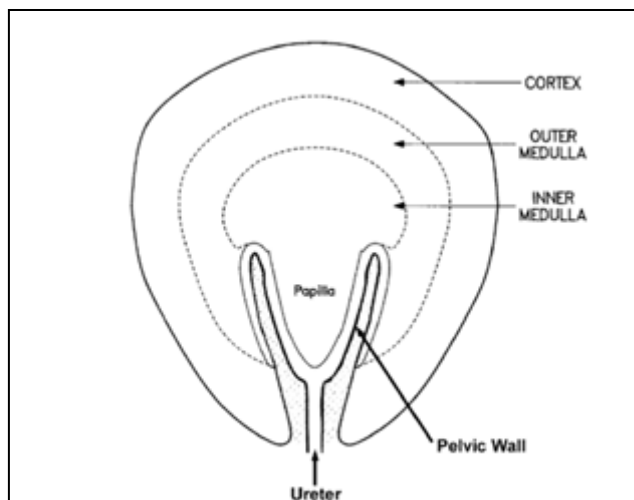
Figure 2. Schematic view of a cross-section of an unipapillate kidney, typical for rat, mouse and rabbit. The unipapillate kidney is constituted from cortex and a medullar region, and has only one papilla compared with the human kidney that is multipapillate. Reproduced from (Knepper, Saidel et al. 2003).

pyramid with a single papilla. Thus, the kidney is named unipapillate (Nielsen, Kwon et al. 2012). The renal pyramid has the base at the interface between the medulla and the cortex. The tip, represented by the papilla is oriented towards the renal hilum. The papilla is surrounded by the renal pelvis, where the final urine accumulates and drains further into the ureter. The surface of the renal pelvis is covered by urothelium, a type of epithelium that is specific to the urinary tract which is also present in ureter, bladder and pelvic urethra.

2.2.2 The renal vascularization

The kidneys are vascularized by the renal arteries, that derive from the abdominal aorta (Nielsen, Kwon et al. 2012). Once they have passed through the hilum, they divide into interlobar arteries, arcuate arteries, and finally cortical radial arteries, that supply the blood to the glomerulus through the afferent arterioles. After the filtration takes place the blood from each glomerulus is collected by the efferent arterioles either in the peritubular capilaries or in the vasa recta. The vasa recta are loop-shaped capillaries present alongside the nephrons in the medulla. The blood reaches then the peritubular venules and continues through the arcuate veins and the interlobar veins. After that, it leaves the kidney via the renal veins. The renal blood flow of the rat is considered to be in average 5-7 ml/min/g of kidney (Steinhausen, Endlich et al. 1990) and the glomerular filtration rate an average of almost 1 ml/min/g of kidney (Fleck 1999).

2.2.3 The nephron and collecting duct system

The nephron is considered to be the functional unit of the kidney. There are approximately 30000 nephrons in an adult rat kidney (Bertram, Soosaipillai et al. 1992). The components of the nephron include the renal corpuscle comprised of the glomerulus and Bowman's capsule and the renal tubule. The latter includes the proximal convoluted tubule, the loop of Henle and the distal convoluted tubule. The initial filtration of the blood passing through the kidney takes place in the renal corpuscle. The glomerulus is a network of interconnected capillaries supplied with blood from an afferent arteriole. It drains into an efferent arteriole. About 20% of the plasma filtrated through the glomeruli passes into Bowman's capsule, forming the primary urine (Haraldsson, Nystrom et al. 2008). This glomerular filtrate is further

processed along the renal tubule and as a result the final urine contains only 1% of the initial water content.
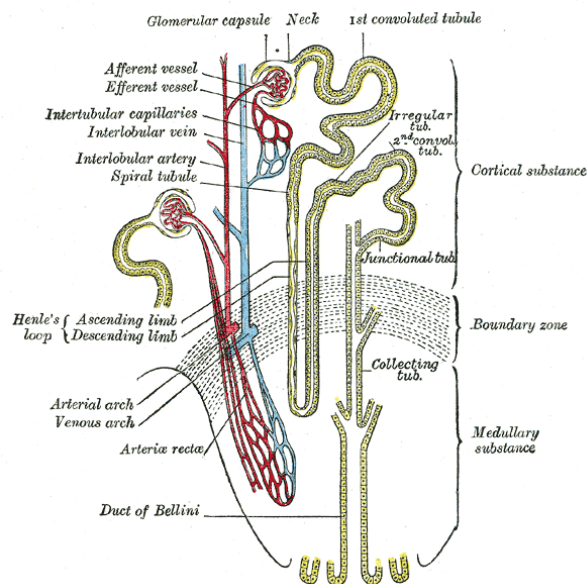
Figure 3. The renal tubule and its vascular supply. From **(Gray and Lewis 1918).**

The collecting duct system is the connection of the nephron to the ureter. It includes the connecting tubules, cortical collecting ducts and medullary collecting ducts. The medullary ducts end at the renal papilla and empty into the renal calyx, where urine is gathered and enters the ureter to leave the kidney.

2.3 Decellularization

Decellularization introduces a new type of scaffold that is derived from natural tissues and organs. The obtained scaffolds are composed only of natural ECM that retains all the necessary properties of the tissue, but contains no cells, which are a major cause of graft incompatibility. During decellularzation the target tissue or organ is exposed to a series of decellularizing agents. The purpose of the treatment is to eliminate the cellular components of the tissue and to preserve the extracellular matrix as much as possible.

A suitable bio-scaffold has a capital importance in the successful generation of a tissue engineered structure. The scaffold has to be biocompatible and resorbable. It must not trigger an immunogenic effect from the host and it has to be able to support and induce the attachment and growth of cells. These cells must then be stimulated to constitute themselves into three dimensional structures, colonize the graft and integrate it into the host organism.

Until now there have been many studies, both *in vitro* and *in vivo*, that demonstrated the use of scaffolds of limited dimensions and their successful integration and functionality. Nevertheless, these models have the disadvantage of a lack of vasculature. Thus, the nutrients and oxygen are only supplied through diffusion from the surrounding tissue (Rouwkema, Rivron et al. 2008). The cells can receive enough oxygen if they are situated at a distance of 100 – 200 µm away from a blood vessel *in vivo* (the diffusion limit of oxygen) (Carmeliet and Jain 2000). This fact greatly restricts the size of the scaffold and consequently the size of the area that can be repaired.

Another limitation encountered at xenogenic biomaterials is their antigenicity. The intended receiver of the graft will exhibit a foreign body response to the replacement tissue. Because the major components of the extracellular matrix, such as collagens, laminin and fibronectin, have a similar structure among different species (Bernard, Chu et al. 1983; Exposito, D'Alessio et al. 1992), they can be well tolerated by xenogenic recipients. The cellular antigens are the factors that play a major role in the immune mediate rejections of the tissue, because they are

recognized as foreign by the immune system of the recipient (Gilbert, Sellaro et al. 2006).

Thus, decellularization of whole organs, such as heart, kidney or liver, theoretically gives the possibility, to generate a remaining scaffold that may be completely biocompatible and non-immunogenic. Besides this, even the vascular network can be kept intact. This can be used to create scaffolds for tissue engineering that can be seeded with cells and uniformly supplied with nutrients in all areas. Moreover, the vascular pedicle, which is used for the perfusion of the decellularization agent, could be employed for a direct blood supply upon implantation.

Figure 4. Decellularization of whole rat heart. The three images are taken in succession during decellularization of a rat heart. The first image on the left shows the organ at the beginning of the treatment, with the native cells contributing to the normal aspect of the heart. The third image shows the organ at the end of the decellularization protocol, when the heart becomes white and semi-transparent, but maintains the original shape. Images part of the study of Ott et al. (Ott, Matthiesen et al. 2008).

2.3.1 Extracellular matrix in tissue engineering

Tissues are constituted of cells and their environment, which is generally termed extracellular matrix (ECM). The ECM provides the structural support, but has also a key involvement in cell signaling, homeostasis, and transmission of external stimuli (Adams and Watt 1993; Chen 2008). ECM can deposit growth factors and their associated proteins. Here, the interactions between ECM and the growth factors can have an important role in the fate of the cells (Rosso, Giordano et al. 2004). On the other hand, cells can also influence the structure and composition of the ECM they reside in. This interaction was defined "dynamic reciprocity" (Bissell, Hall et al. 1982).
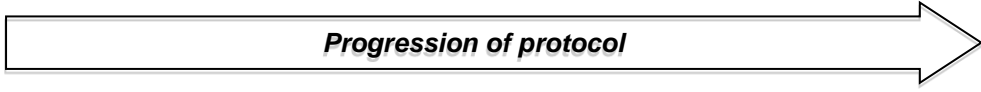
Up to now synthetic scaffolds cannot reproduce the complex signals by which cell behavior is regulated in the living organism. This is why the design of scaffolds based on natural ECM characteristics and components could be the optimal approach in tissue engineering to constructing 3D grafts (Ingber and Levin 2007).

Cell culture substrates were developed that are based on ECM proteins, in order to induce a behavior of the cells similar to that in the natural environment. Such products are used for coating of culture dishes as separate or mixtures of proteins like collagens, laminin, fibronectin, vitronectin, or osteopontin (Zhang, He et al. 2009). Tissue engineered grafts were made by coating synthetic scaffolds with an ECM-based solution (Yun, Kim et al. 2011). Another proposed solution was growing autologous cells on a synthetic mesh-like scaffold *in vitro* until they produce their own ECM. The cells were then removed from the scaffold prior to implantation. The newly produced ECM contained native proteins such as collagens, fibronectin, or laminin and the construct showed very good biocompatibility when implanted (Lu, Hoshiba et al. 2011).

2.3.2 Decellularization agents

There are multiple agents described in the literature, which alone or combined can lead to obtaining acellular scaffolds (Badylak, Taylor et al. 2011; Crapo, Gilbert et al. 2011). Commonly used are physical, chemical and enzymatic methods. Protocols whole organ decellularization have been developed and published. To maximize their efficiency, multiple methods are most of the time combined. A summary of some of the decellularization protocols is made in Table 1 below.

Table 1. Overview of decellularization protocols available in literature for heart, liver, and lung. Adapted from (Badylak, Taylor et al. 2011).

Progression of protocol						
Heart	Freeze –80°C 6 h	Thaw in type 1 H2O 8 h	Perfuse type 1 H2O then PBS 37°C 2 h	0.02% Trypsin 0.05% EDTA 0.05% NaN3 2 h	4% Deoxycholate 2 h	0.1% Peracetic Acid 4% EtOH 1 h	Total ~21 h
Heart	10 µM adenosine 15 min		1% SDS 12 h		1% Triton X-100 30 min	PBS with antibiotics 124 h	Total ~137 h
Lung	8 mM CHAPS 1 M NaCl 25 mM EDTA 2 h		PBS with antibiotics		90 U/ml benzonase	PBS with 10% FBS	Total ~5 weeks
Lung	0.1% SDS 120 min		1% Triton X-100 10 min		PBS with antibiotics 72 h		Total ~74 h
Liver	Freeze –80°C 24 h		0.02% Trypsin 2 h	3% Triton X 18–24 h		Peracetic acid 1 h	Total ~51 h
Liver	Freeze –80°C	4°C PBS overnight	0.01% SDS 24 h · 0.1% SDS 24 h	1% SDS 24 h	1% Triton X-100 30 min	0.1% Peracetic acid 3 h	Total ~88 h
Liver	PBS Freeze 1 week		Freeze/thaw 24 h	11% SDS 5 weeks	DNAase 24 h	DMEM 48 h	Total ~7 weeks

2.3.2.1 Physical methods

The application of physical methods to the tissues has an effect of disrupting the cell membrane. The cellular components must be then washed out of the tissues with the aid of chemical or enzymatic solutions. In this category can be included freeze/thaw cycles, sonication, high pressure and mechanical agitation (Badylak, Taylor et al. 2011).

Repeated freezing and thawing can cause cell lysis by formation of ice crystals inside the cell cytoplasm. This method has been used to decellularize vascular (Wilshaw, Rooney et al. 2011), meniscal (Stapleton, Ingram et al. 2008), cartilaginous (Kheir, Stapleton et al. 2011), or nervous (Haase, Rovak et al. 2003) tissues. The temperature plays an important role in this method, because a too steep or too slow decrease in temperature can adversely affect the extracellular matrix, with irreparable damages occurring. The rests of the cells must be washed out following this procedure.

Mechanical removal of certain cell layers, such as muscle or submucosa in thin tissues, can aid the process of decellularization prior to applying other agents of decellularization (Yang, Zhang et al. 2010). This procedure can simplify the cell removal but the physical degradation of the ECM cannot be avoided.

Applying pressure on a tissue can also yield an acellular matrix, which retains its mechanical properties after the procedure. Successful attempt were made with high hydrostatic pressure on simple tissues like blood vessels (Funamoto, Nam et al. 2010; Negishi, Funamoto et al. 2011) or corneas (Sasaki, Funamoto et al. 2009; Hashimoto, Funamoto et al. 2010), where the ECM is not so densely organized as in parenchymal organs like the kidneys or liver. A disadvantage of this method is the baric formation of ice crystals that may disrupt the ECM ultrastructure (Funamoto, Nam et al. 2010).

A relatively new technique is that of non-thermal irreversible electroporation (NTIRE) (Sano, Neal et al. 2010). By using this method, pulsed electrical fields are used to produce micro pores in the membranes of cells by destabilizing the electrical potential of the cell membrane. The disadvantage of this method is that the elimination of the dead cells is taking place with the help of the immune cells, which implies that this procedure has to be produced *in vivo*.

2.3.2.2 Chemical methods

Acid and alkaline substances can be used on tissues to remove the cytoplasmic and nuclear components (Brown, Freund et al. 2011; Mendoza-Novelo, Avila et al. 2011). They are particularly effective on removal of nucleic acids like RNA and DNA. Sulfuric acid, acetic and peracetic acid and ammonium hydroxide are efficient in removal of cellular components, but have also a negative effect on the components of the ECM. Peracetic acid is also a common antimicrobial agent. When used in decellularization it has almost no effects on the composition of the ECM (Hodde, Janis et al. 2007). Alkaline solutions, on the other hand, have a harsher impact on the ECM, by disrupting the collagen crosslinks and removing the growth factors (Reing, Brown et al. 2010).

Detergents, ionic, anionic or zwitterionic, can thoroughly solubilize cellular membranes, which contain also a lipid layer (Cebotari, Tudorache et al. 2010).

The anionic detergent Triton X-100 (chemical structure presented in Figure 5) has been extensively used in decellularization protocols (Nakayama, Batchelder et al. 2010; De Kock, Ceelen et al. 2011). It was proven that it is efficient on thin tissues, like heart valves, but on thicker tissues, such as heart pericardium, it was not able to remove completely the cellular materials (Grauss, Hazekamp et al. 2005). Triton X-100 has also been shown to decrease the amounts of laminin, fibronectin and glycosaminoglycans (GAGs) from the treated tissues and to reduce their mechanical strength.
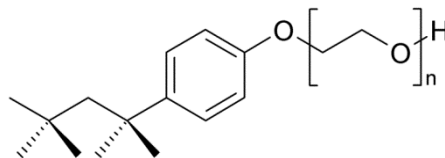
Figure 5. Chemical structure of Triton X-100.

Ionic detergents, such as SDS (Figure 6), are much more effective at removing cells from a tissue, as anionic detergents. On the other hand, they are more prone to denaturize the proteins and disrupt the protein-protein interactions. Cell nuclei and the cytoplasmic protein vimetin can be better removed from dense organs like kidney or liver with the help of SDS, but it has been found that it decreases the ECM contents in growth factors (Reing, Brown et al. 2010).
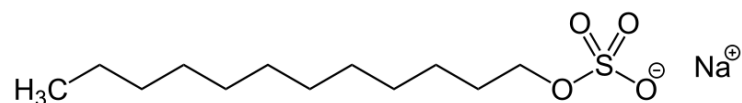
Figure 6. Chemical structure of SDS.

Zwitterionic detergents are another class of detergents that has been used to decellularize tissues. One of the members of this class is CHAPS (Figure 7). It has been shown to be less efficient in removal of cells from compact tissues than from thinner ones, like lungs. The zwitterionic detergents are generally not disrupting the structure of the ECM, as ionic detergents do. In contrast they are not very efficient at removing the cellular components and tend to lower the pressure resistance of

processed tissues. However, the association between these two types of detergents has lead so far to good results in developing acellular bioscaffolds (Table 1).
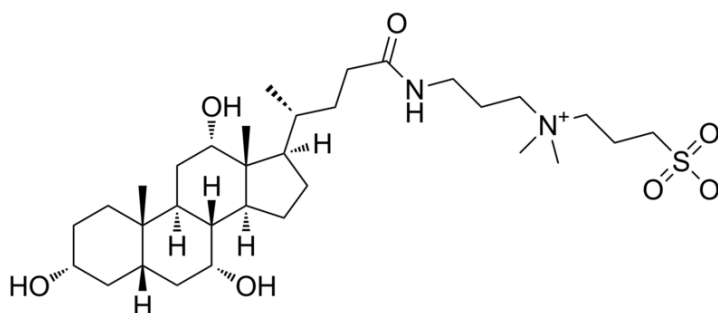
Figure 7. Chemical structure of CHAPS.

2.3.2.3 Enzymatic methods

There are many types of enzymes which can be used in tissue decellularization, in order to enhance the actions of the physical and chemical agents. Known protocols include nucleases, trypsin, lipase, dispase, thermolysin and α-galactosidase (Crapo, Gilbert et al. 2011).

DNases and RNases are nucleases often used to eliminate rests of nucleic acid from the matrix. These enzymes can cleave DNA strands to very small fragments, this way helping in their removal after other cellular components have already been removed (Petersen, Calle et al. 2010; Yang, Zhang et al. 2010).

Trypsin can be very useful at the beginning of the decellularization treatment, to facilitate the penetration of other decellularization agents and is commonly used as such (Rieder, Kasimir et al. 2004). If used alone, its disadvantage is that it requires long incubation times and affects elastin and collagen structure and consequently the mechanical properties of the ECM (Waldrop, Puchtler et al. 1980).

Lipase is used for the removal of the lipids in tissues (Brown, Freund et al. 2011). The enzymes dispase and thermolysin are not efficient alone in decellularizing a tissue, as they can remove only cells at the surface of a tissue and require mechanical abrasion for a complete decellularization (Hopkinson, Shanmuganathan et al. 2008).

The enzyme α-galactosidase is useful for removing the immunogenic cell-surface antigen galactose-α-(1,3)-galactose, which can affect the integration of an acellular scaffold *in vivo* (Xu, Wan et al. 2008).

2.3.3 Techniques of decellularization

The way a decellularization agent is applied to an organ or tissue depends much on the thickness and density of the tissue, the agents used, and the purpose to which the acellular ECM will be used (Crapo, Gilbert et al. 2011).

2.3.3.1 Whole organ perfusion

The decellularization of a whole organ by perfusion through the existing vascular tree can be a very efficient method. This is due to the very fine vascular capillaries that uniformly reach all areas of the organ to minimize the diffusion of the oxygen and nutrients to the cells. This way, the decellularizing solution is delivered throughout the organ and the solubilized cellular materials can be effectively washed out.

Various organs such as heart, liver, kidney, or lungs have been transformed into 3D acellular scaffolds by using this method (Ott, Matthiesen et al. 2008; Ross, Williams et al. 2009; Ott, Clippinger et al. 2010; Petersen, Calle et al. 2010; Uygun, Soto-Gutierrez et al. 2010). Perfusion agents can be solutions of detergents, enzymes, alcohols, acids or bases, which are rinsed out with deionized water or PBS. Following treatment, the scaffolds have a translucent white appearance, and the native organ geometry and the vasculature are preserved.

2.3.3.2 Pressure gradient

Supplementary to enzymatic treatment of hollow tissues, a pressure gradient can be induced across the walls of tissue. The decellularization agent will, therefore, be forced through the tissue walls. This can increase efficiency of the procedure, especially for denser tissue. In a recent study describing this procedure (Prasertsung, Kanokpanont et al. 2008) it was shown that it does not so negatively affect the ultrastructure of the ECM as enzymatic treatment alone. Furthermore, it was shown that by using a pressure gradient collagen was less degraded than by

using agitation, DNA was better removed from the tissue and even a transmural pressure of 5 mmHg increased protein extraction (Montoya and McFetridge 2009).

2.3.3.3 Immersion and agitation

This method can be applied when decellularizing tissues that do not possess vasculature usable for perfusion. Target tissues can be, among others, heart valves, blood vessels, tendons, trachea or skin. The tissues are immersed into a decellularizing agent and subjected to agitation for a certain period of time. The nature of the agent, the duration and intensity of the treatment depends on the characteristics of the tissue. Thicker and denser tissues can require longer treatment times or stronger decellularization agents or combinations thereof, as in the case of skin, trachea, or muscle (Conconi, De Coppi et al. 2005).

2.3.4 Applications of decellularization

Graft materials based on decellularized ECM are already approved by the Food and Drug Administration of the United States of America. They are present on the market and are now in clinical use. Due to the removal of cells there is a minimal possibility of graft rejection. The minimization of infectious diseases transmission by very strict disease testing and in combination with effective sterilization processes made these products a very attractive alternative to autografts or allografts.

One of the commercially available acellular grafts is Alloderm®. It is an acellular human dermal scaffold for which there are currently multiple clinical applications. It was used successfully in the care of burn victims (Hiles, Record Ritchie et al. 2009), in repair of abdominal hernias (Hiles, Record Ritchie et al. 2009), plastic surgery (Gabriel and Maxwell 2011) and even periodontal surgery (Gapski, Parks et al. 2005).

Another clinically used product is CryoValve® SG. It is derived from human cardiac valve that has been decellularized and is successfully used in the replacement of the pulmonary valve in pediatric cardiac surgery (Konuma, Devaney et al. 2009).

In orthopedic surgery was also found applicability for decellularized tissue. Decellularized bone allografts are used on a large scale and in various forms in the treatment of bone defects of large dimensions. Acellular bone can be used as sections of long bones, cancellous or cortical bone chips, tricortical wedges. There are also proprietary allografts, with Graftech, BioCap, or MatriGraft to name just a few.

Even if the application of decellularized scaffolds to regenerate organs in humans seems to be very appealing and straightforward, broad clinical applicability was not yet reached. Nevertheless, a very interesting case on trachea regeneration through decellularization has been published by Macchiarini (Macchiarini, Jungebluth et al. 2008). Here, a 30-year-old female patient with end-stage bronchomalacia has received a bronchus graft prepared from a donor trachea by decellularization. The donor trachea was decellularized, colonized in vitro with autologous epithelial cells and mesenchymal stem-cell-derived chondrocytes and implanted to the recipient. The operation was deemed a success as the airway was functional and of normal appearance at 4 months from the surgery, the patient's quality of life was improved and there were no signs of graft rejection.

3 Aim of the work

The work done so far in tissue engineering is being severely limited by the lack of vascularization in the newly developed tissue structures. This is why the developing of a method that addresses this need is clearly necessary.

The aim of this thesis is to test the applicability of decellularization in providing a new type of vascularized bioscaffold for tissue engineering of bone. For this work the scaffold will be obtained through decellularization of animal tissue, namely rat kidneys. The scaffold will be seeded with cells belonging to C2C12 cell line and with primary human osteoblasts. The acellular scaffold will be beforehand characterized. After seeding, different markers will be investigated, which indicate the viability and functionality of the cells after different periods of *in vitro* culture.

Specifically, this study aims to investigate whether:

- it is possible to generate acellular scaffolds from rat kidneys with a short protocol based on SDS;
- the ECM of the generated scaffold maintains its structural and ultrastructural integrity;
- the generated scaffold can support the growth of human primary osteoblasts on a long term basis;
- the seeded primary human osteoblasts maintain their phenotype when cultured on the rat-derived scaffold.

4 Materials and methods

4.1 Materials

4.1.1 Laboratory devices

Name	Company, Country	Model
Autoclave	H+P Labortechnik AG, Germany	Varioklav
Cell culture incubator	Thermo Fisher Scientific, Germany	Heracell 150
Laboratory centrifuge	Eppendorf AG, Germany	5804R
Microscope	Carl Zeiss Microscopy GmbH, Germany	AxioObserver Z1
Electronic pipette filler	Eppendorf AG, Germany	Easy-Pet®
Sterile work bench	Kendro, Germany	Herasafe HS12
Sterilizer	Binder GmbH, Germany	ED115
Water bath	Grant Instruments, UK	SUB14
Microtome	Microm, Germany	HM 335E
Arthroscopy pump	Arthrex Medizinische Instrumente GmbH, Germany	AR-6475
Photometer	Thermo Fisher Scientific, Germany	Multiskan Ascent
Real-time PCR thermocycler	Applied Biosystems, USA	StepOnePlus
Spectrophotometer	PeqLab Biotechnologie GmbH, Germany	Nanodrop 2000c

4.1.2 Laboratory materials

Name	Company, Country
Main pump tubing	Arthrex Medizinische Instrumente GmbH, Germany
Extension pump tubing	
Glass bottles	Schott AG, Germany
Instruments for dissection	Karl Hammacher GmbH, Germany
Surgical suture 6-0	Ethicon LLC, USA
Catheter 26G	BD infusion therapy, Germany
Catheter 20G	B.Braun Melsungen AG, Germany
Discofix® 3-way Stopcock	
Perfusor®-tubings 150mm	
Syringes 2 ml, 20 ml	
Scalpels no. 21	Feather Safety Razor Co., Ltd., Japan
Microtome blades No.35	
Cover slides	Menzel-Gläser, Germany
Microscope slides	

4.1.3 Cell culture vessels and filters

Name	Company, Country
Cell culture flasks 75 cm²	BD Bioscience, Germany
Cell culture flasks 175 cm²	
Cell culture chamber slides	
Conical tubes 15 ml	
Conical tubes 50 ml	
Cell Strainer 40 µm	
Serological pipettes	Sarstedt AG, Germany
Cell culture dishes 3.5 cm	
Cell culture dishes 10 cm	
Pipette tips	Biozym Scientific GmbH, Germany
Sterile Filter 0.22 µm	Millipore GmbH, Germany

4.1.4 Chemicals

Substance	Company, Country
Alamar Blue	AbD Serotec, Germany
Allura Red AC	Sigma-Aldrich Chemie GmbH, Germany
BRIJ L23 solution	
Phosphate Buffered Saline, pH 7.4	
Stains-all	
Ethanol 70%	Apotheke MRI
Ethanol 96%	
Ethanol 99,8%	
Isopropanol	
Picric Acid saturated	
Acetic Acid Glacial	Merck KGaA, Germany
Hydrogen Peroxide	
Parafolmaldehyde	
Formamide	
SDS Ultra-Pure	Carl Roth GmbH, Germany
Methanol	
Penicillin-Streptomycin	Biochrom AG, Germany
Trypan Blue	
Sterile distilled water	B.Braun Melsungen AG, Germany
Xylol Pharm. Helv. VI	Aug. Hedinger GmbH & Co. KG, Germany

4.1.5 Cell culture media, buffers and supplements

Substance	Company, Country
Dulbecco's MEM w/o Calcium	Biochrom AG, Germany
Dulbecco's MEM Low Glucose	
Dulbecco's MEM High Glucose	
Fetal Bovine Serum Superior (FBS)	
L-Glutamine	
MEM-Vitamins	
HEPES	
Phosphate Buffered Saline Dulbecco's (w/o Ca and Mg) 10x	
Biofreeze	
Trypsin/EDTA (0.05%/0.02% w/v in PBS)	Sigma-Aldrich Chemie GmbH, Germany
β-Glycerophosphate disodium salt hydrate	
Dexamethasone	
L-Ascorbic Acid	
Primocin	Invivogen, USA

4.1.6 Recipes of cell culture media and buffers

Osteoblast growth culture medium	
DMEM without Ca^{2+}	500 ml
FBS	100 ml
HEPES Buffer	10 ml
Penicillin-Streptomycin	5 ml
L-Glutamine	5 ml
MEM Vitamins	5 ml
Dexamethasone	100 nM
L-Ascorbic Acid	285 µM
Osteogenic differentiation culture medium	
Alpha Medium	500 ml
FBS	50 ml
HEPES Buffer	10 ml
Penicillin-Streptomycin	5 ml
L-Glutamine	5 ml
MEM Vitamins	5 ml
Dexamethasone	100 nM
L-Ascorbic Acid	285 µM
β-Glycerophosphate	10 mM
C2C12 cell culture medium	
DMEM High Glucose	500 ml
FBS	50 ml
HEPES Buffer	10 ml
Penicillin-Streptomycin	5 ml
L-Glutamine	5 ml
Dulbecco's phosphate buffered saline (1x)	
Dulbecco's PBS stock solution (10x)	100 ml
Sterile distilled water	900 ml

4.1.7 Histo- and immunohistochemistry solutions and substances

Name of substance	Company, Country
Weigert's Hematoxylin	Apotheke MRI
Mayer's Hematoxylin	
Eosin G	Carl Roth GmbH, Germany
Target Retrieval solution Citrate pH 6.0	Dako GmbH, Germany
Biotin blocking kit	
Protein blocking reagent	
Antibody diluent	
Peroxidase Substrate AEC+	
Vectastain ABC Kit Elite	Vector Laboratories, Inc., USA
SYBR® Green I	Sigma-Aldrich Chemie GmbH, Germany
Alizarin Red S	
Eukitt®	O. Kindler GmbH, Germany
Sirius Red F3B	BDH Chemicals, UK
NBT/BCIP	Roche Diagnostics GmbH, Germany
Kaiser's Glyceringelatin	Merck KGaA, Germany
Tissue-Tek OCT compound	Sakura Finetek GmbH, Germany
Micro-Cut Paraffin	Polysciences, Inc., USA

4.1.8 Decellularization perfusion solutions

Sodium dodecyl sulphate (SDS) solutions				
SDS	2.5 g	5 g	6.6 g	10 g
Distilled water	1000 ml	1000 ml	1000 ml	1000 ml
Final concentration	0.25%	0.50%	0.66%	1.00%
Phosphate buffered saline solution				
Phosphate buffered saline pH 7.4	1 pouch			
Distilled water	1000 ml			

4.1.9 Histology solutions

Hematoxylin and eosin staining solutions	
Mayer's Hematoxylin	100 ml
Eosin G	100 ml + 1 drop Acetic acid glacial
Distilled water	
Alizarin Red S staining solution (pH 4.2)	
Alizarin Red S	1 g
Distilled water	100 ml
NaOH for pH adjustment	
Sirius Red staining solution	
Sirius red F3B	0.5 g
Picric acid saturated aqueous solution	500 ml

4.1.10 *In situ* nick translation assay solutions

Nick translation buffer (10x)	
Tris 1M	1000 µl
MgCl 1M	100 µl
Beta-mercaptoethanol 13M	15 µl
BSA 20 mg/ml	10 µl
Distilled water	875 µl
Nick translation master mix (for one tissue slide)		
dNTPs	dTTP 10 mM	0.8 µl each
	dCTP 10 mM	
	dGTP 10 mM	
Nick Translation Buffer (10x)	4 µl	
Biotin-7-dATP 0.4 mM	2 µl	
Distilled water	29.6µl	
Klenow fragment 2 u/µl	2 µl	
Reaction stopping buffer		
NaCl	8.8 g	
Sodium citrate	4.4 g	
Distilled water	ad 500 ml	

4.1.11 Antibodies for immunohistochemistry

Primary antibodies			
Name	**Company**	**Concentration**	**Incubation time/ temperature**
Laminin	Dako	1:500	2h/RT
Fibronectin		1:500	2h/RT
Vimentin		1:75	1h/RT
Ki-67	Quartett	1:500	2h/RT
Osteocalcin		1:100	1h/RT
Secondary Antibodies			
Name	**Company**	**Concentration**	**Incubation time/ temperature**
Rabbit biotinilated	Vector Laboratories	1:200	30min/RT
Mouse biotinilated		1:200	30min/RT
Isotype controls			
Name	**Company**	**Concentration**	**Incubation time/ temperature**
Normal Rabbit IgG	Peprotech	Corresponding to primary AB	Corresponding to primary AB
Control Mouse IgG			

4.1.12 Real time quantitative PCR

Ready-to-use kits and solutions	
Name	**Company, Country**
Quantitect Reverse Transcription Kit	Qiagen GmbH, Germany
TaqMan® PreAmp Master Mix (2x)	Applied Biosystems, USA
TaqMan® Gene Expression Master Mix	Applied Biosystems, USA
High Pure FFPE RNA Micro Kit	Roche Diagnostics GmbH, Germany

Primer assays			
Gene Name	**Full Name**	**Assay Code**	**Company**
COL1A1	collagen, type I, alpha 1	Hs 00164004_m1	Applied Biosystems, USA
TP53	tumor protein p53	Hs 00996818_m1	
PHEX	phosphate regulating endopeptidase homolog, X-linked	Hs 01011692_m1	
MEPE	matrix extracellular phosphoglycoprotein	Hs 00220237_m1	
PDPN	podoplanin	Hs 00366766_m1	
ALPL	alkaline phosphatase, liver/bone/kidney	Hs 01029144_m1	
RUNX2	runt-related transcription factor 2	Hs 00231692_m1	
SP7	Sp7 transcription factor (osterix)	Hs 01866874_s1	
GAPDH	glyceraldehyde-3-phosphate dehydrogenase	4352934E	

4.2 Methods

4.2.1 Isolation of primary human osteoblasts

The human osteoblasts were isolated from donors that underwent endoprosthetic reconstructive surgeries in the Orthopedics Clinic of Klinikum rechts der Isar, Munich, Germany. For simplification, in this work the term osteoblasts will be used, although the cells belong to a pre-stage of mature osteoblasts. The femoral heads removed during surgery were transported under sterile conditions to the laboratory, where the cell isolation was performed using the primary explant culture method (Jonsson, Frost et al. 1999). The tissue was cut in small pieces and placed in 175 cm² cell culture flasks containing Alpha Medium supplemented with 10% FBS, 1% glutamine, 1% Pen-Strep and 2% HEPES. These were then kept in a cell culture incubator at a constant temperature of 37°C and 5% CO_2 atmosphere. First medium change was done after 3 days, when medium was substituted with osteoblast growth medium. Thereafter, culture medium was changed every 3 days. Within two weeks cells were growing out of the bone pieces. After reaching confluence, they were transferred to other cell culture flasks for further culture and expansion.

4.2.2 Cell culture
4.2.2.1 Cultivation of C2C12 cells and primary human osteoblasts

The C2C12 cells and the primary human osteoblasts were cultured in cell culture flasks and well-plates incubated at a temperature of 37°C and in an atmosphere with 5% CO_2 and 100% humidity, in standard cell culture incubators. The compositions of culture media specific for each cell type are presented in Section 4.1.6. All cell culture procedures were carried out under a sterile laminar flow hood. The culture medium was changed once every 3-4 days, by discarding the old medium and replacing the same volume of new medium under sterile conditions. Shortly before use, the cell culture medium specific for osteoblast cell culture was supplemented with dexamethasone and L-ascorbic acid-2-phosphate. Cells were cultured until they reached 80% confluence and then they were either used for experiments or subcultured.

4.2.2.2 Subculturing the cell population

The subculturing procedure was performed by removal of the culture medium using sterile pipettes, followed by rinsing with sterile 1x D-PBS, and incubation 5-10 minutes with Trypsin/EDTA. Cell culture flasks were carefully shaken to detach the cells and culture medium was added to inactivate the Trypsin. Afterwards, the cell suspension was transferred to sterile plastic 50 ml conical tubes and centrifuged at 250 g, 22°C, for 10 minutes. Thereafter, the supernatant was removed from the tubes and the pellet of cells was resuspended in fresh medium. This cell suspension was passed through a 40 µm cell strainer and counted. The appropriate number of cells was placed into new cell culture flasks.

4.2.2.3 Cell counting

Counting of the cells was done using the Neubauer improved hemocytometer, pictured in Figure 8A. It consists of a thick rectangular glass slide with an H-shaped central area that is subdivided into two square counting areas. Each counting area is divided into nine 1 mm² squares, and of these, the four corner ones are further divided into sixteen smaller squares (Figure 8B). A cover glass is placed at 0.1 mm over the counting areas (Figure 8C).
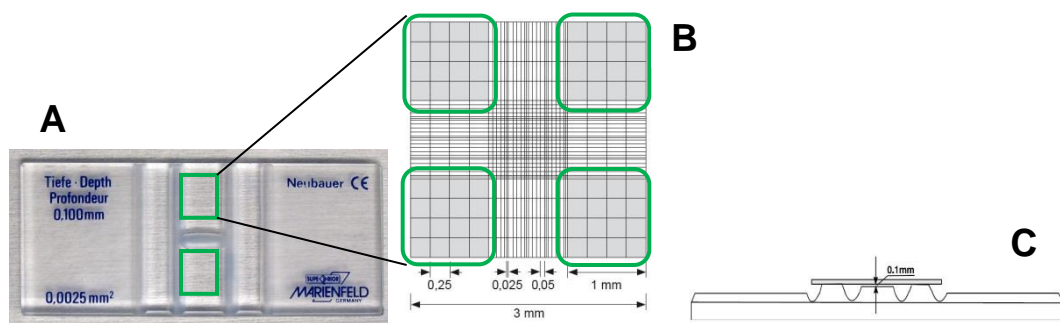
Figure 8. Neubauer improved hemocytometer. (A) Photograph of the haemocytometer. The two counting chambers are outlined with green color. (B) Diagram of counting chamber with gridlines. The cell suspension is pipetted into the counting chamber and cells from the 4 counting regions (green outline) are counted. Side view of Neubauer improved hemocytometer with cover glass (C).

After being enzymatically detached from the culture flasks with trypsin-EDTA, the vital cells were counted. For the counting procedure, a mixture of 20 µl

Trypan Blue and 20 µl cell suspension was prepared in 500 µl Eppendorf reaction tubes. After 5 minutes of incubation, 10 µl of this mixture was pipetted into the counting chambers of the hemocytometer and the cells visible in the corner 1 mm² squares were counted in both counting areas. The number of vital cells in 1 ml suspension was calculated with the following formula:

$$Number\ of\ vital\ cells\ /\ ml = \frac{Counted\ cells}{8} \times 10^4 \times Dilution\ factor$$

The population doubling time (DT) was calculated with the formula

$$DT = \frac{(t - t_0) \times \ln 2}{\ln(N - N_0)}$$

where t and t_0 are the times at which the cells were counted, and N and N_0 are the cell numbers at times t and t_0, respectively.

4.2.2.4 Induction of matrix mineralization

One of the characteristics of the human osteoblasts *in vitro* is that they are able to mineralize the extracellular matrix they produce. The induction of matrix mineralization was performed on cells in 6-well cell culture plates.

When cells grown in cell culture flasks reached 80% confluence, they were detached from the culture flasks with Trypsin/EDTA, counted, centrifuged in 50 ml conical tubes, and resuspended in fresh Osteoblast growth culture medium. The cells were then plated in three 6-well cell culture plates, at a density of approximately 5000 cells/cm² and cultured in osteoblast growth medium until they reached 80% confluence. At this point, the medium was replaced as follows: in 3 wells of each well plate the medium was replaced with osteoblast growth culture medium and used as control; in the remaining 3 wells of each plate the medium was changed to osteogenic differentiation culture medium. The medium was changed for all wells every 3 days. The cells were cultured for 7, 14 or 21 days. After the plates were removed from culture, the cells were prepared for the investigation of the mineralized deposits or alkaline phosphatase.

4.2.2.5 Assessing the time of cell attachment to growth substrate

The time necessary for cells to attach to the substrate *in vitro* was assessed prior to seeding the cells into the scaffolds. This was accomplished by performing time lapse microscopy of cells cultured in Petri dishes.

Human osteoblast-like cells in passage 3 were subcultured and placed in 3.5 cm diameter Petri dishes. For microscopy, immediately after subculture the Petri dishes were placed inside a Zeiss PM S1 incubation chamber set at 37°C and 5% CO_2 concentration. Phase contrast micrographs were taken each minute for 4.5 hours, with the Zeiss MRc digital camera and Axiovision 4.8.2 software.

4.2.3 Kidney harvesting

The kidneys were harvested from male and female Lewis rats, weighing between 350 g and 450 g. The animals were housed and cared for according to the institutional guidelines on the care and use of the experimental animals. Briefly, the rats were anesthetized and euthanized. The abdominal area of the animal was disinfected with 70% ethanol and the abdominal cavity was opened with a longitudinal incision. The kidneys were exposed and removed through blunt excision. The organs were then placed in 50 ml conical tubes filled with PBS and placed on ice for a period of 1 to 3 hours. The harvested kidneys were stored at -80°C for at least 7 days, until further use.

4.2.4 Decellularization
4.2.4.1 Perfusion system

The perfusion system consisted of the pump and the tubing. The pump used was an Arthrex arthroscopy pump model Continuous Wave III AR-6475. The tubes used for the pump consisted of two connectable parts. After assembly, one end of the tube was inserted into the reservoir of liquid, represented by glass bottles of 1000 ml. The other end of the tube was connected to a three-way-stopcock that was in turn connected to a perfusion extension line. The catheter that was attached to the kidney was connected by the extension line to the rest of the perfusion system.

4.2.4.2 Kidney preparation and decellularization

After carefully removing the connective and adipose tissue from the kidney without damaging the parenchyma, a 20G venous catheter was introduced into the renal artery and fixed by suture with 5-0 surgical wire. The catheter was connected through a Luer-Lock connector to the perfusion system, respectively to the perfusion extension line. Perfusion of the organ was made with a pressure of 100 mmHg at room temperature. A series of solutions was then circulated through the system. The solution succession and duration of the perfusion is described in Table 2.

Table 2. Decellularization protocol.

Step no.	Solution	Duration (minutes)
1.	Distilled water	10
2.	SDS	30
3.	Distilled water	10
4.	SDS	30
5.	Distilled water	60
6.	Distilled water with 5% Pen-Strep	60*

*- step was performed under sterile laminar flow hood; sterile solution

The concentration of the SDS solutions was chosen based on available literature and it ranged between 0.25% and 1% SDS in distilled water.

At the end of the decellularization protocol, the kidney scaffolds were stored until recellularization in sterile distilled water with 5% Pen-Strep in 50 ml conical tubes at 4°C for up to 2 days.

4.2.4.3 Confirmation of SDS removal from kidney scaffold

To verify the removal of SDS from the scaffolds prior to seeding with human osteoblast-like cells, the measurement of the SDS in the washing solutions was performed. A 5-step washing protocol was established, whereby after decellularization, the kidney scaffold was washed 5 times with distilled water, 1

hour each wash. Samples were taken at the end of each hour of washing and they were used for the SDS detection.

The SDS measurement protocol was adapted after a study by Rusconi (Rusconi, Valton et al. 2001), who describes the quantitation based on the use of the dye stains-all. The color of stains-all changes from intense fuchsia to yellow upon addition of SDS. Furthermore, this color change is gradual and proportional to the amount of SDS added to the stains-all solution, thus allowing its use to reliably quantitate SDS in biochemical samples by means of a visible light spectrophotometer.

A stock solution of stains-all was prepared by mixing 1 mg of stains-all in 1 ml isopropanol/water (1/1, v/v). This solution was stored in the dark at 4°C. A stains-all working solution for immediate use was prepared from 1 ml stock solution, 1 ml formamide, and 18 ml distilled water (final concentration of stains-all 90 mM).

A volume of 10 µl from each of the 5 washing samples was pipetted in a 96-well plate, each sample in 5 replicates. Additionally, a row of standard solutions consisting of known concentrations of SDS was pipetted in 3 replicates. Thereafter, 150 µl of the stains-all working solution was pipetted in each well and thoroughly mixed. The samples were measured at a wavelength of 450 nm with a spectrophotometer. The concentration of SDS was determined according to a standard curve. The limit of detection (LOD) of the assay was calculated according to the formula (McNaught, Wilkinson et al. 1997):

$$LOD = y + 3 * s$$

The y value represents the mean value of the blank measure, and s value is the standard deviation of the blank measure.

4.2.4.4 Arterial tree visualization

The decellularization procedure yields a transparent acellular organ. In order to verify the patency of the arterial system after decellularization, a colored substance was employed, that when injected via the renal artery would be visible

through the scaffold. To obtain this substance, firstly porcine gelatin was mixed with distilled water at 60°C to produce a gelatin solution of 0.5% concentration. When cooled this solution becomes more viscous, and the precision of the infusion increases. Before cooling, 20 ml gelatin solution was colored red with 10 µg Allura Red AC dye. At a temperature of 30°C the viscosity was considered suitable and the solution was carefully injected through the attached catheter into the renal artery, until the arterial branches were visualized in a red color through the translucent scaffold.

4.2.5   Recellularization of the kidney scaffolds

Approximately 10×10^6 cells were used for the recellularization protocol. Cells from four 175 cm² culture flasks were trypsinized, centrifuged, resuspended in 10 ml warm culture medium, passed through a 40 µm cell strainer, and counted using a haemocytometer. The kidney scaffold was perfused for 60 minutes with warm osteoblast growth culture medium before the infusion of cells took place, in order to equilibrate the pH inside the scaffold and provide the necessary nutrients for a successful cellular attachment. The equilibrated kidney attached to the catheter was placed to a sterile 50 ml conical tube in order to minimize the number of cells introduced into the culture vessel during seeding. The cell suspension was aspirated into a 20 ml single-use syringe and infused into the kidney using the arterial catheter via a three-way stop cock, in two steps, 10 min apart, ca. 5 ml of cell suspension each step. The kidney was then replaced in the culture vessel of the perfusion system and placed in a cell culture incubator, at 37°C in 5% CO_2 atmosphere. After a period of 4 hours to allow the cells to attach to the kidney scaffold, the pump was started and set to a pressure of 50 mmHg. After 24 h the pressure was set to 100 mmHg and the perfusion was maintained for a period of 1 day or 14 days for C2C12 cells and 1 day, 5 days or 14 days for osteoblasts. The culture medium was changed twice a week. At the end of the culture period, the scaffolds were removed from the culture vessels and cut at the level of the hilum in two halves by a transversal section with a scalpel. One half was transferred to a sterile 15 ml conical tube and immediately placed at -80°C for storage. The other half was placed in plastic tissue cassettes, fixed in 4% paraformaldehyde for 24 hours, and processed further for histological procedures.

4.2.6 Metabolic activity assay of cells cultured in kidney scaffolds

A resazurin stock solution 800 mM was prepared from resazurin sodium salt and DPBS. This solution was then sterile filtered through a 22 nm filter and stored frozen in 50 ml conical tubes at -20°C. To assess the metabolic activity of the seeded cells in dynamic 3D culture, a working solution of resazurin was prepared by adding 25 ml of the stock solution of resazurin to 250 ml culture medium, followed by thorough mixing; the mixture of resazurin and medium was recirculated through the reseeded kidney scaffold at 37°C and 5% CO_2 atmosphere. After a period of 24h, the resazurin solution was replaced by fresh culture medium and a sample of resazurin solution was pipetted into a 96-well plate, 100 µL/well, and analyzed with a spectrophotometer at wavelengths of 595 nm and 560 nm.

4.2.7 Histology
4.2.7.1 Paraffin embedding

Tissue samples were placed in tissue cassettes and fixed for 24 hours in 4% paraformaldehyde. The cassettes were then processed for dehydration with an automatic tissue processor. The program of this device is described in Table 3.

Table 3. Dehydration protocol

Step no.	Step	Duration (minutes)
1.	70% Ethanol	60
2.	70% Ethanol	60
3.	80% Ethanol	60
4.	80% Ethanol	60
5.	96% Ethanol	60
6.	96% Ethanol	60
7.	99,8% Ethanol	60
8.	99,8% Ethanol	60
9.	99,8% Ethanol/Xylol (1/1 v/v)	60
10.	Xylol	60

After the program was completed the samples were manually embedded into paraffin blocks. This step was accomplished by placing the sample into clean metal molds which were then filled with paraffin and kept in place until the paraffin

hardened. The blocks were then stored at room temperature until they were sectioned.

4.2.7.2 Paraffin-embedded tissue sections

Tissue sections at a thickness of 3 µm were cut with a rotary microtome. After they were cut, the sections were transferred to a water bath at a temperature of 40°C, and then mounted on glass microscope slides. The slides were dried overnight at 50°C to remove any water remaining under the section. After drying, sections were stored until utilized.

4.2.7.3 Deparaffinization

Paraffin was removed and the tissue sections rehydrated before they were stained. The deparaffinization step consisted in rinsing the tissue slides in a series of solutions that is described in Table 4.

Table 4. Deparaffininzation protocol.

Step no.	Step	Time (minutes)
1.	Xylol	10
2.	Xylol	10
3.	Ethanol 99.8%	5
4.	Ethanol 99.8%	5
5.	Ethanol 96%	5
6.	Ethanol 96%	5
7.	Ethanol 70%	5
8.	Ethanol 70%	5
9.	Distilled water	5
10.	PBS	5

4.2.7.4 Frozen sections

The preparation of frozen tissue sections, or cryosections, is a histological procedure used for quickly obtaining of tissue sections for microscopic analysis. It can also be very useful when sensitive targets could be destroyed by paraffin embedding. In the present work, cryosections were used to analyze the presence of the enzyme alkaline phosphatase, which would be inactivated during processing for paraffin embedding, in the acellular kidney scaffolds seeded with

osteoblasts. This enzyme is present in osteoblasts and plays a key role in the mineralization of the bone extracellular matrix.

Tissue samples intended for frozen sectioning were stored at -80°C. Before sectioning, the samples were moved to a container with liquid nitrogen to avoid degradation and keep the tissues in a frozen state. Each sample was mounted onto the specimen disk with OCT-compound, placed inside the cryostat and cut. The temperature of the cryostat was set at -20°C, the specimen holder at -20°C and knife holder at -23°C. Sections were made at 7 µm thickness and were collected on glass slides. They were then allowed to dry at room temperature overnight and stored at -20°C until needed.

4.2.7.5 Histochemistry
4.2.7.5.1 Hematoxylin and eosin staining

The hematoxylin and eosin staining (H&E staining) is the most used staining in histopathology and histochemistry laboratories.

The hematoxylin stain can be used as a primary stain or as a counterstaining in combination with other histological or immunohistochemical procedures. The hematoxylin binds to basophilic structures: the elements from a cell's nucleus, such as chromatin, chromosomes, nucleoli, centrioles and nuclear membrane, but also to mitochondria, element of the cytoplasm. There are three most used types of hematoxylin, depending on the formulation of the dye. The alum hematoxylins are the widest used (Mayer's, Gill's), they contain aluminum salts and are good nuclear stains giving the color blue when submerging in alkaline solutions. Iron hematoxylin (Weigert's, Heidenhein's) contains iron salts and gives the color black or gray. The tungsten hematoxylin (Mallory's) contains a salt of the phosphotungtic acid and is used for staining muscle striations.

The eosin is a xanthene dye available in multiple forms: eosin Y (yellow), B (blue) or S (ethyl eosin, alcohol soluble). The eosin Y is a tetrabromo derivate of fluorescein and is the widest used in histology. It is an acidic dye and binds to basic structures of tissues or cells such as protein compounds (cell cytoplasm,

extracellular matrix). Eosin stains these in shades of red or pink with a good contrast to the basophylic structures stained by the hematoxylin.

As a first step in the H&E staining, the FFPE tissue sections were deparaffinized and rinsed in distilled water. Afterwards, the slides were immersed in a solution of Mayer's hematoxylin for 5 minutes. Then, they were rinsed for 15 minutes in running tap water for bluing the hematoxylin. The slides were then immersed for 1 minute in eosin Y solution (0.5% in water), after which they were shortly rinsed in distilled water to remove the excess dye. Then the slides were dehydrated by successive immersion in 70%, 96% and 100% ethanol solutions, cleared in xylol, mounted in Eukitt mounting medium and covered.

4.2.7.6 Fluorescent staining of DNA in scaffolds

SYBR Green I is a synthetic dye from the cyanine family. It has a very high affinity for double stranded DNA (dsDNA), although it can also bind to single stranded DNA or RNA but to a much lesser extent than dsDNA. This is why it is used frequently in molecular biology for the detection of dsDNA in samples. When bound to nucleic acids and stimulated with light at a wavelength of 497 nm, the SYBR Green I dye emits light at a wavelength of 520 nm.

For the imagistic detection of dsDNA in the native and decellularized tissue samples with SYBR Green I dye, FFPE tissue sections were first deparaffinized, rinsed in distilled water and TBS buffer. The samples were then incubated for 30 minutes at room temperature in the dark with a 1:10000 SYBR-Green I solution in TBS buffer. After being rinsed two times in TBS buffer to remove unbound dye, the slides were mounted in fluorescence mounting medium. Thereafter the samples were imaged.

4.2.7.6.1 Sirius Red staining

Sirius red is a red acidic azo dye frequently used to visualize collagen I and III fibers in tissue sections. When examined under bright field microscopy, the stained collagen fibers appear bright red on a pale yellow background. The dye

binds to the basic groups of the collagen molecule through its acid sulphonic groups and permits very sensitive detection of collagen in tissue sections.

Before performing the staining, the paraffin-embedded tissue slides were deparaffinized and rinsed in distilled water. They were then incubated for 10 minutes in a solution of Weigert's hematoxylin to stain the cell nuclei and washed for 10 minutes in running tap water. Sirius Red working staining solution was prepared by adding 0.5 g of Sirius red F3B powder to 500ml saturated solution of picric acid. The tissue slides were incubated in the Sirius red working solution for 60 minutes. Afterwards, the slides were rinsed twice for 5 minutes with 0.5% (v/v) acetic acid glacial in tap water. The staining procedure was concluded after dehydration in ethanol of increased concentrations (70%, 96% and 100%), clearing in xylol, mounting in Eukitt mounting medium and covered.

4.2.7.6.2 Alizarin Red S staining

The alizarin red staining is extensively used in the identification of deposits containing calcium phosphate, calcium carbonate or calcium oxalate. Alizarin red stains calcium phosphate, the component of bone in the form of hydroxyapatite, at pH 4.2.

Alizarin Red S staining solution was prepared and the pH was adjusted to 4.2 with NaOH solution. Tissue sections were deparaffinized and rinsed in distilled water. Slides were immersed into the staining solution and incubated for 30 min. Afterwards they were rinsed in distilled water to remove the unbound dye, mounted in Kaiser's Jelly mounting medium and covered.

4.2.7.6.3 Alkaline phosphatase staining

The presence of the enzyme alkaline phosphatase on tissue sections or cultured cells was verified with the NBT/BCIP assay (Nitro blue tetrazolium chloride/5-Bromo-4-chloro-3-indolyl phosphate, toluidine salt). The reaction is based on the dephosphorylation of the BCIP by the alkaline phosphatase. This reaction yields a product which is oxidized by the NBT to a dark-blue precipitating dye that is very little soluble in water or lipid. The working solution was prepared

shortly before use from ready-to-use tablets by adding one tablet of NBT/BCIP in 10 ml dH$_2$O.

After preparation, the working solution is applied on cells grown on cell culture chamber slides or on frozen tissue sections. The samples were incubated with the solution for 30 minutes at room temperature, after which they were rinsed in Tris buffer two times, mounted in aqueous mounting medium and covered.

4.2.7.7 Immunohistochemistry (IHC)

The immunohistochemical staining is a method of detecting certain markers on tissues or cells with the help of specific antibodies. IHC is based on the principle of antigen-antibody reaction. In the human body, the antibodies are generally produced by the lymphocytes and their purpose is to specifically recognize their corresponding antigen located on a foreign tissue, cell or even molecule. At the molecular level, the antigens are typically proteins or polysaccharides. The part of the antigen where the antibody attached itself is the epitope and can be made of just a few aminoacids. A large antigen can have multiple epitopes, and each one of them can be recognized by different antibodies. The recognition of antigens by the antibodies depends on the conformation of the protein. The antigens might not be detected when they are not on the surface of the protein.

Antibodies used in molecular biology are typically produced in animals. IHC can be applied on sections of formalin-fixed or frozen tissues, or on fixed cultured cells. It is a method less quantifiable than ELISA or immunoblotting, but it has the advantage of providing the location of the antigen on tissues or cells.

There are a number of basic steps when performing an IHC staining. First, the primary antibody is applied onto the sample and it will bind to the corresponding antigen. Then, the secondary antibody is applied, which is directed against the primary antibody. The secondary antibody can be conjugated with a fluorescent probe and the complex visualized via fluorescent microscopy, or can be conjugated with an enzyme that will cleave a substrate and thus produce a color at the location of the antigen-antibody complex, visualized by bright-field

microscopy. In the current work, the second method was used, namely visualization by bright-field microscopy. In this case, it is taken advantage of the very strong affinity of the protein avidin for biotin, known also as vitamin H. The secondary antibody is readily complexed with avidin, and then an enzyme complexed with biotin is added, in this case peroxydase, which binds to the avidin on the secondary antibody. In the presence of a proper substrate, the peroxydase will produce a colored precipitate at the location of the detected antigen, which can be easily visualized.

The protocol for IHC staining was performed on FFPE tissue slides. A summary of the protocol is presented in Table 5.

Table 5. Summary of IHC protocol.

Step no.	Procedure
1.	Block endogenous peroxydase
2.	Avidin block
3.	Biotin block
4.	Antigen retrieval
5.	Protein block
6.	Primary antibody application
7.	Secondary antibody application
8.	Peroxydase complex application
9.	Chromogenic peroxydase substrate
10.	Counterstain
11.	Mount and cover the slides

The tissue sections were first deparaffinized according to the protocol in Table 4 and rinsed in distilled water. Afterwards the endogenous peroxidase was blocked in a 3% solution of hydrogen peroxide in methanol (v/v) for 30 minutes, followed by two times rinsing in PBS. The next step was blocking the endogenous biotin in the tissue sections by using the Biotin-Blocking System from Dako. This system has two components, an avidin solution and a biotin solution. First, the avidin solution was applied onto the tissue sections and incubated for 10 minutes to block the biotin in the samples. After the slides were rinsed once in PBS, they were incubated for 10 minutes with the biotin solution to block the residual biotin-binding activity of the avidin molecule, followed by two times rinsing in PBS. The next step was the heat induced antigen retrieval. The tissue slides were placed in

a plastic coplin jar with sodium citrate buffer (pH 6) which was placed in a microwave oven. The microwave was set to 600W. After 5 minutes, the coplin jar was removed from the oven and refilled with buffer. The jar was placed again in the oven that was set to 500W and started for another 2 minutes. The coplin jar was removed from the oven, left to cool for 5 minutes, and the slides were rinsed two times in PBS. Thereafter the samples were incubated for 30 minutes with Protein Block solution (Dako) to inhibit the non-specific staining. Afterwards, the slides were not rinsed and the Protein Block was tapped off. They were wiped dry around the specimens, and the samples were incubated with the primary antibodies. The type of the antibodies, the working dilution and the incubation time are described in Table 6.

Table 6. Primary antibodies, their working dilutions, incubation times and controls

Primary antibody	Dilution	Incubation time (minutes)
Laminin	1:500	60
Fibronectin	1:250	60
KI-67	1:500	60
Osteocalcin	1:100	60
Vimentin	1:500	60

The slides were then rinsed two times in PBS 0.1% Brij-L23. The sections were incubated with the secondary antibody, according to Table 7.

Table 7. Secondary antibodies, their dilution, and incubation time

Secondary antibody	Dilution	Incubation time (minutes)
Biotinylated Goat Anti-Rabbit	1:200 in PBS	30
Biotinylated Horse Anti-Mouse	1:200 in PBS	30

After the incubation time and two times rinsing in PBS with Brij, the tissue sections were incubated with the Vectastain Elite ABC system for 30 minutes. The tissue slides were rinsed again two times in PBS with Brij, and the chromogen was applied. After an incubation of 7 minutes the slides were rinsed in PBS two times. Counterstaining was done with hematoxylin. The slides were mounted in Kaiser's Jelly and covered.

4.2.7.8 In-situ nick translation assay (ISNT)

Apoptosis is a type of cellular death occurring in response to physiological signals or stress. Apoptosis can be triggered by the normal turnover in organs and also during embryogenesis. Certain molecular biochemical and morphological changes are caused by apoptotic death. One of the specific events during apoptosis is the DNA damage. This can be detected by using the ISNT assay already described in literature (Gold, Schmied et al. 1993).
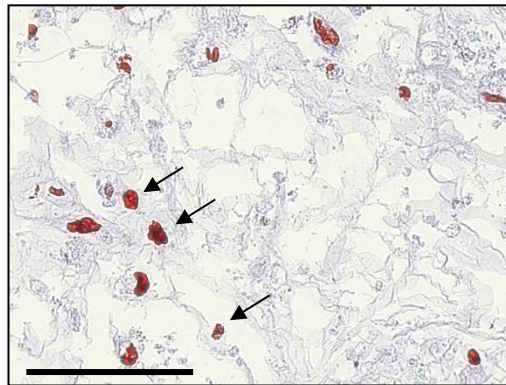
Figure 9. Appearance of nuclei from cells positive for apoptosis detected by ISNT assay used as positive control. The positive nuclei were stained red by the assay. Scale bar represents 100 μm.

One of the advantages of this method is that it reveals the location of the DNA damage by precise marking of DNA strand breaks. The protocol used to perform the assay is described in Table 8.

Table 8. *In situ* **nick-translation procedure.**

Step no.	Procedure	Duration (minutes)
1.	Deparaffinization and rehydration	
2.	Wash in distilled water	5
3.	Proteinase K 1:1000	20
4.	Wash in distilled water	5
5.	Block endogenous peroxydase	20
6.	Wash in distilled water	5
7.	Nick Buffer 1x	10
8.	Discard nick buffer without rinsing	
9.	Nick translation mix	65 at 37°C
10.	Termination buffer	15
11.	Wash in PBS	10
12.	FCS 1% in PBS	10
13.	Wash in PBS	5
14.	ABC reagent	30
15.	Wash in PBS	5
16.	AEC Chromogen	7
17.	Wash in PBS	5
18.	Hematoxylin	1
19.	Tap water	5
20.	Mount in Kaiser's Jelly and cover	

4.2.8 DNA extraction from paraffin-embedded tissue

The DNA concentration from each sample was used for the quantification of the DNA content in decellularized samples.

DNA extraction was performed from paraffin sections with the QIAamp DNA FFPE Tissue Kit. For each sample, two tissue sections, 10 μm thicknesses each, were cut with a rotary microtome. The tissue sections were placed in 1.5 ml reaction tubes. The protocol was followed as described in the manufacturer's instructions. The DNA contents of the resulting solutions was measured with a Nanodrop spectrophotometer and expressed in μg/μl.

4.2.9 Gene expression analysis at mRNA level using real time PCR
4.2.9.1 RNA extraction from paraffin embedded tissue

RNA was extracted from FFPE tissue with the High Pure FFPE RNA Micro Kit (Roche Applied Science, Germany). Two tissue slices, each of 10 μm thickness, were placed into a 1.5 ml reaction tube, deparaffinized by adding 800 μl

xylene, vortexed, and incubated at RT for 5 min. The xylene was then removed by 400 µl ethanol 98.6%, vortexed and centrifuged at 12000 rpm for 4 min at RT. The supernatant was carefully removed, 1000 µl ethanol 98.6% were added and mixed through vortexing, followed by centrifugation at 12000 rpm for 4 min at RT. The supernatant was carefully removed and extraction procedure was continued according to manufacturer's instructions. RNA was eluted in RNase-free water, quantified spectrophotometrically, and stored at -80°C until further use.

4.2.9.2 Synthesis of cDNA

RNA extracted from paraffin samples was converted in cDNA used for gene expression quantification by real time PCR. The cDNA synthesis was performed with the Quantitect Reverse Transcription Kit (Qiagen, Germany). For each reaction 1 µg RNA was used. Subsequent steps, including removal of genomic DNA (gDNA), were made according to the manufacturer instructions. At the end of the reaction the samples were diluted to a final concentration of 10 ng/µl and the preamplification of the template was done with TaqMan® PreAmp Master Mix (2x) (Applied Biosystems, USA), according to the manufacturer instructions. The primers used for preamplification are found in section 4.1.12.

4.2.9.3 TaqMan-based real time PCR

The TaqMan real time PCR method involves a fluorogenic probe that enables the detection of a specific PCR product as it accumulates during the PCR reaction (Heid, Stevens et al. 1996). TaqMan procedure specifically detects the target gene sequence and nonspecific products do not affect the accuracy of quantification, as is the case of DNA binding dyes. TaqMan assays employ a sequence-specific, fluorescent-labeled oligonucleotide probe called the TaqMan probe, in addition to the sequence-specific primers. The probe contains a fluorescent reporter at the 5' end and a quencher at the 3' end. When intact, the fluorescence of the reporter is quenched due to its proximity to the quencher. During the combined annealing/extension step of the amplification reaction, the probe hybridizes to the target and the dsDNA-specific 5'→3' exonuclease activity of nuclease (thermostable polymerases) cleaves off the reporter. As a result, the

reporter is separated from the quencher, and the resulting fluorescence signal is proportional to the amount of amplified product in the sample (Figure 10).
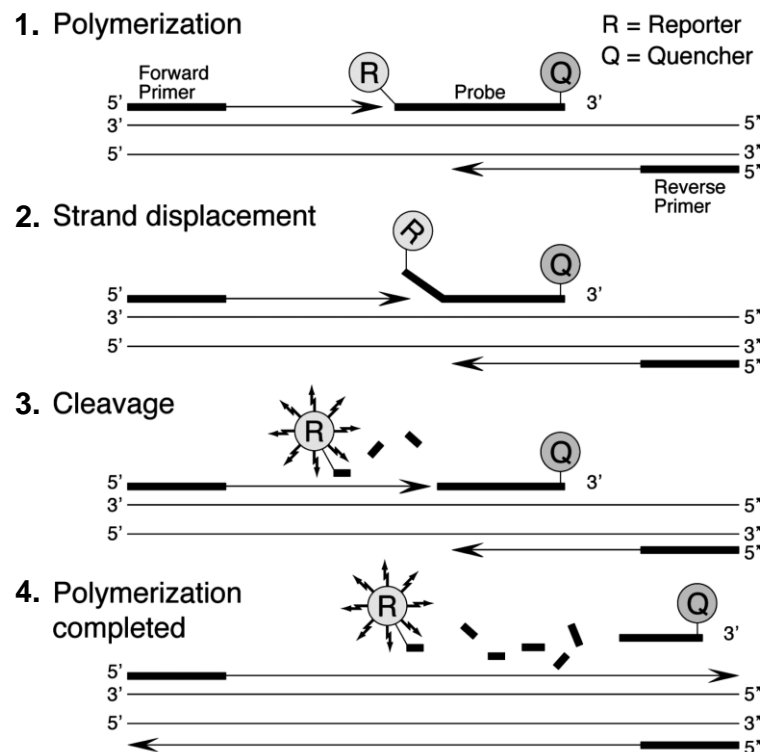
Figure 10. Overview of TaqMan®- Probe-Based Assay Chemistry. 1. A fluorescent reporter (R) and quencher (Q) are attached to the 5', respectively 3', ends of a TaqMan probe. **2.** When the probe is intact, the reporter dye emmision is quenched. **3.** During each extension cycle, the DNA polymerase cleaves the reporter dye from the probe. **4.** Once separated from the quencher, the reporter dye emits its characteristic fluorescence. Adapted from TaqMan protocol book (2002).

Transcript levels of osteogenic related genes were determined using the ready to use TaqMan® Gene Expression Master Mix (Applied Biosystems, USA). The cDNA template was equivalent to 20 ng RNA for each PCR reaction. Measurements were performed in triplicates; a non-template blank served as a negative control. Amplification curves and gene expression were normalized to the housekeeping gene *GAPDH*. Primers for the genes *COL1A1, BGLAP, TP53, PHEX, MEPE, PDPN, ALPL, RUNX2, SP7, and GAPDH* were purchased from Life Technologies GmbH (Darmstadt, Germany) as ready-to-use primer mix as shown in section 4.1.12. The PCR program was set as follows: denaturation for 2 min at 50°C followed by 10 min at 95°C, and amplification for 40 cycles. Each cycle comprised of 15 seconds at 95°C and 60 seconds at 60°C. The device used was StepOnePlus (Life Technologies GmbH, Germany).

Data analysis of the quantitative PCR (qPCR) consists in comparing the amplification curve in the exponential phase of different targets with the amplification curve of a housekeeping gene, which serves as internal control. The analysis of gene expression was done by using the previously described $2^{-\Delta\Delta CT}$ method (Schmittgen and Livak 2008) and the following formula:

$$2^{-\Delta\Delta C_T} = 2^{-(\Delta C_{T\,sample} - \Delta C_{T\,calibrator})}$$

$$\Delta C_T = mean\ C_{T\,target} - mean\ C_{T\,GAPDH}$$

Data represent fold change in gene expression normalized to an internal control gene (GAPDH), and relative to a calibrator (not seeded primary human osteoblasts).

4.2.10 Statistical evaluation

Data are presented as mean ± SEM. Statistical analysis was performed with GraphPad Prism (GraphPad Software Inc, USA). For single comparison Mann-Whitney U test was used. The significance of differences was: * for p<0.05; ** for p<0.01; *** for p<0.0001.

5 Results

5.1 Morphological characterization of C2C12 cells under light microscopy

In order to evaluate the potential of the decellularized kidney scaffold to sustain three-dimensional cell culture, the C2C12 mouse myoblastic cell line (Yaffe and Saxel 1977) was tested.

Cells were grown in C2C12 cell culture medium and were subcultured before reaching 90% confluence, in order to avoid terminal differentiation towards myotubes. The microscopic aspect of the cells in culture is shown in Figure 11.
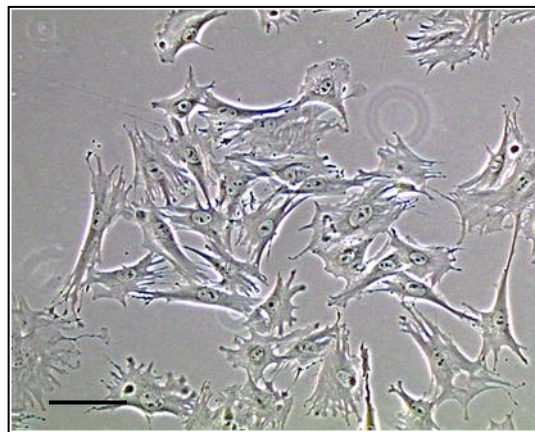
Figure 11. Phase-contrast micrograph of C2C12 cells in culture. C2C12 cells present typical myoblast morphology, thick in the middle and tapered at the end, with multiple cytoplasmatic processes. Scale bar represents 100 μm.

C2C12 cells present a fibroblastic morphology. They have spindle shape morphology, thick in the middle, a relatively large nucleus and 1-3 nucleoli.

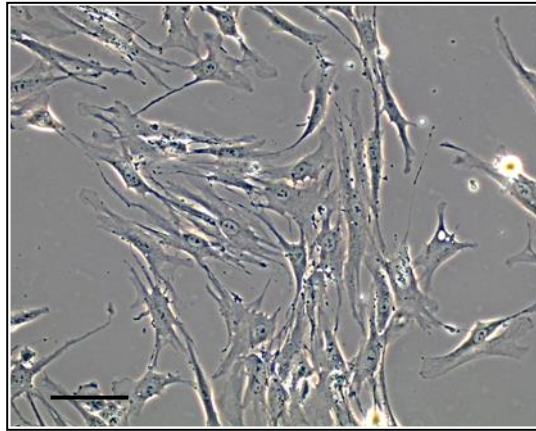## 5.2 Culture of primary human osteoblasts

5.2.1 Cell characterization

5.2.1.1 Morphology

The primary human osteoblasts were isolated from femoral heads of patients undergoing total hip replacement. Phase contrast micrographs show the morphology of this type of cells in culture (Figure 12). They are characterized morphologically by small cell bodies with few long and thin cell processes. The cell

body contains a round nucleus with large nucleolus, which is surrounded by finely scattered chromatin particles.

Figure 12. Phase-contrast micrograph of primary human osteoblasts in culture. Cells were grown in osteoblast-specific medium, and homogenously exhibited the typical "spindle" morphology throughout the cell culture period with a large spherical nucleus. Scale bar represents 100 µm.

5.2.1.2 Attachment time of the human bone cells on plastic substrate

Due to the method of seeding the cells and of scaffold perfusion, it was necessary to assess the approximate time required for the cells to attach to their substrate. Figure 13 shows an example of time-lapse microscopy carried out on human osteoblast-like cells utilized for seeding the acellular kidney scaffold. The total duration of the experiment was 4.5 hours. The micrographs below were taken at the beginning of the experiment (minute 0) and at 15 minutes, 2 hours, 4 hours and 4.5 hours thereafter.
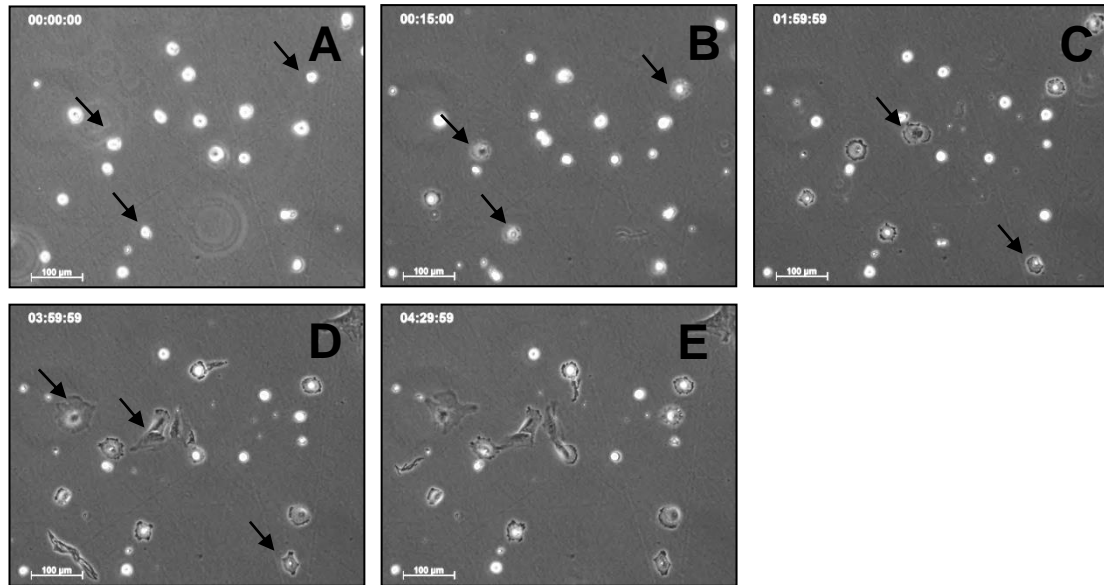
Figure 13. Example of time-lapse microscopy of human osteoblast-like cells. (A) Cell were seeded into cell culture dishes and placed under the microscope inside a special incubation chamber, without any cells being attached, where they were photographed every minute for a total of 4.5 hours during attachement. (B) The first cells started to attach after 15 minutes of incubation (arrows), but were still retaining the round shape, sign that the attachment was only superficial. (C) After 2 hours more cells were attached. (D)(E) After an incubation period of 4 hours firmly attached cells were observed. Scale bars represent 100 μm.

In Figure 13A, immediately after seeding, no attached cells were seen. After 15 minutes, the first cells started to attach, pointed by arrows in Figure 13B and C. Four hours after starting the experiment, cells were attached and spread on the surface of the culture dish. This process continued to develop in the next 30 minutes without major differences.

5.2.1.3 Cell growth

Cell growth was assessed by successively calculating the population doubling time and using an established mathematical formula. Cells from two donor patients were used for this measurement. The doubling time was calculated for cells between passage 3 and 7 in 2-dimensional culture. It was found that, in average, the primary human bone cells had a doubling time of 38.55 h in passage 3 and 63.8 h in passage 7. The graph resulted from these observations is presented in Figure 14.
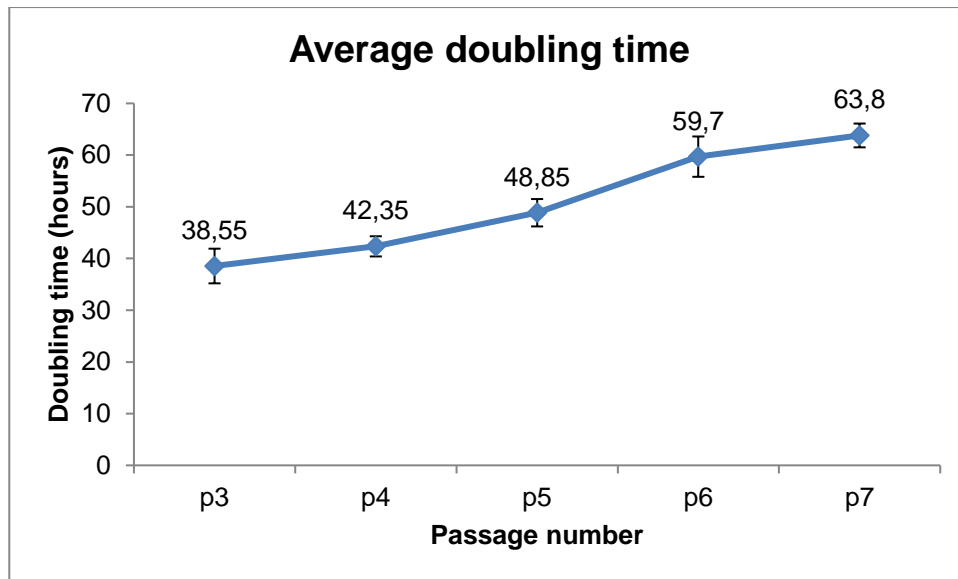
Figure 14. Population doubling time of primary human osteoblasts. The doubling time of two cell populations was calculated. The time necessary for a population doubling increased from passage 3 to passage 7 in the investigated cells.

5.2.1.4 Functional characterization

The human osteoblasts cultured *in vitro* have shown they were positive for alkaline phosphatase (Figure 15A). Furthermore, they produced a matrix containing collagen type-I detected by immunocytochemistry (ICC) (Figure 15B).
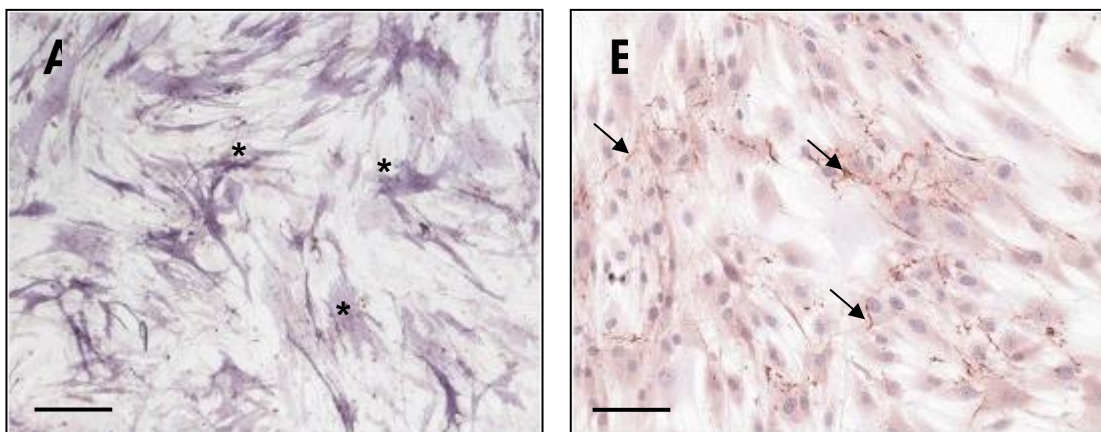
Figure 15. Human osteoblast cells exhibit typical characteristics of bone cells. (A) The cultured cells were positive for alkaline phosphatase; examples marked with asterisks (*). **(B)** The cells produced an extracellular matrix *in vitro* that contained also collagen type I (arrows) detected by ICC. Scale bars represent 100 µm.

Osteoblasts are member of the mesenchymal cell line (Caplan 1991) and a characteristic of these cells is that they contain vimentin filaments in the cytoplasm. Vimentin is one of the class III intermediate filament (IF) proteins, and is present in all mesenchymal cells (Cattoretti, Andreola et al. 1988). The presence of vimentin was investigated by ICC. Figure 16 shows human primary bone cells positive for vimentin.
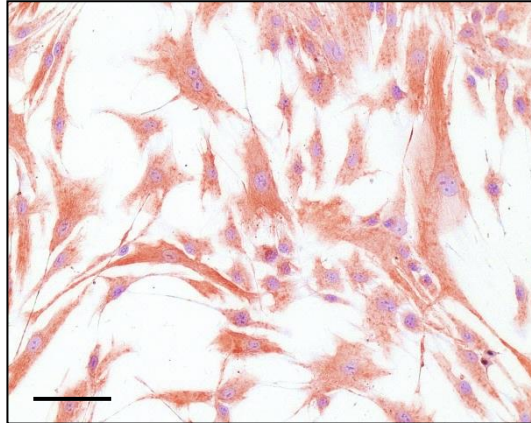
Figure 16. Vimentin immunocytochemical staining on human osteoblast cells. The presence of vimentin fibers in the cell cytoplasm is characteristic for cells originating from the mesenchymal cell lineage. The red color represents positive cells; counterstaining of nuclei with hematoxylin (blue). Scale bar 100 µm.

5.2.2 Human osteoblasts under osteogenic conditions
5.2.2.1 Matrix mineralization capacity

The primary human osteoblasts were cultured in osteogenic induction culture medium over a period of maximum 21 days, in order to verify their mineralization capacity. As control, cells were cultured also in osteoblast growth media. The mineralization was demonstrated by the Alizarin Red S staining that colors the mineral deposits red (Figure 17).

Time of culture	Macroscopic		Microscopic	
	Growth medium	Ostegenic medium	Growth medium	Ostegenic medium
7 days				
14 days				
21 days				
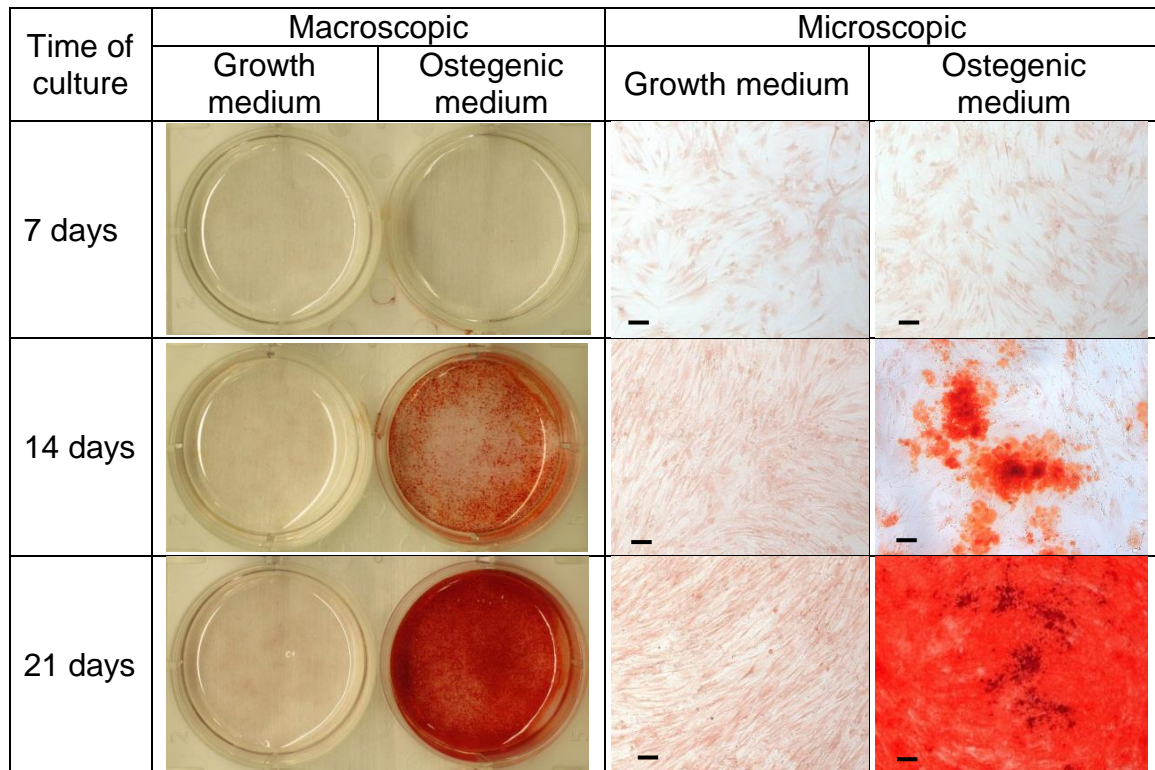
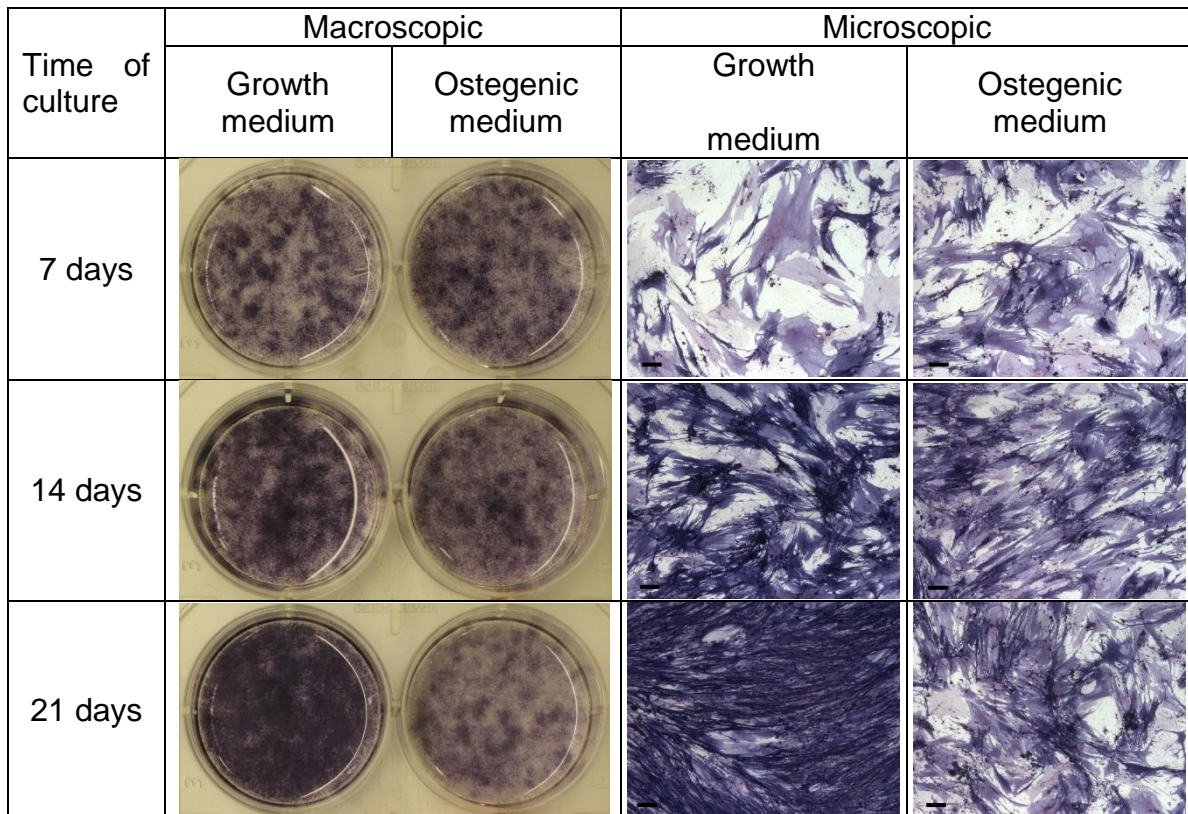**Figure 17. Assessment of mineralization capacity with Alizarin Red S staining.** Human osteoblasts were capable of inducing mineralization of the ECM *in vitro*, when cultured under osteogenic conditions. The first signs of mineralization appear after 14 days of culture, showed by distinct areas stained bright red. After 21 days almost the entire culture surface is positively stained. By contrast, cells cultured in osteoblast growth medium showed very weak staining. Red color represents the mineralized matrix stained with Alizarin Red S. Scale bars represent 100 µm.

5.2.2.2 Investigation of alkaline phosphatase

Investigation of the presence of alkaline phosphatase over the 21-day culture period showed that the intensity of the ALP staining was increasing over the time of culture in the cells cultured in the growth medium. In contrast, the cells grown in mineralization induction medium showed a decrease in intensity (Figure 18), characteristic for mature osteoblasts.

| Time of culture	Macroscopic		Microscopic	
	Growth medium	Ostegenic medium	Growth medium	Ostegenic medium
7 days				
14 days				
21 days				

Figure 18. Alkaline phosphatase staining of cells cultured in growth and respectively osteogenic differentiation medium for up to 21 days. Culture of osteoblastic cells in growth medium maintained their phenotype. Over the culture period there was an increase in their number and expression of ALP. At the same time, the cells cultured in osteogenic differentiation medium had slower proliferation and were less positive for ALP. The dark blue areas are ALP-positive. Scale bars represent 100 μm.

5.3   Confirmation of decellularization

The rat kidneys were decellularized according to the protocol presented in section 4.2.4. The decellularization was considered successful based on the macroscopic and histologic investigations, as well as the quantity of DNA measured in the acellular matrix.

### 5.3.1   Macroscopic appearance of acellular rat kidneys

At the end of the decellularization procedure, the rat kidneys had a white and translucent aspect. Moreover, the kidneys had kept their original form, and the consistency was similar to the native organ. Figure 19 presents the macroscopic aspect of the native (A) and decellularized (B) rat kidney.
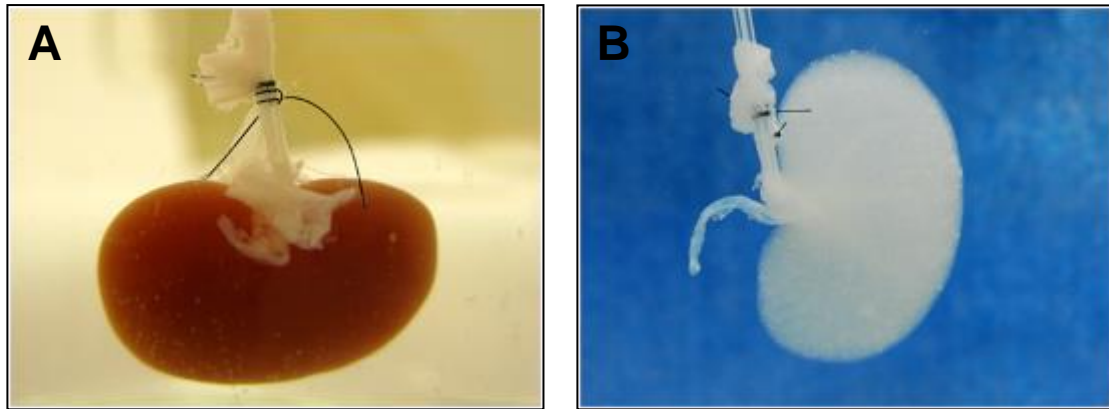
Figure 19. Macroscopic aspect of native (A) and decellularized (B) rat kidney. The acellular rat kidney maintained the shape it had in native state and became translucent due to the loss of cells.

5.3.2 Blood vessel integrity of the acellular scaffolds

The integrity of the rat kidney arterial tree was verified by injection of a gel containing Allura Red AC into the renal artery of the decellularized kidney. The transparent scaffold allowed the visualization of the red gel inside the arteries. The vascular tree of the decellularized kidney maintained its patency following the decellularization protocol (Figure 20).
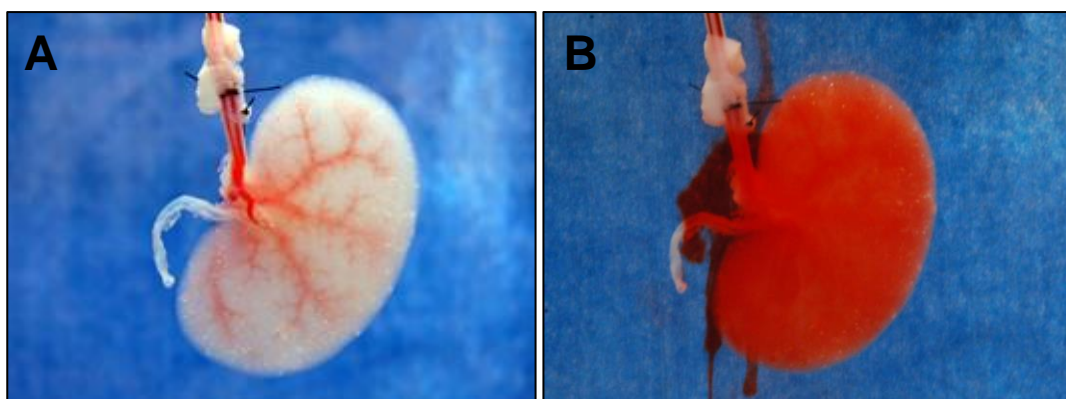
Figure 20. Decellularized rat kidney scaffold injected with an Allura Red AC-containing gel. The decellularized rat kidney was injected via the renal artery with colored semi-liquid gelatin. **(A)** Because of the kidney translucency, the arterial branches of the kidney could be distinguished colored red. **(B)** The acellular kidneys could be completely colored, indicating that the internal circulation of the kidney was still patent in the whole organ after decellularization.

5.3.3 Detergent removal from the scaffolds

The removal of SDS from the scaffold was confirmed by photometrical measurement of the contents of the detergent in subsequent washing solutions. Based on the measurement of the standards, the limit of detection (LOD) of the assay was found to be 0.005% SDS. The results of the assay have shown that all the measured samples were under LOD of the assay.

5.3.4 Histological investigation of the acellular scaffolds

The loss of cells following decellularization was confirmed by H&E staining of slices from paraformaldehyde-fixed paraffin-embedded samples of native and decellularized rat kidneys (Figure 21).
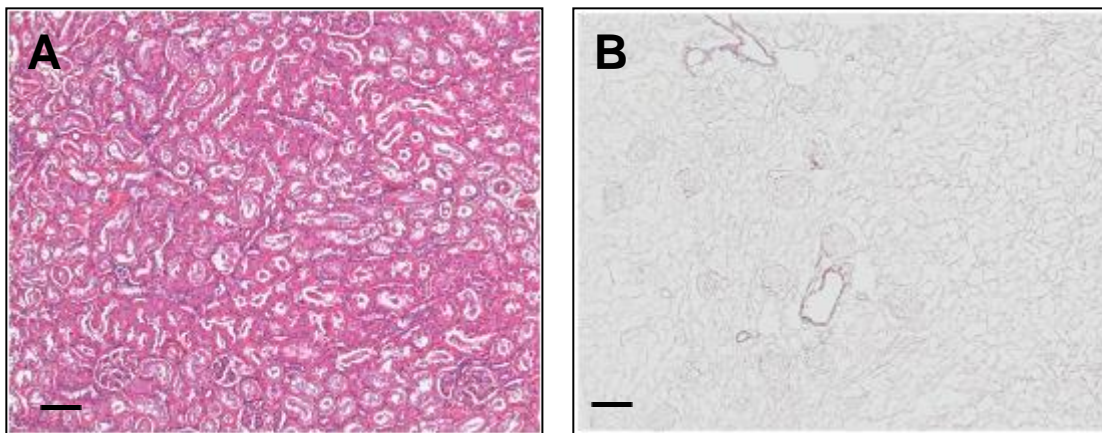
Figure 21. Hematoxylin and eosin stain of native (A) and decellularized (B) kidneys. In samples from native kidneys, the eosin stained the cytoplasm of the cells and extracellular matrix with red and the hematoxylin stained the nuclei blue. In the decellularized samples, the absence of cells was confirmed by weak eosin staining and absence of cell nuclei. Scale bars represent 100 µm.

5.3.5 Fluorescent detection of DNA in acellular scaffolds

To visually detect any remnants of DNA in the newly created scaffold, the SYBR Green I staining was used. The SYBR Green I specifically binds to double-stranded DNA (dsDNA), but also to single-stranded DNA (ssDNA) or RNA. Once bound to the nucleic acid, SYBR Green I produces a green fluorescence when stimulated with light at 450-490 nm wavelength. As seen in Figure 22, there were no visible cell nuclei in the decellularized kidney scaffold, after perfusion with 0.66% SDS for one hour.
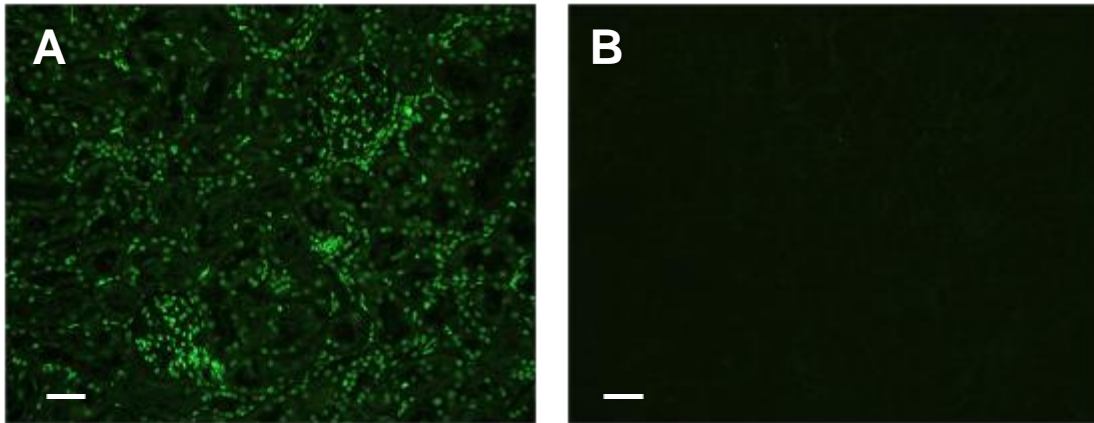
Figure 22. SYBR Green I nuclear fluorescent staining. Native (A) and decellularized (B) rat kidney. Cell nuclei are stained bright green in the native kidney tissue sample, whereas no staining can be observed in the decellularized sample. Scale bars represent 100 µm.

5.3.6 DNA contents of the acellular scaffolds

DNA was extracted from paraffin-embedded native and decellularized kidney samples, to precisely determine its quantity. The extraction of nucleic acids from FFPE tissues has been described as an alternative to extraction from fresh or lyophilized samples (Klopfleisch, Weiss et al. 2011). The results of this measurement are shown in Figure 23. Here, it can be seen that in the decellularized samples contained no detectable DNA.
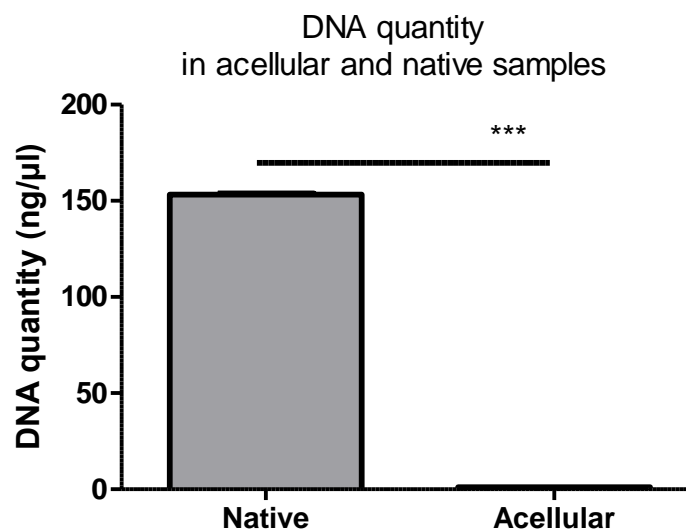
**Figure 23. DNA measurement from native and decellularized rat kidneys.** In the decellularized rat kidneys, the quantity of DNA was situated under the detection limit of the instrument of 2 ng/µl.

5.4   Investigation of the rat kidney matrix after decellularization

The extracellular matrix is generally composed of collagens, proteoglycans and noncollagenous glycoproteins. The collagens have the major role of providing the ECM with resistance and strength. They represent a proportion of more than 50% of the ECM, with collagen type I being the most frequent. Laminin and fibronectin are noncollagenous glycoproteins that play an important role in cellular adhesion and growth.

5.4.1   Collagen contents of the acellular scaffolds

Collagen type I and III can be detected in histological sections using the Sirius Red staining (Figure 24). This method was applied to verify the presence of these two types of collagen in sections of native and decellularized kidneys. The staining was positive on samples from both before and after the decellularization on the ECM of the rat kidney.
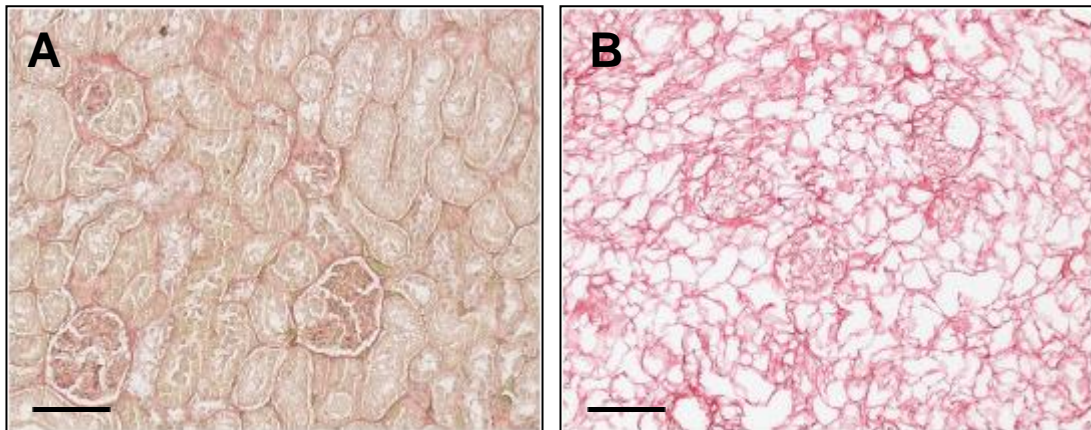
Figure 24. Sirius Red staining for collagen of native (A) and decellularized (B) kidneys. The extracellular matrix of the kidney contains various types of collagen, mostly type I and III. These appear red when stained with the Sirius Red reagent in the tissue specimens analyzed under light microscopy. The lack of cells in the decellularized kidney emphasized the large proportion of collagen by the more intense red color. The red color represents positive staining for collage I and III; counterstaining of nuclei with hematoxylin (blue). Scale bars represent 100 µm.

5.4.2   Investigation of extracellular matrix after decellularization

Laminin and fibronectin were investigated by IHC. Their presence was confirmed in the ECM of native and decellularized rat kidneys (Figure 25).
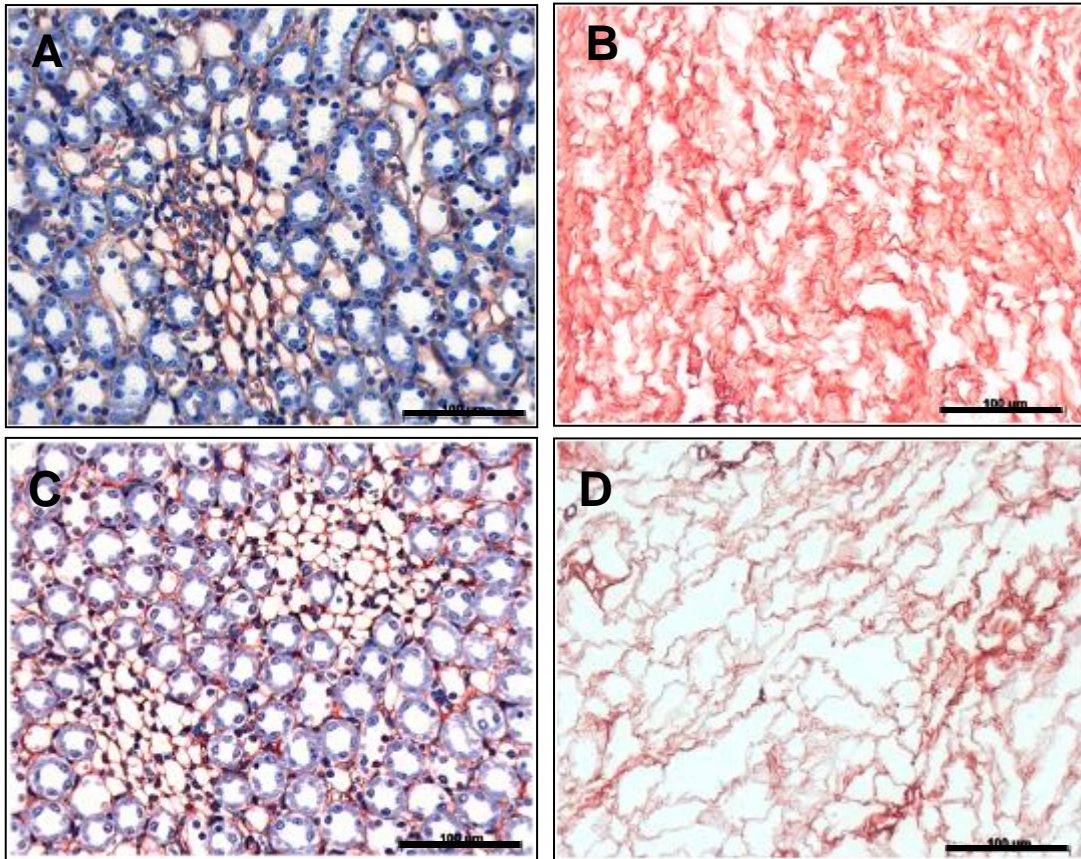
Figure 25. IHC staining of native (A, C) and decellularized (B, D) kidneys for laminin (A, B) and fibronectin (C, D). The red color represents positive staining for laminin (first row) and fibronectin (second row); counterstaining of nuclei with hematoxylin (blue). Scale bars represent 100 µm.

5.5   Seeding the decellularized rat kidney matrix with C2C12 cells

As a preliminary experiment, the acellular rat kidney scaffold was seeded with C2C12 mouse myoblasts. The C2C12 grow much faster that the human primary osteoblastic cells in culture, therefore the number of cells required for seeding was rapidly reached. Moreover, by using the C2C12, the unnecessary use of the harder-to-obtain primary human cells was avoided and the experimental setup was optimized.

The seeding of cells was carried out as described in Section 4.2.5. Briefly, the approximately ten million cells were aspirated into a sterile syringe and seeded through infusion in the arterial catheter. The seeded scaffolds were cultured for 24 hours or 14 days, two kidney scaffolds for each time period. Thereafter, histochemical and immunohistochemical procedures were performed on slices

from the paraformaldehyde-fixed paraffin embedded samples after the culture periods.

Cells were detected in the reseeded kidney scaffolds with the H&E staining both after 24 hours and 14 days of culture (Figure 26). After the first 24 hours, the C2C12 cells were mostly attached to the glomerular area. At the end of the 14 days of culture the cells had proliferated and continued to spread to more areas of the acellular scaffold.
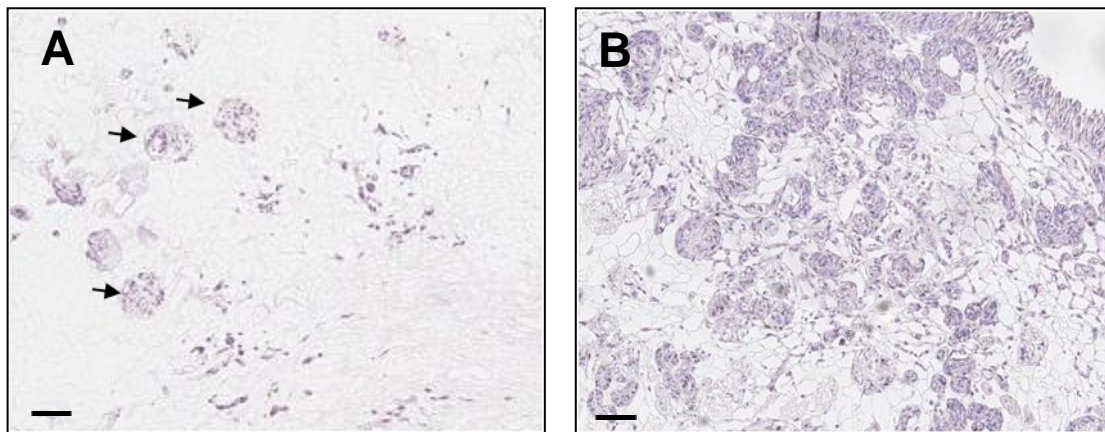
Figure 26. Decellularized kidney scaffold seeded with C2C12 cells at 24 hours (A) and 14 days (B) after seeding, stained with H&E. After 1 day of culture, the seeded cells were present only in certain regions of the scaffold, especially in the glomeruli (arrows). After 14 days, the cells have proliferated and migrated, covering a greater proportion of the scaffold. The blue color represents nuclei stained with hematoxylin (blue). Scale bars represent 100 µm.

5.6 Seeding the rat kidney matrix with human osteoblasts

After the compatibility of the scaffold with the C2C12 cells was proven, the experiments were focused on the culture of primary human osteoblasts in the three-dimensional environment. The culture time periods were set to 24 hours, 5 days and 14 days. In contrast to experiments with C2C12, an extra time point at 5 days was set in order to have a better understanding of the growth of the osteoblasts inside the scaffold. A number of five kidney scaffolds for each culture period were seeded with human osteoblasts.

5.6.1 Investigation of the metabolic activity of the seeded cells

In order to evaluate the metabolic activity of the cells across the 3D culture period, a resazurin-based assay was carried out. Resazurin assays are commercially available and are frequently used to assess cell viability *in vitro* and the cellular response to toxic stimulants (Czekanska 2011). The resazurin is reduced by the viable cells to rezosurfin. The proportion of rezosurfin/resazurin is assessed by measurement of absorbance at 570 and 600 nm wavelengths with a spectrophotometer.

For applying the resazurin-based assay to the culture in 3D conditions, certain modifications were made to it, as described in chapter 4.2.6. After perfusion with the resazurin-supplemented medium, the absorbance of the samples was measured with a photometric plate reader. The results of the assay are summarized in

Figure 27.

During day 6 of culture, the cells had a 0.72-fold decrease in metabolic activity (p=0.0358) compared with day 2. There was a 1.07-fold and 1.095-fold increase of metabolic activity on day 11 (p=0.2087), respectively day 14 (p=0.0358), compared with day 2.
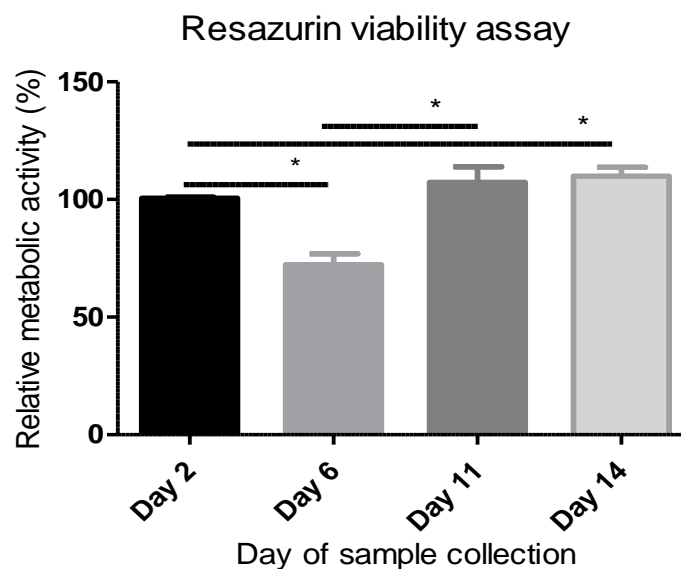
Figure 27. Resazurin viability assay of cells cultured in 3D environment at different points in time over the 2-week culture period. The graph shows the absorbance of the medium samples after 2, 6, 11 and 14

days of 3D culture, respectively, in percentage against the average value obtained at day 2 of culture, taken as the reference point. There was a decrease of cell metabolic activity after 6 days, followed by an increase after 11 and 14 days of culture of the seeded scaffolds.

5.6.2 Histological investigations

From each scaffold seeded with human osteoblasts, both paraffin embedded and frozen samples were prepared. The majority of the histological investigations were made on thin slices from FFPE samples. Only the staining for ALP was done on frozen sections.

5.6.2.1 Hematoxylin and eosin staining

The first histological procedure that showed the spreading of cells after each of the culture durations was the H&E staining. This confirmed that the human osteoblasts were able to attach to and colonize the acellular kidney scaffold after 1, 5 and 14 days of 3D culture (Figure 28).
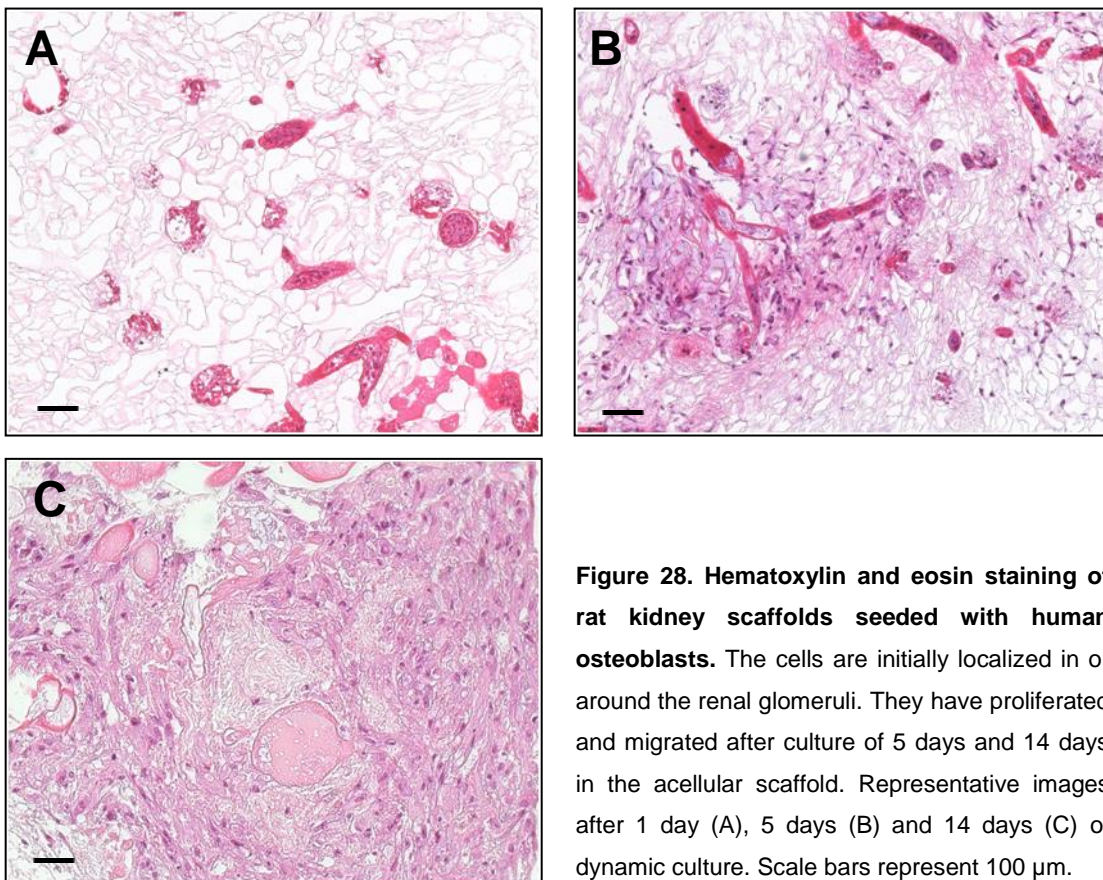
Figure 28. Hematoxylin and eosin staining of rat kidney scaffolds seeded with human osteoblasts. The cells are initially localized in or around the renal glomeruli. They have proliferated and migrated after culture of 5 days and 14 days in the acellular scaffold. Representative images after 1 day (A), 5 days (B) and 14 days (C) of dynamic culture. Scale bars represent 100 μm.

5.6.2.2 Alkaline phosphatase staining on frozen sections

The enzyme alkaline phosphatase (ALP) is contained in the matrix vesicles (MV) and released by the osteoblasts (Anderson 1995). It plays a key role in the mineralization of the extracellular matrix of bone by catalyzing the release of inorganic phosphate (P_i) from ATP and by modulating the bridging of MVs to the extracellular matrix (Narisawa, Frohlander et al. 1997).

Alkaline phosphatase was present on the human osteoblasts, which were injected into the kidney scaffolds, as already shown in Figure 15 (A). The same assay was positive also on frozen sections from the kidney scaffolds recellularized with human osteoblasts that were maintained in dynamic culture for 1, 5 and 14 days (Figure 29).
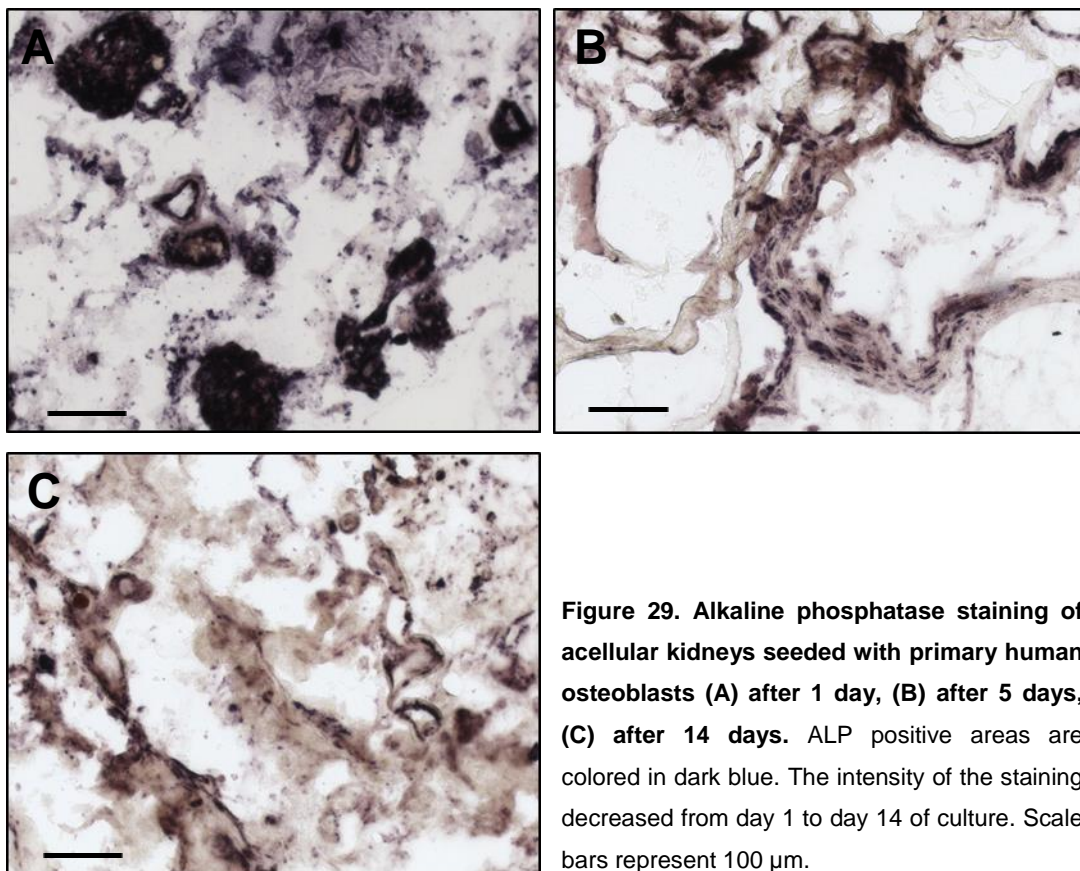
Figure 29. Alkaline phosphatase staining of acellular kidneys seeded with primary human osteoblasts (A) after 1 day, (B) after 5 days, (C) after 14 days. ALP positive areas are colored in dark blue. The intensity of the staining decreased from day 1 to day 14 of culture. Scale bars represent 100 µm.

5.6.2.3 Detection of apoptosis by "in situ nick translation"

Apoptosis or programmed cell death is a very important control mechanism of normal cell turnover (Wijsman, Jonker et al. 1993). It can be triggered by a wide range of cellular signals, both extracellular and intracellular, which are initiated as response to different types of stress - membrane damage, heat, radiation, or hypoxia (Elmore 2007).

The tested samples have shown different amounts of cells that were in the process of apoptosis, depending on the duration they have been cultured in the kidney acellular matrix (Figure 30). The apoptotic cells have typical morphology, with a round shape and condensed nucleus sometimes divided into multiple fragments.

Figure 30. Apoptosis detection assay on slices from osteoblast-seeded kidney scaffolds cultured in 3D. Kidney scaffold seeded for 24h (A), 5 days (B), and 14 days (C). Red color represents positive staining for apoptotic cells. There are more positive cells (arrows) after 1 day and 14 days of culture, but very few after 5 days. Counterstaining of nuclei was made with hematoxylin (blue color). Scale bars represent 100 µm.

5.6.2.4 Immunohistochemistry

5.6.2.4.1 Staining of proliferation marker Ki-67

Ki-67 is a protein encoded by the Mki67 gene and it is a marker of cellular proliferation (Gerdes, Lemke et al. 1984). It is present in the cell during the G1, S, G2 and M stages of cell cycle and is missing during the G0 stage. Ki-67 can be detected in tissue samples by using immunohistochemistry and is a very important tool to assess cellular proliferation potential.

Detecting the protein Ki-67 in samples seeded with C2C12 cells showed that almost all cells were in proliferative state (data not shown). Human osteoblasts present in the kidney scaffold showed a decrease in proliferation rate over the time of culture, with the most proliferating cells present in the samples cultured for 24 h and 5 days. After 14 days, almost all cells in the investigated samples were in the resting stage, negative for Ki-67 (Figure 31).

Figure 31. Ki-67 immunohistochemistry on osteoblast-seeded kidney scaffolds. The nuclear red staining shows cell nuclei positive for Ki-67 in proliferative state. Arrows show examples of positive cells. Counterstaining of nuclei was made with hematoxylin (blue color). Scale bars represent 100 µm.
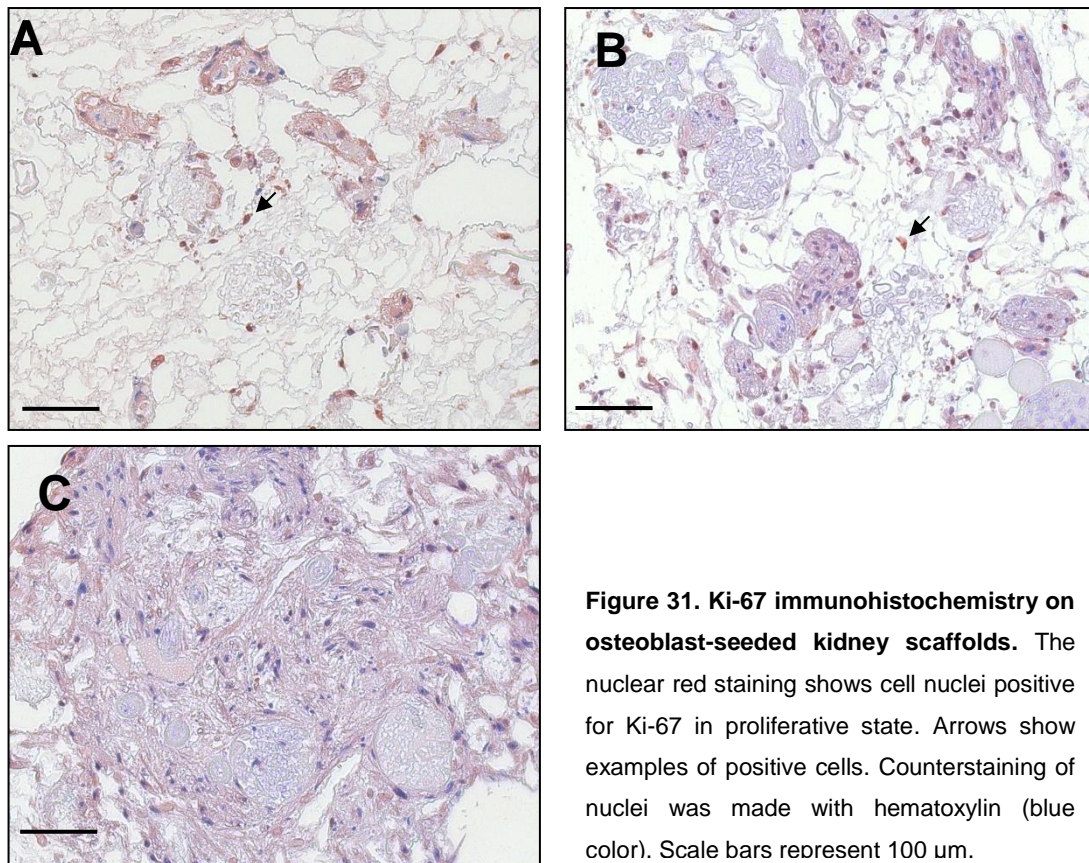
5.6.2.4.2 Staining of osteocalcin

Osteocalcin is a Ca^{2+}-binding bone and dentin specific non-collagenous protein secreted by the osteoblasts and osteocytes (Lian and Gundberg 1988; Gundberg 2003). It has three glutamic acid (Gla) residues, which can be γ-

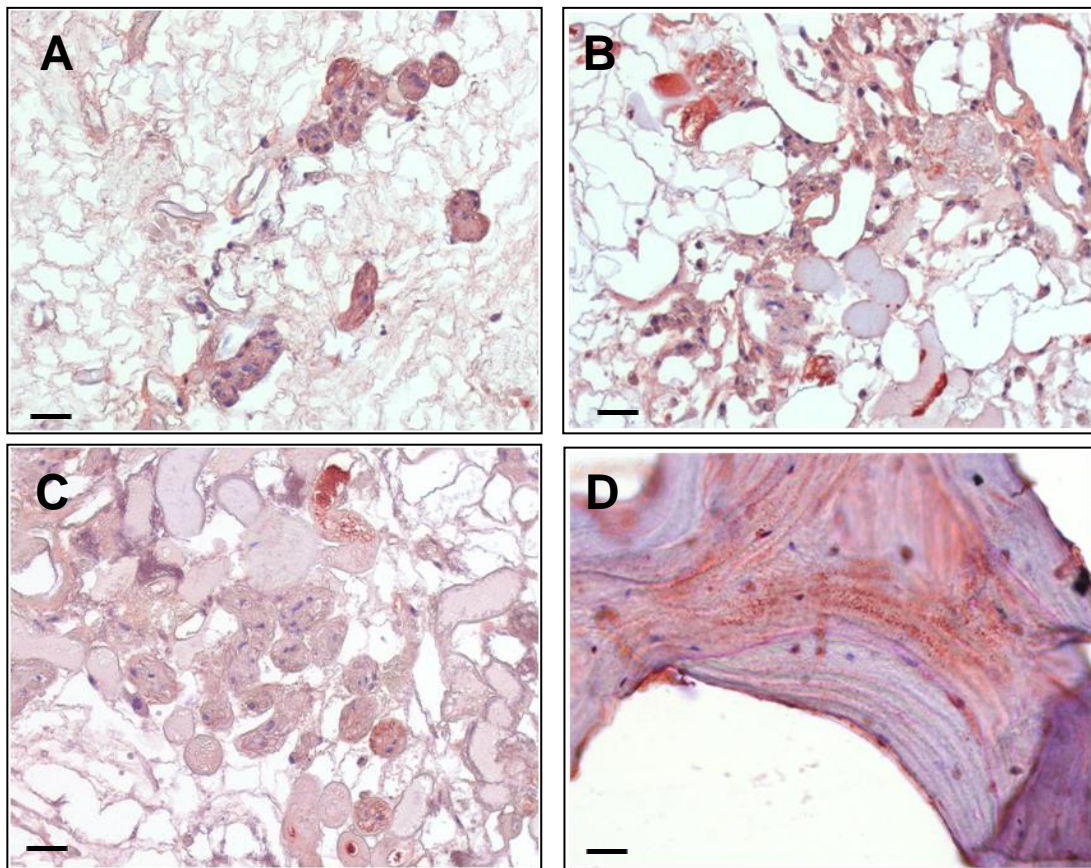carboxylated. When the Gla residues undergo carboxylation, they confer osteocalcin the capability to bind calcium phosphate or hydroxyapatite (Berkner 2008).

The presence of osteocalcin in recellularized samples was verified by immunohistochemistry and tested positive, as shown in Figure 32.

Figure 32. Osteocalcin immunohistochemical staining on decellularized rat kidney seeded with osteoblasts and cultured for 1 day (A), 5 days (B), or 14 days (C). Normal human bone (D) was used as positive control. Osteocalcin-positive areas are colored red. Counterstaining of the nuclei was made with hematoxylin (blue color). Scale bars represent 100 µm.

5.6.2.4.3 Staining of vimentin

Vimentin is a major intermediate filament family member. It is expressed in all normal cells belonging to the mesenchymal lineage. This protein is also known to maintain cellular integrity and provide resistance against stress. Vimentin staining was performed on osteoblast-seeded rat kidney matrixes cultured for 1, 5, or 14 days. The staining was positive in all samples, as shown in Figure 33.
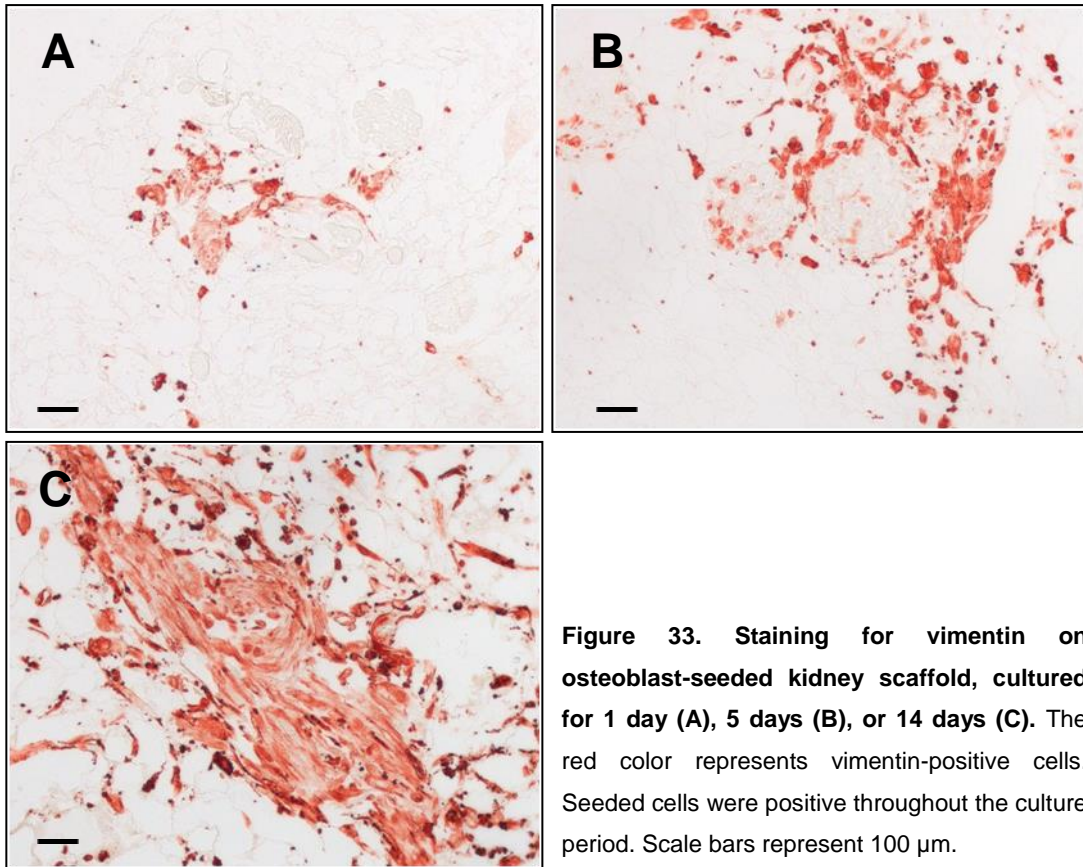
Figure 33. Staining for vimentin on osteoblast-seeded kidney scaffold, cultured for 1 day (A), 5 days (B), or 14 days (C). The red color represents vimentin-positive cells. Seeded cells were positive throughout the culture period. Scale bars represent 100 μm.

5.6.3   Gene expression quantification through real time PCR

The expression of several genes known for their connection to the populations of osteoblasts and osteocytes were investigated by real time PCR, in total RNA extracted from acellular rat kidneys seeded with human primary osteoblasts and cultivated for 1, 5, and 14 days. Of the genes specific for the osteoblast lineage, the expression of the following genes was analyzed: alkaline phosphatase *(ALPL)*, collagen type I *(COL1A1)* and the transcription factors *RUNX2* and osterix *(OSX)*. Depending on their environment, the human osteoblasts are known to terminally differentiate towards osteocytes, therefore genes specific for this cell type were also included in the investigation, namely podoplanin *(PDPN or E11)* and *PHEX*. Another gene included in the investigation was *TP53* that encodes protein p53. It responds to diverse cellular stresses to regulate target genes that induce cell cycle arrest, apoptosis, senescence, DNA repair, or changes in metabolism. The results of the PCR examination are presented in Figures 34 - 37.

5.6.3.1 Gene expression quantification of alkaline phosphatase and collagen type I

The expression of genes *ALPL* and *COL1A1* are presented in Figure 34. Compared with 1 day of culture, the expression of *ALPL* was reduced 0.031-fold on day 5 (p<0.0001) and 0.0303-fold on day 14 (p<0.0001). The expression of *COL1A1* was found to be reduced 0.0625-fold in constructs after 5 days 0.0625-fold (p<0.0001) and 0.015-fold after 14 days 0.0625-fold (p<0.0001) compared with 1 day of culture.
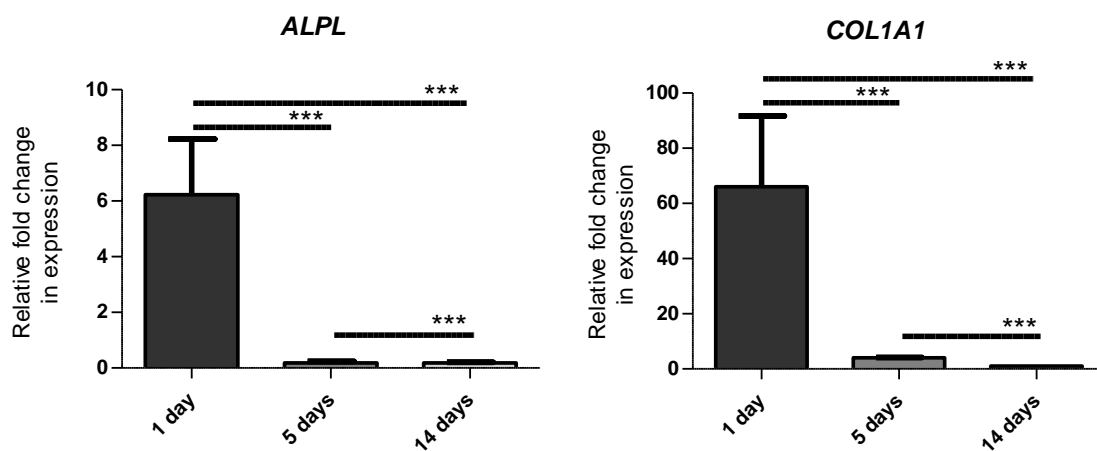
Figure 34. Real time PCR gene expression of osteoblast-specific genes alkaline phosphatase (*ALPL*) and collagen type I (*COL1A1*) (n=3).

5.6.3.2 Gene expression quantification of transcription factors osterix and RUNX2

The transcription factors *OSX* and *RUNX2* are key regulators of bone cell differentiation. The results of their gene expression investigation are presented in Figure 35. The expression of *RUNX2* decreased 0.57-fold from day 1 to day 5 (p<0.0001) and 0.71-fold to day 14 (p<0.0001) of culture in the acellular scaffold. The expression of *OSX* increased 1346.2-fold after 5 days (p<0.0001) and 1954.4-fold after 14 days (p<0.0001) of culture compared with day 1.
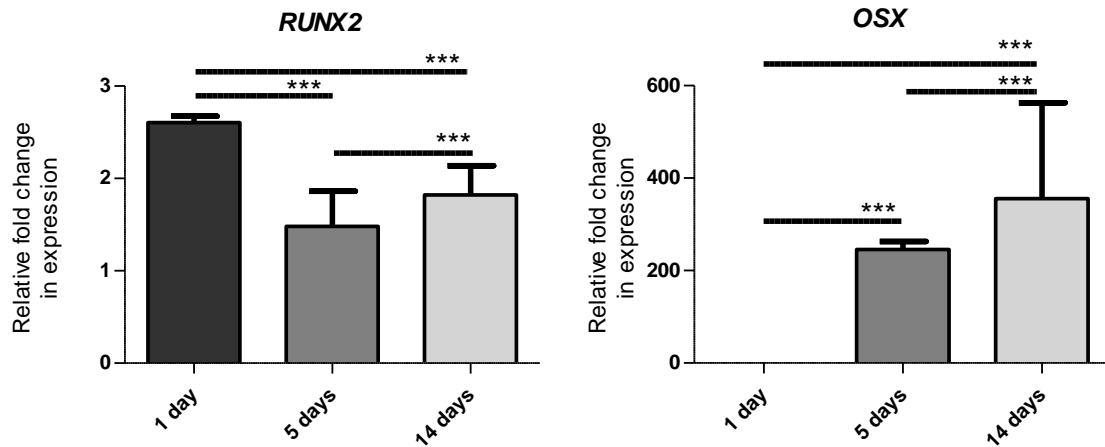
Figure 35. Quantification of *RUNX2* and *OSX* gene expressions by real time PCR (n=3).

5.6.3.3 Gene expression quantification of osteocyte markers PDPN, PHEX and MEPE

PDPN, PHEX and MEPE are among markers identified in osteocytes. PDPN appears on early osteocytes, PHEX was identified on both early and mature osteocytes, and MEPE is strongly expressed during the mineralization of bone. The PCR investigation showed that *PDPN* and *PHEX* are expressed in the analyzed samples during the whole culture period and their expression was variable (Figure 36). Compared with day 1, after 5 days *PHEX* had a 1.64-fold increased expression (p<0.0001) and after 14 days a 0.52-fold decreased expression (p=0.2000). When compared to day 1, the level of *PDPN* decreased 0.28-fold after 5 days (p<0.0001) and increased 1.26-fold after 14 days (p=0.5333). The gene expression of *MEPE* could not be detected in any sample.
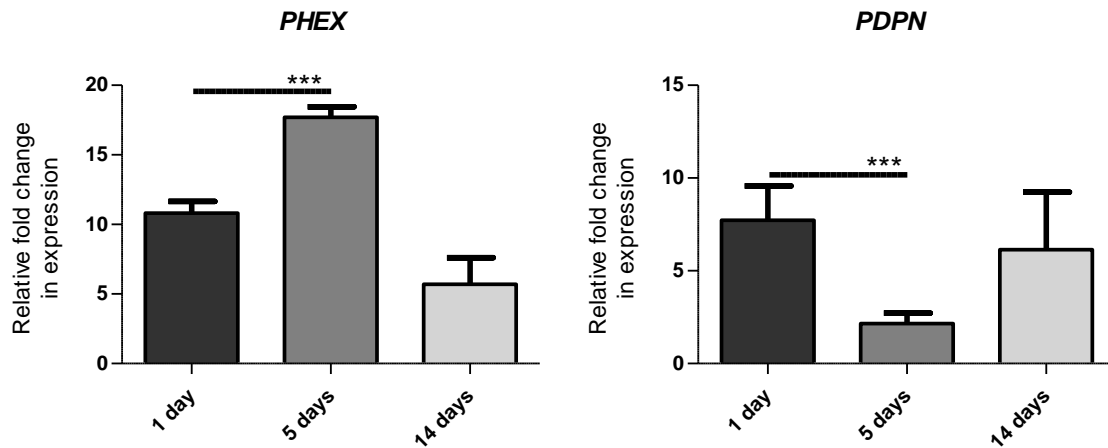
Figure 36. Quantification of osteocyte-specific genes *PHEX* and podoplanin (*PDPN*) by real time PCR (n=3).

5.6.3.4 Gene expression quantification of TP53

TP53 is the gene that encodes the protein p53, which plays roles in activation of apoptosis, but also cell senescence and differentiation. The investigation of the *TP53* expression at mRNA level by qPCR (Figure 37) revealed a 2.64-fold increased expression after 5 days compared with day 1 ($p<0.0001$). After 14 days of culture, the expression increased 1.24-fold compared with day 1 ($p<0.0001$).
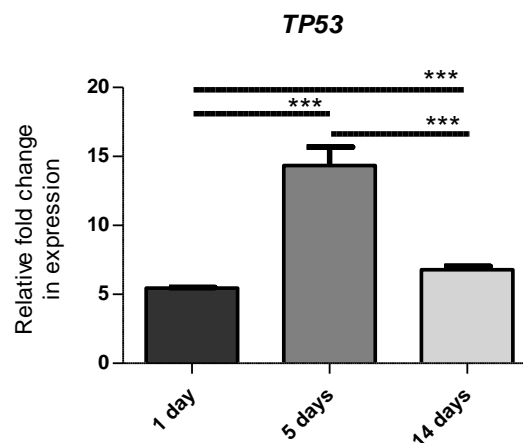
Figure 37. Real time PCR investigation of gene *TP53* in samples cultured for 1, 5 and 14 days (n=3).

6 Discussion

The field of tissue engineering has come a long way since its establishment as a separate field, almost three decades ago. Many medical breakthroughs related to this scientific domain have been made. Here, artificial tissues, as skin, cartilage, or urinary bladder were composed, to name just a few (Berthiaume, Maguire et al. 2011). These were very important steps that brought a partial, or even complete, solution to medical problems that, until then, seemed unsolvable. The healing of burned patients could be made faster and with fewer complications. For patients with end-stage bladder disease in need of cystoplasty the successful development of artificial urinary bladders could be the long awaited solution. Furthermore, cartilage tissue engineering was already successfully transferred to the clinic and helped thousands of patients to recover from traumatic cartilage damage up to now (Berthiaume, Maguire et al. 2011).

An area with high demand for solutions is bone regenerative medicine (Stylios, Wan et al. 2007). The bone is a very complex tissue that has the potential of self-repair. Under certain conditions, however, the bone's healing capacity cannot compensate for the extent of the injury and the fracture does not heal. Treatment options have been developed that aim to improve the regeneration process. Unfortunately, the success rate is still low and the treatment costs still very high (Salter, Goh et al. 2012). Up to now, the most successful technique and the current *gold standard* is autologous bone grafting, which involves harvesting of bone from areas in the body such as the iliac crest (Calori, Mazza et al. 2011). Although requiring a very invasive procedure and being highly limited by the size of the graft, there are no problems of graft rejection or immune reactions.

With help of biomaterials, it has been tried to build synthetic constructs that neither involve invasive surgery nor are dimensionally limited. These can be specifically tailored to the needs of the patient (Carson and Bostrom 2007). These constructs are usually porous and are based on biocompatible materials, such as ceramics, hydroxyapatite or synthetic fibers (Carson and Bostrom 2007). These are implanted into the patient, and can be combined with autologous cells for improved integration, this approach representing a tissue engineering application.

However, the major drawback of current tissue engineered tissues is that the thickness of the construct cannot exceed a few millimeters (Stylios, Wan et al. 2007). This limit exists because of the lack of vascularization of the artificial tissues (Berthiaume, Maguire et al. 2011). Without vascular supply, the cells inside the scaffolds can only be provided with nutrients and oxygen by diffusion through the pores in the scaffold. Diffusion can be sufficient to nourish the cells in tissues of limited thickness, as skin and cartilage. In case of tissue engineering of solid tissues creation of a vascular supply is prerequisite for cell survival. Today, one of the current challenges in tissue engineering is the establishment of vascularization of the composed constructs (Sukmana 2012).

6.1 Characterization of cells

There were two cell types used for the recellularization experiments. These were the mouse myoblastic cell line C2C12 and primary human osteoblasts. The cells were grown under normal cell culture conditions and were characterized.

The C2C12 cells had typical morphology already described in literature for this cells type (Yaffe and Saxel 1977; Blau, Pavlath et al. 1985). Additionally the proliferation rate was very high, with a population doubling time of 12 hours as mentioned in literature (Rossi, Charlton et al. 1997; Robey, Saiget et al. 2008). This feature helped achieve the necessary cell number for the preliminary experiments in a very short time.

The primary human osteoblasts were isolated from human femoral head cancellous bone. They had an average doubling time of over 4 times higher than the doubling time of the C2C12 cells, meaning that necessary culture time until seeding was longer.

The cells were seeded in the vascular tree of the scaffold, where they had to be attached when the perfusion was started. Time-lapse microscopy can be employed to assess the time of cell adhesion to a substrate (Leung, Kakar et al. 1994). A similar experiment was performed on primary human osteoblasts placed on plastic substrate. This experiment showed that the majority of cells were attached to the substrate after 4 hours. This result was used to set the time the

cells were allowed to attach after seeding into the acellular scaffolds. After that time period the perfusion was started.

The populations of human bone cells were positive for alkaline phosphatase and they also produced collagen type I. These are characteristics of cells originating in bone tissue (Nacher, Serrano et al. 1999). A common feature of all cells from the mesenchymal lineage is the presence of vimentin filaments in the cytoplasm (Eriksson, Dechat et al. 2009). The cells used in this work were tested for vimentin and found positive. In addition, osteoblasts hold the capacity to produce mineralized deposits when cultured in osteogenic differentiation media. This was proven and was in agreement with already published reports (Gotoh, Hiraiwa et al. 1990; Kasperk, Wergedal et al. 1995).

6.2 Decellullarization of whole organs

By using decellularized extracellular matrix as scaffolds for tissue engineering, one can utilize two of their most important features. First, the scaffolds have a preexistent vascular network conserved even after the decellularization process. Second, they consist of natural components such as collagen or elastin.

In the present work, acellular scaffolds were obtained from whole rat kidneys by decellularization with the detergent sodium dodecyl sulfate (SDS). This organ has dimensions above the current size limitation in tissue engineering. The present study serves as proof of principle of the utilization of acellular organ scaffolds in constructing engineered bone tissues. The rat kidney can be efficiently decellularized with detergent solutions by using the arterial system as intake and venous and urinary systems as outtake. These systems remain afterwards the basis for seeding the cells into the scaffolds, as well as for the subsequent nourishment and removal of the metabolites.

With its complex internal architecture composed mainly of tubular structures, the kidney-derived scaffold has a very high potential of being a suitable basis for developing artificial tissues. This tubular structure can insure that it can

be perfused throughout in a sufficient quantity, as to maintain the viability of the construct on a long-term basis.

With the help of the detergent sodium dodecyl sulfate (SDS) it was possible to develop a very efficient and reliable decellularization protocol for whole rat kidneys. Therewith, a xenogenic scaffold for tissue engineering can be obtained. There are several reports in literature of similar protocols that were applied on other organs such as liver or lungs (Ott, Clippinger et al. 2010; Uygun, Soto-Gutierrez et al. 2010). There are, however, different methods that can be used to achieve decellularized organs: chemical, physical or enzymatic. These methods, used separately or in any combination, can yield comparable satisfactory results, although until now, none of the protocols already present in literature can be considered a standard in this field.

With the protocol developed during this work, complete decellularization of a rat kidney was possible in just one hour of detergent perfusion, with SDS in a concentration of 0.66% (w/v). It makes this method a very effective, cost-efficient and fast way of obtaining scaffolds for tissue engineering.

The success of the decellularization procedure was analyzed by different means: macroscopically, histologically and residual DNA measurement.

As already presented by previous studies (Ott, Matthiesen et al. 2008; Nakayama, Batchelder et al. 2010; Uygun, Soto-Gutierrez et al. 2010), the first indicator of the complete decellularization was the general translucency of the organ after being perfused with the SDS. Its shape and consistency were similar to the native organ, but all the cells were removed by the perfusion solution. An advantage of this translucency is that it is possible to verify the patency of the vascular network remaining in the matrix by injection of a colored gel in the renal artery, as described in a previous work (Uygun, Soto-Gutierrez et al. 2010). The main arterial branches of the kidney are distinctly observable inside the decellularized organ, as they are carrying the red Allura Red gel from the hilum through the vascular ramifications (Figure 20). The injection of the red dye can be continued until the whole acellular kidney becomes colored and the small vascular branches cannot be distinguished anymore. This proved the fact that the vascular

network was still capable of functioning, from the larger interlobar arteries to the capillaries.

The acellular kidney was prepared for histological analysis. The first investigation performed, hematoxylin and eosin staining, has revealed that there were no cell nuclei present in the decellularized samples. The ECM had the gross aspect of a honeycomb, but nevertheless structures of the kidney such as the renal papilla or the glomeruli were preserved.

An important concern in the use of xenografts is their immunogenicity. Here, especially DNA is very important to be absent from artificial scaffold used for tissue engineering (Choi, Choi et al. 2012). Nevertheless, studies have shown (Gilbert, Freund et al. 2009) that, although there is residual DNA present in commercially available scaffolds that were derived from ECM, these materials do not cause host responses. This fact points out that a certain quantity of foreign material is needed to induce a response.

The presence of DNA was verified on samples of the decellularized kidney first with the fluorescent SYBR® Green I dye that binds to nuclear material and second by direct measurement of the DNA quantity by spectrophotometry. The fluorescent assay showed no more visible DNA residues in the acellular matrix. That confirmed the initial results from hematoxylin and eosin staining. In addition, a direct measurement of the matrix DNA content was carried out. DNA was extracted from thin sections of paraformaldehyde-fixed paraffin embedded native and decellularized kidneys. The quantity of DNA in acellular samples was below the detection limit of the assay (2 ng/µl dsDNA) and similar to the negative control sample. This result confirmed that virtually all DNA was efficiently removed with the developed decellularization protocol.

To ensure that the SDS detergent is thoroughly washed out of the scaffolds after decellularization, the kidney effluent was investigated for SDS content. After performing the experiments, it emerged that there was an SDS concentration of under 0.005% SDS in the washing solution. It was reported in literature that this concentration was not toxic for human cells (Babich and Babich 1997). This

indicated that the environment provided by the acellular kidney scaffold is not toxic for the cells seeded therein.

For further tissue engineering application, it is of considerable importance that the obtained biomatrix has the necessary qualities to make the process of cell attachment and growth possible. A key role in this process is played by the extracellular matrix (ECM) of the scaffold. More and more ECM proteins are being investigated for their role in cell attachment and migration (Kuschel, Steuer et al. 2006). ECM proteins such as collagen I, laminin and fibronectin are among those that have already been proven to promote cell attachment and mobility (Clyman, McDonald et al. 1990). After the native cells have been removed with the SDS, the ECM will become the structure the seeded cells will first come in contact to and where they will subsequently attach.

The extracellular matrix is located in the space remaining between the cells of a tissue. It is produced by the cells and is composed of many macromolecules that bind to each other to form a complex mixture (Alberts 2008). There are four main types of macromolecules in the ECM: collagens, non-collagenous glycoproteins, glycosaminoglycans and proteoglycans (Rozario and DeSimone 2010).

There are 28 known types of collagen (Gordon and Hahn 2010) and collagen type I is the most abundant (Di Lullo, Sweeney et al. 2002). Related to the weight of the ECM, the collagens constitute 90% of the total dry weight of the ECM (van der Rest and Garrone 1991). In the ECM of the kidney and other organs, collagen type I, III and IV are most frequent (Mounier, Foidart et al. 1986; Lemley and Kriz 1991).

The presence of the collagen in the acellular kidney scaffold was assessed with the Sirius red staining. This is a very well established and reliable method of investigating the presence of collagen I, II, and III in tissues (Junqueira, Bignolas et al. 1979; James, Bosch et al. 1990). Sirius Red staining on rat kidney was clearly positive on sections of the native and decellularized tissues. This was an indicator that the general structure of the extracellular matrix of the kidney was preserved during the decellularization procedure. Collagen has a very important

role in providing the ECM with strength and stability. It consists of three polypeptide chains that coil around each other to form a right-handed superhelix (Petersen, Calle et al. 2012). It was therefore assumed that the seeded ECM would withstand the *in vitro* culture period and the matrix would not rupture or burst.

The major non-collagenous proteins in the ECM are the laminins and fibronectin. The laminins are the main component of basal membranes (Paulsson 1992). These two protein families are present also in the kidney (Lemley and Kriz 1991). While fibronectin mediates the connection of the cells to the basal membranes (Alberts 2008), the laminins are essential to organizing the sheet structure of the basal membrane (McKee, Harrison et al. 2007). The immunohistochemical stainings performed on sections of decellularized kidney revealed the presence of the two ECM proteins even after the treatment with SDS and decellularization.

6.3   Recellularization of the bioscaffolds

6.3.1   Reseeding acellular scaffolds with C2C12 cells

The C2C12 mouse myoblastic cells line has been previously used successfully to recellularize perfusion-decellularized organs (Akhyari, Aubin et al. 2011). The advantage of this cell line is the small doubling time of 13 hours (McMahon, Anderson et al. 1994). This allowed fast setup of the preliminary experiments by quickly obtaining the necessary number of cells. Nevertheless, one cannot predict how these cells, or others, will react to this new type of scaffold. Decellularization can lead to different scaffold characteristics, which may not be suitable for the cells.

The preliminary results obtained from the experiments with C2C12 cells showed high seeding efficiency with high number of cells present in the scaffold after the 3D culture periods. After the first day of 3D culture, the cells were uniformly distributed in the acellular organ and grouped mostly around the glomeruli and vessels. This was consistent with the work of Uygun et al (Uygun, Soto-Gutierrez et al. 2010) who demonstrated comparable results after seeding rat hepatocytes into the artery of acellular rat livers. Several conclusions could be

drawn from these results. The seeding method is efficient, the seeded cells survive and proliferate for 14 days within the bioscaffolds and they migrate from the vessels further inside the scaffold. The distribution of the cells within the scaffolds on day 14 confirmed that the cells were well nourished and oxygenated not only in the superficial layers of the scaffold. This demonstrates the functionality of the vascular network through which medium was perfused.

6.3.2 Reseeding acellular scaffolds with human cells

The osteoblasts were seeded to the bioscaffolds, using the same protocol as for the C2C12 cells. As expected, the human osteoblasts were also capable of adhering to the kidney scaffold, roughly in the same manner as the C2C12 cells. Cell size could also play a role in the distribution of seeded cells inside the kidney scaffold, due to the intricate tubular system of the organ. If the cells cannot go through vessels of a certain diameter, a uniform seeding of the whole organ cannot be achieved. Therefore, smaller vessels are clogged with cells, blocking the circulation of the perfusion medium in the kidney. It was reported that the mean diameter of the C2C12 myoblasts in suspension was around 14 µm (Kazi and Lang 2010), while the osteoblasts were measured at 20 to 30 µm (Puckett, Pareta et al. 2008). The obtained results show similar and uniform distribution of the osteoblasts and C2C12. This illustrates that the size of the cells is within the diameter of the capillaries of the rat kidney scaffold and allows for a uniform distribution of cells. An alternative method of seeding the cells would be by direct injection into the acellular scaffold. However, this would cause irreparable damage to the scaffold and the seeded cells would not be evenly distributed throughout the matrix.

For better characterization of the osteoblast growth inside the scaffold, three culture durations were chosen: 24 hours, 5 days and 14 days after the seeding of cells.

The assessment of the vitality of the cells with a resazurin assay has already been shown in literature (Dienstknecht, Ehehalt et al. 2010). It is a reliable tool for evaluation of cell number and viability in culture without cell perturbation. This method has also been applied during 14-day 3D culture of scaffolds seeded

with human osteoblasts. The analysis of the assay showed an increase in viability towards the last day of culture. Furthermore, with this method the status of the construct could be monitored without interrupting the experiment.

The H&E staining was the first histological investigation performed on the samples. It quickly provided information regarding the presence and distribution of the cells in the matrix, as well as the internal morphology of the construct. The tissue sections from the samples cultured for 5 days had a different histological appearance based on the H&E staining, compared with the 24 hour- or 14 day-cultured constructs. Characteristic for sections from the 24 hour-cultures was the presence of the cells within or in the vicinity of the glomerular capillaries and in larger blood vessels, described also in previous work (Uygun, Soto-Gutierrez et al. 2010). This could be explained by the method of seeding the cells into in the renal artery. From the 5-day time point onward, cells could be found in higher numbers in the areas surrounding the glomeruli and even further inside the scaffold, loosely scattered and away from the initial attachment sites. On the other hand, hardly any cells could be observed in the renal medulla. This could occur due to the separation of the vascular and urinary compartments of the kidney. The medulla contains mainly structures belonging to the urinary compartment, whereas the cells were seeded into the vascular one.

The presence of cells in acellular scaffolds after longer culture periods was proven also in previous studies, such as the works of Uygun *et al.* (Uygun, Soto-Gutierrez et al. 2010) and Baptista *et al.* (Baptista, Siddiqui et al. 2011). Their experiments showed that cells could still be found after culture in a liver decellularized scaffold for 5, respectively 7 days. The studies on lung acellular scaffolds by Ott *et al.* (Ott, Clippinger et al. 2010) and Petersen *et al.* (Petersen, Calle et al. 2010) confirmed that constructs could be maintained for up to 9, respectively 8 days in the 3D culture environment. In contrast, the current work describes the successful attempt of cultivating cells in an acellular whole organ scaffold for a longer duration. After a 3D culture period of 14 days, cells could still be found in sections from the scaffolds. These had nonetheless a different aspect compared to the ones cultured for 1 day and 5 days. The cells were now tightly

grouped, forming more compact colonies. There were also morphological signs of apoptosis and certain areas where cellular debris could be seen.

The Ki-67 immunohistochemical staining, used to identify dividing cells, was performed in addition to the apoptosis detection assay. This staining illustrated the proliferation potential of the cells seeded in the kidney scaffolds at the three reference points of 24 hours, 5 days and 14 days after seeding. The highest amount of Ki-67 positive cells was found at 24 hours. The Ki-67 staining performed on monolayer cell cultures showed a similar fraction of positive cells. The number of positive cells decreased until day 14 of 3D culture, when not many positive cells could be identified. There are various signaling pathways that control the proliferation of mesenchymal stem cells (Lemon, Waters et al. 2007). The proliferation and differentiation of these cells in monolayer culture occur differently than in three dimensional environments (Cukierman, Pankov et al. 2001). Therefore, one can expect that the human osteoblasts seeded into the acellular kidney matrix behave differently than in 2D culture due to the radical differences in the growth conditions. The cells used for seeding were taken from early passages (at the earliest in the 3rd passage and at the latest in passage 7), where there is a sufficient number of proliferating cells. This can lead to the hypothesis that after 14 days in 3D culture, the cells have reached a stationary phase in their growth. This behavior has been observed in cells cultured on 3D scaffolds and it has been associated with stress caused by lack of nutrients, or by physical limitations of the scaffold (Moussavi-Harami, Duwayri et al. 2004).

The rate of apoptosis, or programmed cell death, was verified with the highly specific nick translation assay. When the cell undergoes apoptosis, its DNA is cleaved by endonucleases in a specific manner. Apoptosis occurs naturally in tissues and is essential to maintaining a healthy cell population. Cells that are no longer needed or not functioning properly are constantly removed by apoptosis (Hengartner 2000). The assay performed to detect apoptosis revealed that at the three time points the seeded cells had different degrees of apoptosis. Apoptotic cells in higher numbers were found after 24 hours of 3D culture, possibly due to the stress involved in the seeding procedure and the change of growth environment. Cells cultured in the kidney scaffolds for 5 days have shown very

rare signs of apoptosis. By contrast, the rate of apoptosis increased again after 14 days. This was not necessarily triggered by harmful stimuli. A possible cause could have been the absence of dividing cells, which produced resulted in aging of the cell population.

One of the questions raised during the project was whether the kidney-based scaffold originating from rat would have an effect on the human osteoblasts characteristics. Therefore, the presence of three typical osteoblastic markers was investigated, namely alkaline phosphatase, osteocalcin and vimentin.

The alkaline phosphatase (ALP) is an enzyme typically present in osteoblasts and it can be considered one of the markers for this type of cells (Bonucci and Nanci 2001). The presence of ALP was investigated on cells in monolayer cell culture (2D) and also on sections from kidney scaffolds seeded with these cells cultured in 3D conditions. Samples cultured for 1 day and 5 days were strongly positive for ALP. Interestingly, at 14-day point of culture the intensity of the staining decreased. One hypothesis that could explain this result would be a further maturation of the osteoblasts towards osteocytes. This cell type has lower ALP activity (van der Plas, Aarden et al. 1994). The scaffolds were not cultured in differentiation medium, therefore the probable trigger for this change could be the kidney ECM itself.

Osteocalcin is one of the proteins found to be specifically produced by osteoblastic cells (Lee, Sowa et al. 2007). It is, after collagens, the most abundant protein in the extracellular matrix of bone and plays a central role in its mineralization (Knepper-Nicolai, Reinstorf et al. 2002). Through the stainings performed on scaffolds seeded with human osteoblasts, it was possible to confirm the presence of osteocalcin in the constructs seeded with osteoblasts after 1, 5, and 14 days of 3D culture. There is a similar aspect of the stainings at these reference points, regarding the amount of positive tissue detected. This constitutes an interesting result, because it could lead to the hypothesis that most of the osteocalcin is secreted by the cells in the first days of culture. Thereafter, the cellular secretion decreased, but the osteocalcin remained in the scaffold for the rest of the culture period. It is known that osteocalcin can bind to type I collagen (Prigodich and Vesely 1997). Moreover, the collagen fibers have similar gene

sequences and structures across vertebrates (Ramirez, Boast et al. 1990). Therefore, the osteocalcin secreted by the human osteoblasts could bind to the collagen already present in the decellularized kidney scaffold.

Vimentin is a known marker for mesenchymal stem cells, which forms type III intermediate filament in the cell cytoplasm (You, Kublin et al. 2011). It is a marker for the mesenchymal linage, to which the osteoblasts belong (Satelli and Li 2011). In addition, it can also be found in osteocytes (Shapiro, Cahill et al. 1995). The immunohistochemical staining for vimentin was performed on both human osteoblasts cultured in 2D and those seeded in the acellular kidney scaffolds. It was found that the stainings were positive in all cases. The cytoplasm of the cells was stained in a distinct pattern that revealed the ubiquitous presence and arrangement of the vimentin filaments in the cells. The vimentin staining performed on samples from the seeded kidney scaffolds cultured for 1 day, 5 days and 14 days in 3D conditions showed that the vast majority of cells were positive for this mesenchymal cell marker over the culture period.

Several genes described in literature to be specifically expressed in osteogenic lineage were analyzed by real time PCR. Interestingly, the results of the gene expression investigation have pointed at a possible differentiation of the seeded osteoblastic cells into cells with osteocyte features at the end of the 14-day 3D culture.

The expression of alkaline phosphatase (*ALPL*) and collagen type I (*COL1A1*) have significantly decreased from day 1 of culture to almost non-detectable levels after 14 days. This corresponded to published work that reports that in differentiated osteoblasts, the levels of *ALP* and *COL1A1* are decreasing with progression of differentiation (Dallas and Bonewald 2010). These results point to the fact that the acellular scaffold could induce in the seeded cells a differentiation effect similar to that obtained after culturing them longer under specific differentiation conditions.

The gene expressions of *RUNX2* and osterix (*OSX*) in samples analyzed in the current work had an opposite evolution during the time of culture. The expression of *RUNX2* was found to significantly decrease from 1 day of culture to

5 days and 14 days. *OSX* exibited a statistically significant increase in expression compared with day 1 after 5 days and 14 days. Runx2 and osterix are transcription factors essential for developments of the osteogenic linage, with osterix being a gene downstream of Runx2 (Komori 2006). Osterix is known to be essential to osteoblast differentiation and bone mineralization. It additionally plays an essential role in the cell-specific genetic program of osteocytes (Zhou, Zhang et al. 2010). Runx2 triggers the expression of bone-specific genes at an early stage in osteoblast differentiation, but also maintains the osteoblastic cells in an immature stage (Komori 2006). It can be hypothesized, that cells seeded into the acellular scaffold changed their phenotype during the culture time towards mature osteoblasts and possibly osteocytes.

The gene expressions of *PHEX* and *PDPN,* markers found in osteocytes, were also analyzed from samples of kidney seeded with human primary osteoblasts. In samples cultured for 5 days, *PHEX* was expressed significantly higher than in those cultured for 1 day and higher than samples cultured for 14 days. In the investigated samples, the gene expression of *PDPN* in the samples cultured for 5 days was significantly lower than in those cultured for 1 day and lower than in samples cultured for 14 days. It is described in current literature that genes *PDPN* and *PHEX* appear in bone cells once the process of differentiation has begun (Dallas and Bonewald 2010). The positive expression of the markers *PDPN* and *PHEX* corresponds with the decrease in the expression of *RUNX2* and the increase in *OSX*. This fact points to a modification of the phenotype of the seeded cells from osteoblastic towards osteocytes. This correlates well with the decrease in gene expression of both *ALPL* and *COL1A1* as already mentioned in literature (Komori 2006).

6.4 Conclusion

This work presents a method of tissue engineering vascularized bone, developed by seeding primary human osteoblasts into decellularized rat kidneys. For decellularization, whole rat kidneys were perfused with a detergent solution containing SDS. The decellularization protocol resulted in a cell-free and non-toxic scaffold with a functional vascular network. Moreover, the matrix kept the original

shape of the organ and still contained important extracellular matrix proteins: collagen, fibronectin and laminin. The vascular pedicle was successfully used for recellularizing the acellular scaffold with human bone cells. Cells could be grown *in vitro* in 3D conditions for at least 14 days. Furthermore, immunohistochemical stainings proved the cells preserved osteogenic characteristics, such as expression of ALP, vimentin, osteocalcin. Investigations of proliferation and apoptosis on the seeded constructs showed a decrease in proliferation and increase in apoptosis after the 14-day culture period, pointing towards an aging of the cell population. Additionally, expressions of osteogenic genes and transcription factors were analyzed by real time PCR. The results indicated a maturation of the seeded osteoblastic cells into cells with osteocytic characteristics. In conclusion, this study succeeded in developing bioscaffolds from whole decellularized rat kidneys that supported the growth of human bone cells. Therefore, this method has a great potential to bringing important contributions to the field of bone tissue engineering.

6.5 Study limitations

During the course of this study, several limitations have emerged. A relatively high number of primary human cells was necessary for a sufficient seeding of the scaffold, despite its small size. This limits possible up-scaling of the tissue engineered construct. The technical setup of the experimental assembly was relatively complicated. Routine interventions, such as medium change, were difficult and could potentially compromise the experiment due to contamination. Furthermore, this assembly required a larger space that regular cell culture operations. Another difficulty was to assess the status of the constructs and the cells within without interrupting the experiment.

6.6 Future perspectives

There are still improvements that need to be made to this work, to become a relevant alternative to current tissue engineering techniques. Firstly, optimizations could be made to the technical side of the experimental work for easier interaction. Specifically simplifying the construction of the assembly will lead to easier operation and lower risk of contamination.

The ultimate goal of this work is to find clinical applicability in bone regenerative medicine. The defects that have to be repaired in humans are often larger in size. Therefore, a larger acellular organ is needed for these situations. Moreover, the acellular scaffolds must be endothelialized to reduce the risk of blood clotting when the construct will be implanted and connected to the blood supply. Thus exposure of collagen-containing basement membrane to the circulation has to be avoided. Clotting would lead to blocked blood vessels and therewith necrosis of the graft. Additionally, the culture time of the constructs has to be optimized to find the best time point for the transplantation of the grafts. At this point, the cells within must be able to withstand the change in their growth conditions. Also, the cells have to be in a sufficient number to trigger the remodeling of the implanted graft towards a bone-like tissue.

7 Summary

Tissue engineering of bone constructs is developing into a very attractive branch of regenerative medicine. The growing need for bone substitutes combined with the insufficient number of tissue donors has focused the interest on tissue engineering solutions. One new type of scaffolds for tissue engineering is based on decellularized whole organs. The major advantage of this method is that it produces a scaffold containing a ready-to-use vascular network. These bioscaffolds inhere the potential to overcome the current size limitations in tissue engineering. Recently, this technology was successfully used to compose the type of organ from which the scaffolds originated. In the current work we tested the compatibility of human bone cells with an acellular scaffold derived from rat kidney and investigated the potential of this method to be applied in regeneration of bone.

An acellular scaffold was obtained through decellularization of whole rat kidneys. The complete removal of cells was initially proven by H&E staining and confirmed by the fluorescent SYBR Green I dye, as well as by measuring the DNA content of the acellular organ. The scaffolds are rich in collagen as shown by the picrosirius red staining and also contain fibronectin and laminin, major proteic constituents of the basal lamina. These factors are essential for the cell attachment. The scaffolds were seeded with primary human osteoblasts. The obtained constructs were cultured for a maximum of 14 days under dynamic conditions. They were investigated at 1, 5 and 14 days after seeding the cells by histochemical and immunohistochemical procedures. These experiments showed that the seeded cells are able to attach and proliferate in the kidney scaffold and survive the 14-day culture period. Here, a part of cells entered apoptosis, but the metabolic activity of the population could be proven. Moreover, the cells secreted alkaline phosphatase and osteocalcin, two typical osteoblast markers, over the culture period, indicating that they kept their phenotype despite the xenogenic nature of the scaffold. Real-time PCR analysis of the expression of typical osteoblast genes was also performed. This showed that over the culture period, the cells progressively exhibited characteristics of mature osteoblasts or osteocytes.

To conclude, the present work shows that the method of generating biological constructs holds great promise in the field of tissue engineering of bone and regeneration of bone defects. Nevertheless, further investigations need to be made to optimize the culture conditions, to precisely characterize the cells during the *in vitro* culture period and ultimately, to test the *in vivo* applicability of this method.

8 References

AAOS-Orthopaedic-Device-Forum (2010). The evolving role of bone-graft substitutes. American Academy of Orthopaedic Surgeons 77th Annual Meeting, New Orleans, Lousiana, American Academy of Orthopaedic Surgeons.

Adams, J. C. and Watt, F. M. (1993). "Regulation of development and differentiation by the extracellular matrix." Development 117(4): 1183-1198.

Akhyari, P., Aubin, H., Gwanmesia, P., Barth, M., Hoffmann, S., Huelsmann, J., Preuss, K. and Lichtenberg, A. (2011). "The quest for an optimized protocol for whole-heart decellularization: a comparison of three popular and a novel decellularization technique and their diverse effects on crucial extracellular matrix qualities." Tissue Eng Part C Methods 17(9): 915-926.

Alberts, B. (2008). Molecular biology of the cell. New York, Garland Science.

Albrektsson, T. and Johansson, C. (2001). "Osteoinduction, osteoconduction and osseointegration." Eur Spine J 10 Suppl 2: S96-101.

Anderson, H. C. (1995). "Molecular biology of matrix vesicles." Clin Orthop Relat Res(314): 266-280.

Babich, H. and Babich, J. P. (1997). "Sodium lauryl sulfate and triclosan: in vitro cytotoxicity studies with gingival cells." Toxicol Lett 91(3): 189-196.

Badylak, S. F., Taylor, D. and Uygun, K. (2011). "Whole-organ tissue engineering: decellularization and recellularization of three-dimensional matrix scaffolds." Annu Rev Biomed Eng 13: 27-53.

Baptista, P. M., Siddiqui, M. M., Lozier, G., Rodriguez, S. R., Atala, A. and Soker, S. (2011). "The use of whole organ decellularization for the generation of a vascularized liver organoid." Hepatology 53(2): 604-617.

Berkner, K. L. (2008). "Vitamin K-dependent carboxylation." Vitam Horm 78: 131-156.

Bernard, M. P., Chu, M. L., Myers, J. C., Ramirez, F., Eikenberry, E. F. and Prockop, D. J. (1983). "Nucleotide sequences of complementary deoxyribonucleic acids for the pro alpha 1 chain of human type I procollagen. Statistical evaluation of structures that are conserved during evolution." Biochemistry 22(22): 5213-5223.

Berthiaume, F., Maguire, T. J. and Yarmush, M. L. (2011). "Tissue engineering and regenerative medicine: history, progress, and challenges." Annu Rev Chem Biomol Eng 2: 403-430.

Bertram, J. F., Soosaipillai, M. C., Ricardo, S. D. and Ryan, G. B. (1992). "Total numbers of glomeruli and individual glomerular cell types in the normal rat kidney." Cell Tissue Res 270(1): 37-45.

Biosystems, A. (2002). TaqMan® One-Step RT-PCR Master Mix Reagents Kit Protocol.

Bissell, M. J., Hall, H. G. and Parry, G. (1982). "How does the extracellular matrix direct gene expression?" J Theor Biol 99(1): 31-68.

Blair, H. C., Robinson, L. J. and Zaidi, M. (2005). "Osteoclast signalling pathways." Biochem Biophys Res Commun 328(3): 728-738.

Blau, H. M., Pavlath, G. K., Hardeman, E. C., Chiu, C. P., Silberstein, L., Webster, S. G., Miller, S. C. and Webster, C. (1985). "Plasticity of the differentiated state." Science 230(4727): 758-766.

Boivin, G. and Meunier, P. J. (2003). "The mineralization of bone tissue: a forgotten dimension in osteoporosis research." Osteoporos Int 14 Suppl 3: S19-24.

Bonucci, E. and Nanci, A. (2001). "Alkaline phosphatase and tartrate-resistant acid phosphatase in osteoblasts of normal and pathologic bone." Ital J Anat Embryol 106(2 Suppl 1): 129-133.

Brown, B. N., Freund, J. M., Han, L., Rubin, J. P., Reing, J. E., Jeffries, E. M., Wolf, M. T., Tottey, S., Barnes, C. A., Ratner, B. D. and Badylak, S. F. (2011). "Comparison of Three Methods for the Derivation of a Biologic Scaffold Composed of Adipose Tissue Extracellular Matrix." Tissue Engineering Part C-Methods 17(4): 411-421.

Brown, B. N., Freund, J. M., Han, L., Rubin, J. P., Reing, J. E., Jeffries, E. M., Wolf, M. T., Tottey, S., Barnes, C. A., Ratner, B. D. and Badylak, S. F. (2011). "Comparison of three methods for the derivation of a biologic scaffold composed of adipose tissue extracellular matrix." Tissue Eng Part C Methods 17(4): 411-421.

Bruder, S. P. and Fox, B. S. (1999). "Tissue engineering of bone. Cell based strategies." Clin Orthop Relat Res(367 Suppl): S68-83.

Bruder, S. P., Kraus, K. H., Goldberg, V. M. and Kadiyala, S. (1998). "The effect of implants loaded with autologous mesenchymal stem cells on the healing of canine segmental bone defects." J Bone Joint Surg Am 80(7): 985-996.

Bruder, S. P., Kurth, A. A., Shea, M., Hayes, W. C., Jaiswal, N. and Kadiyala, S. (1998). "Bone regeneration by implantation of purified, culture-expanded human mesenchymal stem cells." J Orthop Res 16(2): 155-162.

Bucholz, R. W. (2002). "Nonallograft osteoconductive bone graft substitutes." Clin Orthop Relat Res(395): 44-52.

Calori, G. M., Mazza, E., Colombo, M., Ripamonti, C. and Tagliabue, L. (2011). "Treatment of long bone non-unions with polytherapy: indications and clinical results." Injury 42(6): 587-590.

Caplan, A. I. (1991). "Mesenchymal stem cells." J Orthop Res 9(5): 641-650.

Carmeliet, P. and Jain, R. K. (2000). "Angiogenesis in cancer and other diseases." Nature 407(6801): 249-257.

Carrel, A. (1912). "On the Permanent Life of Tissues Outside of the Organism." J Exp Med 15(5): 516-528.

Carrel, A. and Burrows, M. T. (1911). "Cultivation of Tissues in Vitro and Its Technique." J Exp Med 13(3): 387-396.

Carrel, A. and Lindbergh, C. A. (1935). "The Culture of Whole Organs." Science 81(2112): 621-623.

Carson, J. S. and Bostrom, M. P. (2007). "Synthetic bone scaffolds and fracture repair." Injury 38 Suppl 1: S33-37.

Carter, D. R., Beaupre, G. S., Giori, N. J. and Helms, J. A. (1998). "Mechanobiology of skeletal regeneration." Clin Orthop Relat Res(355 Suppl): S41-55.

Cattoretti, G., Andreola, S., Clemente, C., D'Amato, L. and Rilke, F. (1988). "Vimentin and p53 expression on epidermal growth factor receptor-positive, oestrogen receptor-negative breast carcinomas." Br J Cancer 57(4): 353-357.

Cebotari, S., Tudorache, I., Jaekel, T., Hilfiker, A., Dorfman, S., Ternes, W., Haverich, A. and Lichtenberg, A. (2010). "Detergent decellularization of heart valves for tissue engineering: toxicological effects of residual detergents on human endothelial cells." Artif Organs 34(3): 206-210.

Chen, C. S. (2008). "Mechanotransduction - a field pulling together?" J Cell Sci 121(Pt 20): 3285-3292.

Choi, Y. C., Choi, J. S., Kim, B. S., Kim, J. D., Yoon, H. I. and Cho, Y. W. (2012). "Decellularized Extracellular Matrix Derived from Porcine Adipose Tissue as a Xenogeneic Biomaterial for Tissue Engineering." Tissue Eng Part C Methods.

Clyman, R. I., McDonald, K. A. and Kramer, R. H. (1990). "Integrin receptors on aortic smooth muscle cells mediate adhesion to fibronectin, laminin, and collagen." Circ Res 67(1): 175-186.

Conconi, M. T., De Coppi, P., Di Liddo, R., Vigolo, S., Zanon, G. F., Parnigotto, P. P. and Nussdorfer, G. G. (2005). "Tracheal matrices, obtained by a detergent-enzymatic method, support in vitro the adhesion of chondrocytes and tracheal epithelial cells." Transpl Int 18(6): 727-734.

Crapo, P. M., Gilbert, T. W. and Badylak, S. F. (2011). "An overview of tissue and whole organ decellularization processes." Biomaterials 32(12): 3233-3243.

Cukierman, E., Pankov, R., Stevens, D. R. and Yamada, K. M. (2001). "Taking cell-matrix adhesions to the third dimension." Science 294(5547): 1708-1712.

Czekanska, E. M. (2011). "Assessment of cell proliferation with resazurin-based fluorescent dye." Methods Mol Biol 740: 27-32.

Dallas, S. L. and Bonewald, L. F. (2010). "Dynamics of the transition from osteoblast to osteocyte." Ann N Y Acad Sci 1192: 437-443.

De Kock, J., Ceelen, L., De Spiegelaere, W., Casteleyn, C., Claes, P., Vanhaecke, T. and Rogiers, V. (2011). "Simple and quick method for whole-liver decellularization: a novel in vitro three-dimensional bioengineering tool?" Arch Toxicol 85(6): 607-612.

Di Lullo, G. A., Sweeney, S. M., Korkko, J., Ala-Kokko, L. and San Antonio, J. D. (2002). "Mapping the ligand-binding sites and disease-associated mutations on the most abundant protein in the human, type I collagen." J Biol Chem 277(6): 4223-4231.

Dienstknecht, T., Ehehalt, K., Jenei-Lanzl, Z., Zellner, J., Muller, M., Berner, A., Nerlich, M. and Angele, P. (2010). "Resazurin dye as a reliable tool for determination of cell number and viability in mesenchymal stem cell culture." Bull Exp Biol Med 150(1): 157-159.

Elmore, S. (2007). "Apoptosis: a review of programmed cell death." Toxicol Pathol 35(4): 495-516.

Eriksson, J. E., Dechat, T., Grin, B., Helfand, B., Mendez, M., Pallari, H. M. and Goldman, R. D. (2009). "Introducing intermediate filaments: from discovery to disease." J Clin Invest 119(7): 1763-1771.

Exposito, J. Y., D'Alessio, M., Solursh, M. and Ramirez, F. (1992). "Sea urchin collagen evolutionarily homologous to vertebrate pro-alpha 2(I) collagen." J Biol Chem 267(22): 15559-15562.

Fleck, C. (1999). "Determination of the glomerular filtration rate (GFR): methodological problems, age-dependence, consequences of various surgical interventions, and the influence of different drugs and toxic substances." Physiol Res 48(4): 267-279.

Fu, H., Doll, B., McNelis, T. and Hollinger, J. O. (2007). "Osteoblast differentiation in vitro and in vivo promoted by Osterix." J Biomed Mater Res A 83(3): 770-778.

Funamoto, S., Nam, K., Kimura, T., Murakoshi, A., Hashimoto, Y., Niwaya, K., Kitamura, S., Fujisato, T. and Kishida, A. (2010). "The use of high-hydrostatic pressure treatment to decellularize blood vessels." Biomaterials 31(13): 3590-3595.

Gabriel, A. and Maxwell, G. P. (2011). "Evolving role of alloderm in breast surgery." Plast Surg Nurs 31(4): 141-150.

Gapski, R., Parks, C. A. and Wang, H. L. (2005). "Acellular dermal matrix for mucogingival surgery: a meta-analysis." J Periodontol 76(11): 1814-1822.

Gauthier, O., Bouler, J. M., Weiss, P., Bosco, J., Daculsi, G. and Aguado, E. (1999). "Kinetic study of bone ingrowth and ceramic resorption associated with the implantation of different injectable calcium-phosphate bone substitutes." J Biomed Mater Res 47(1): 28-35.

Gerdes, J., Lemke, H., Baisch, H., Wacker, H. H., Schwab, U. and Stein, H. (1984). "Cell cycle analysis of a cell proliferation-associated human nuclear antigen defined by the monoclonal antibody Ki-67." J Immunol 133(4): 1710-1715.

Gilbert, T. W., Freund, J. M. and Badylak, S. F. (2009). "Quantification of DNA in biologic scaffold materials." J Surg Res 152(1): 135-139.

Gilbert, T. W., Sellaro, T. L. and Badylak, S. F. (2006). "Decellularization of tissues and organs." Biomaterials 27(19): 3675-3683.

Gold, R., Schmied, M., Rothe, G., Zischler, H., Breitschopf, H., Wekerle, H. and Lassmann, H. (1993). "Detection of DNA fragmentation in apoptosis: application of in situ nick translation to cell culture systems and tissue sections." J Histochem Cytochem 41(7): 1023-1030.

Gordon, M. K. and Hahn, R. A. (2010). "Collagens." Cell Tissue Res 339(1): 247-257.

Gotoh, Y., Hiraiwa, K. and Nagayama, M. (1990). "In vitro mineralization of osteoblastic cells derived from human bone." Bone Miner 8(3): 239-250.

Grauss, R. W., Hazekamp, M. G., Oppenhuizen, F., van Munsteren, C. J., Gittenberger-de Groot, A. C. and DeRuiter, M. C. (2005). "Histological evaluation of decellularised porcine aortic valves: matrix changes due to different decellularisation methods." European Journal of Cardio-Thoracic Surgery 27(4): 566-571.

Gray, H. and Lewis, W. H. (1918). The Urinary Organs. Anatomy of the human body. Philadelphia ; New York, Lea & Febiger,.

Gundberg, C. M. (2003). "Matrix proteins." Osteoporos Int 14 Suppl 5: S37-40; discussion S40-32.

Haase, S. C., Rovak, J. M., Dennis, R. G., Kuzon, W. M., Jr. and Cederna, P. S. (2003). "Recovery of muscle contractile function following nerve gap repair with chemically acellularized peripheral nerve grafts." J Reconstr Microsurg 19(4): 241-248.

Harada, S. and Rodan, G. A. (2003). "Control of osteoblast function and regulation of bone mass." Nature 423(6937): 349-355.

Haraldsson, B., Nystrom, J. and Deen, W. M. (2008). "Properties of the glomerular barrier and mechanisms of proteinuria." Physiol Rev 88(2): 451-487.

Hashimoto, Y., Funamoto, S., Sasaki, S., Honda, T., Hattori, S., Nam, K., Kimura, T., Mochizuki, M., Fujisato, T., Kobayashi, H. and Kishida, A. (2010). "Preparation and characterization of decellularized cornea using high-hydrostatic pressurization for corneal tissue engineering." Biomaterials 31(14): 3941-3948.

Heid, C. A., Stevens, J., Livak, K. J. and Williams, P. M. (1996). "Real time quantitative PCR." Genome Res 6(10): 986-994.

Hengartner, M. O. (2000). "The biochemistry of apoptosis." Nature 407(6805): 770-776.

Hiles, M., Record Ritchie, R. D. and Altizer, A. M. (2009). "Are biologic grafts effective for hernia repair?: a systematic review of the literature." Surg Innov 16(1): 26-37.

Hodde, J., Janis, A., Ernst, D., Zopf, D., Sherman, D. and Johnson, C. (2007). "Effects of sterilization on an extracellular matrix scaffold: part I. Composition and matrix architecture." J Mater Sci Mater Med 18(4): 537-543.

Hopkinson, A., Shanmuganathan, V. A., Gray, T., Yeung, A. M., Lowe, J., James, D. K. and Dua, H. S. (2008). "Optimization of amniotic membrane (AM) denuding for tissue engineering." Tissue Eng Part C Methods 14(4): 371-381.

Ingber, D. E. and Levin, M. (2007). "What lies at the interface of regenerative medicine and developmental biology?" Development 134(14): 2541-2547.

Jahangir AA, N. R., Mehta S, Sharan A, the Washington Health Policy Fellows (2008). "Bone-graft substitutes in orthopaedic surgery." AAOS Now 2(1).

James, J., Bosch, K. S., Aronson, D. C. and Houtkooper, J. M. (1990). "Sirius red histophotometry and spectrophotometry of sections in the assessment of the collagen content of liver tissue and its application in growing rat liver." Liver 10(1): 1-5.

Janicki, P. and Schmidmaier, G. (2011). "What should be the characteristics of the ideal bone graft substitute? Combining scaffolds with growth factors and/or stem cells." Injury 42 Suppl 2: S77-81.

Jonsson, K. B., Frost, A., Nilsson, O., Ljunghall, S. and Ljunggren, O. (1999). "Three isolation techniques for primary culture of human osteoblast-like cells: a comparison." Acta Orthop Scand 70(4): 365-373.

Junqueira, L. C., Bignolas, G. and Brentani, R. R. (1979). "Picrosirius staining plus polarization microscopy, a specific method for collagen detection in tissue sections." Histochem J 11(4): 447-455.

Kasperk, C., Wergedal, J., Strong, D., Farley, J., Wangerin, K., Gropp, H., Ziegler, R. and Baylink, D. J. (1995). "Human Bone Cell Phenotypes Differ Depending on Their Skeletal Site of Origin." Journal of Clinical Endocrinology & Metabolism 80(8): 2511-2517.

Kassem, M., Abdallah, B. M. and Saeed, H. (2008). "Osteoblastic cells: differentiation and trans-differentiation." Arch Biochem Biophys 473(2): 183-187.

Kazi, A. A. and Lang, C. H. (2010). "PRAS40 regulates protein synthesis and cell cycle in C2C12 myoblasts." Mol Med 16(9-10): 359-371.

Kheir, E., Stapleton, T., Shaw, D., Jin, Z., Fisher, J. and Ingham, E. (2011). "Development and characterization of an acellular porcine cartilage bone matrix for use in tissue engineering." J Biomed Mater Res A 99(2): 283-294.

Kimelman, N., Pelled, G., Helm, G. A., Huard, J., Schwarz, E. M. and Gazit, D. (2007). "Review: gene- and stem cell-based therapeutics for bone regeneration and repair." Tissue Eng 13(6): 1135-1150.

Klopfleisch, R., Weiss, A. T. and Gruber, A. D. (2011). "Excavation of a buried treasure--DNA, mRNA, miRNA and protein analysis in formalin fixed, paraffin embedded tissues." Histol Histopathol 26(6): 797-810.

Knepper-Nicolai, B., Reinstorf, A., Hofinger, I., Flade, K., Wenz, R. and Pompe, W. (2002). "Influence of osteocalcin and collagen I on the mechanical and biological properties of Biocement D." Biomol Eng 19(2-6): 227-231.

Knepper, M. A., Saidel, G. M., Hascall, V. C. and Dwyer, T. (2003). "Concentration of solutes in the renal inner medulla: interstitial hyaluronan as a mechano-osmotic transducer." Am J Physiol Renal Physiol 284(3): F433-446.

Komori, T. (2003). "Requisite roles of Runx2 and Cbfb in skeletal development." J Bone Miner Metab 21(4): 193-197.

Komori, T. (2006). "Regulation of osteoblast differentiation by transcription factors." J Cell Biochem 99(5): 1233-1239.

Konuma, T., Devaney, E. J., Bove, E. L., Gelehrter, S., Hirsch, J. C., Tavakkol, Z. and Ohye, R. G. (2009). "Performance of CryoValve SG decellularized pulmonary allografts compared with standard cryopreserved allografts." Ann Thorac Surg 88(3): 849-854; discussion 554-845.

Kronenberg, H. M. (2003). "Developmental regulation of the growth plate." Nature 423(6937): 332-336.

Kulkarni, R. N., Bakker, A. D., Everts, V. and Klein-Nulend, J. (2012). "Mechanical loading prevents the stimulating effect of IL-1beta on osteocyte-modulated osteoclastogenesis." Biochem Biophys Res Commun 420(1): 11-16.

Kuschel, C., Steuer, H., Maurer, A. N., Kanzok, B., Stoop, R. and Angres, B. (2006). "Cell adhesion profiling using extracellular matrix protein microarrays." Biotechniques 40(4): 523-531.

Lee, N. K., Sowa, H., Hinoi, E., Ferron, M., Ahn, J. D., Confavreux, C., Dacquin, R., Mee, P. J., McKee, M. D., Jung, D. Y., Zhang, Z., Kim, J. K., Mauvais-Jarvis, F., Ducy, P. and Karsenty, G. (2007). "Endocrine regulation of energy metabolism by the skeleton." Cell 130(3): 456-469.

Lemley, K. V. and Kriz, W. (1991). "Anatomy of the renal interstitium." Kidney Int 39(3): 370-381.

Lemon, G., Waters, S. L., Rose, F. R. and King, J. R. (2007). "Mathematical modelling of human mesenchymal stem cell proliferation and differentiation inside artificial porous scaffolds." J Theor Biol 249(3): 543-553.

Leung, T., Kakar, A., Hobkirk, J. A. and Thorogood, P. (1994). "Behaviour of fibroblasts during initial attachment to a glass-ceramic implant material in vitro: a time-lapse video-micrographic study." Biomaterials 15(12): 1001-1007.

Levenberg, S., Rouwkema, J., Macdonald, M., Garfein, E. S., Kohane, D. S., Darland, D. C., Marini, R., van Blitterswijk, C. A., Mulligan, R. C., D'Amore, P. A. and Langer, R. (2005). "Engineering vascularized skeletal muscle tissue." Nat Biotechnol 23(7): 879-884.

Lian, J. B. and Gundberg, C. M. (1988). "Osteocalcin. Biochemical considerations and clinical applications." Clin Orthop Relat Res(226): 267-291.

Lindbergh, C. A. (1935). "An Apparatus for the Culture of Whole Organs." J Exp Med 62(3): 409-431.

Lu, H., Hoshiba, T., Kawazoe, N. and Chen, G. (2011). "Autologous extracellular matrix scaffolds for tissue engineering." Biomaterials 32(10): 2489-2499.

Macchiarini, P., Jungebluth, P., Go, T., Asnaghi, M. A., Rees, L. E., Cogan, T. A., Dodson, A., Martorell, J., Bellini, S., Parnigotto, P. P., Dickinson, S. C., Hollander, A. P., Mantero, S., Conconi, M. T. and Birchall, M. A. (2008). "Clinical transplantation of a tissue-engineered airway." Lancet 372(9655): 2023-2030.

McKee, K. K., Harrison, D., Capizzi, S. and Yurchenco, P. D. (2007). "Role of laminin terminal globular domains in basement membrane assembly." J Biol Chem 282(29): 21437-21447.

McMahon, D. K., Anderson, P. A., Nassar, R., Bunting, J. B., Saba, Z., Oakeley, A. E. and Malouf, N. N. (1994). "C2C12 cells: biophysical, biochemical, and immunocytochemical properties." Am J Physiol 266(6 Pt 1): C1795-1802.

McNaught, A. D., Wilkinson, A. and International Union of Pure and Applied Chemistry. (1997). Compendium of chemical terminology : IUPAC recommendations. Oxford Oxfordshire ; Malden, MA, Blackwell Science.

Meijer, G. J., de Bruijn, J. D., Koole, R. and van Blitterswijk, C. A. (2007). "Cell-based bone tissue engineering." PLoS Med 4(2): e9.

Mendoza-Novelo, B., Avila, E. E., Cauich-Rodriguez, J. V., Jorge-Herrero, E., Rojo, F. J., Guinea, G. V. and Mata-Mata, J. L. (2011). "Decellularization of pericardial tissue and its impact on tensile viscoelasticity and glycosaminoglycan content." Acta Biomater 7(3): 1241-1248.

Montoya, C. V. and McFetridge, P. S. (2009). "Preparation of ex vivo-based biomaterials using convective flow decellularization." Tissue Eng Part C Methods 15(2): 191-200.

Mounier, F., Foidart, J. M. and Gubler, M. C. (1986). "Distribution of extracellular matrix glycoproteins during normal development of human kidney. An immunohistochemical study." Lab Invest 54(4): 394-401.

Moussavi-Harami, F., Duwayri, Y., Martin, J. A. and Buckwalter, J. A. (2004). "Oxygen effects on senescence in chondrocytes and mesenchymal stem cells: consequences for tissue engineering." Iowa Orthop J 24: 15-20.

Nacher, M., Serrano, S., Marinoso, M. L., Garcia, M. C., Bosch, J., Diez, A., Lloreta, J. and Aubia, J. (1999). "In vitro synthesis of type I collagen: Quantification of carboxyterminal propeptide of procollagen type I versus tritiated proline incorporation." Calcified Tissue International 64(3): 224-228.

Nakayama, K. H., Batchelder, C. A., Lee, C. I. and Tarantal, A. F. (2010). "Decellularized rhesus monkey kidney as a three-dimensional scaffold for renal tissue engineering." Tissue Eng Part A 16(7): 2207-2216.

Narisawa, S., Frohlander, N. and Millan, J. L. (1997). "Inactivation of two mouse alkaline phosphatase genes and establishment of a model of infantile hypophosphatasia." Dev Dyn 208(3): 432-446.

Negishi, J., Funamoto, S., Kimura, T., Nam, K., Higami, T. and Kishida, A. (2011). "Effect of treatment temperature on collagen structures of the decellularized carotid artery using high hydrostatic pressure." J Artif Organs 14(3): 223-231.

Nerem, R. M. (1991). "Cellular engineering." Ann Biomed Eng 19(5): 529-545.

Nielsen, S., Kwon, T.-H., Fenton, R. A. and Prætorious, J. (2012). Anatomy of the Kidney. Brenner & Rector's the kidney. M. W. Taal, B. M. Brenner and F. C. Rector. Philadelphia, PA, Elsevier/Saunders,: 1 online resource.

Ott, H. C., Clippinger, B., Conrad, C., Schuetz, C., Pomerantseva, I., Ikonomou, L., Kotton, D. and Vacanti, J. P. (2010). "Regeneration and orthotopic transplantation of a bioartificial lung." Nat Med 16(8): 927-933.

Ott, H. C., Matthiesen, T. S., Goh, S. K., Black, L. D., Kren, S. M., Netoff, T. I. and Taylor, D. A. (2008). "Perfusion-decellularized matrix: using nature's platform to engineer a bioartificial heart." Nat Med 14(2): 213-221.

Paulsson, M. (1992). "Basement membrane proteins: structure, assembly, and cellular interactions." Crit Rev Biochem Mol Biol 27(1-2): 93-127.

Petersen, T. H., Calle, E. A., Colehour, M. B. and Niklason, L. E. (2012). "Matrix composition and mechanics of decellularized lung scaffolds." Cells Tissues Organs 195(3): 222-231.

Petersen, T. H., Calle, E. A., Zhao, L., Lee, E. J., Gui, L., Raredon, M. B., Gavrilov, K., Yi, T., Zhuang, Z. W., Breuer, C., Herzog, E. and Niklason, L. E. (2010). "Tissue-engineered lungs for in vivo implantation." Science 329(5991): 538-541.

Phan, T. C. A., Xu, J. and Zheng, M. H. (2004). "Interaction between osteoblast and osteoclast: impact in bone disease." Histology and Histopathology 19(4): 1325-1344.

Prasertsung, I., Kanokpanont, S., Bunaprasert, T., Thanakit, V. and Damrongsakkul, S. (2008). "Development of acellular dermis from porcine skin using periodic pressurized technique." J Biomed Mater Res B Appl Biomater 85(1): 210-219.

Prigodich, R. V. and Vesely, M. R. (1997). "Characterization of the complex between bovine osteocalcin and type I collagen." Arch Biochem Biophys 345(2): 339-341.

Puckett, S., Pareta, R. and Webster, T. J. (2008). "Nano rough micron patterned titanium for directing osteoblast morphology and adhesion." Int J Nanomedicine 3(2): 229-241.

Ramirez, F., Boast, S., D'Alessio, M., Lee, B., Prince, J., Su, M. W., Vissing, H. and Yoshioka, H. (1990). "Fibrillar collagen genes. Structure and expression in normal and diseased states." Ann N Y Acad Sci 580: 74-80.

Reing, J. E., Brown, B. N., Daly, K. A., Freund, J. M., Gilbert, T. W., Hsiong, S. X., Huber, A., Kullas, K. E., Tottey, S., Wolf, M. T. and Badylak, S. F. (2010). "The effects of processing methods upon mechanical and biologic properties of porcine dermal extracellular matrix scaffolds." Biomaterials 31(33): 8626-8633.

Rieder, E., Kasimir, M. T., Silberhumer, G., Seebacher, G., Wolner, E., Simon, P. and Weigel, G. (2004). "Decellularization protocols of porcine heart valves differ importantly in efficiency of cell removal and susceptibility of the matrix to recellularization with human vascular cells." J Thorac Cardiovasc Surg 127(2): 399-405.

Robey, T. E., Saiget, M. K., Reinecke, H. and Murry, C. E. (2008). "Systems approaches to preventing transplanted cell death in cardiac repair." J Mol Cell Cardiol 45(4): 567-581.

Robinson, C. M., McLauchlan, G., Christie, J., McQueen, M. M. and Court-Brown, C. M. (1995). "Tibial fractures with bone loss treated by primary reamed intramedullary nailing." J Bone Joint Surg Br 77(6): 906-913.

Ross, E. A., Williams, M. J., Hamazaki, T., Terada, N., Clapp, W. L., Adin, C., Ellison, G. W., Jorgensen, M. and Batich, C. D. (2009). "Embryonic stem cells proliferate and differentiate when seeded into kidney scaffolds." J Am Soc Nephrol 20(11): 2338-2347.

Rossi, F., Charlton, C. A. and Blau, H. M. (1997). "Monitoring protein-protein interactions in intact eukaryotic cells by beta-galactosidase complementation." Proc Natl Acad Sci U S A 94(16): 8405-8410.

Rosso, F., Giordano, A., Barbarisi, M. and Barbarisi, A. (2004). "From cell-ECM interactions to tissue engineering." J Cell Physiol 199(2): 174-180.

Rouwkema, J., Rivron, N. C. and van Blitterswijk, C. A. (2008). "Vascularization in tissue engineering." Trends Biotechnol 26(8): 434-441.

Rozario, T. and DeSimone, D. W. (2010). "The extracellular matrix in development and morphogenesis: a dynamic view." Dev Biol 341(1): 126-140.

Rusconi, F., Valton, E., Nguyen, R. and Dufourc, E. (2001). "Quantification of sodium dodecyl sulfate in microliter-volume biochemical samples by visible light spectroscopy." Anal Biochem 295(1): 31-37.

Safadi, F. F., Barbe, M. F., Abdelmagid, S. M., Rico, M. C., Aswad, R. A., Litvin, J. and Popoff, S. N. (2009). Bone Structure, Development and Bone Biology. Bone pathology. J. S. Khurana. Dordrecht ; New York, Humana Press: xiii, 416 p.

Salgado, A. J., Coutinho, O. P. and Reis, R. L. (2004). "Bone tissue engineering: state of the art and future trends." Macromol Biosci 4(8): 743-765.

Salter, E., Goh, B., Hung, B., Hutton, D., Ghone, N. and Grayson, W. L. (2012). "Bone tissue engineering bioreactors: a role in the clinic?" Tissue Eng Part B Rev 18(1): 62-75.

Sano, M. B., Neal, R. E., 2nd, Garcia, P. A., Gerber, D., Robertson, J. and Davalos, R. V. (2010). "Towards the creation of decellularized organ constructs using irreversible electroporation and active mechanical perfusion." Biomed Eng Online 9: 83.

Sasaki, S., Funamoto, S., Hashimoto, Y., Kimura, T., Honda, T., Hattori, S., Kobayashi, H., Kishida, A. and Mochizuki, M. (2009). "In vivo evaluation of a novel scaffold for artificial corneas prepared by using ultrahigh hydrostatic pressure to decellularize porcine corneas." Mol Vis 15: 2022-2028.

Satelli, A. and Li, S. (2011). "Vimentin in cancer and its potential as a molecular target for cancer therapy." Cell Mol Life Sci 68(18): 3033-3046.

Schmittgen, T. D. and Livak, K. J. (2008). "Analyzing real-time PCR data by the comparative C-T method." Nature Protocols 3(6): 1101-1108.

Service, R. F. (2000). "Tissue engineers build new bone." Science 289(5484): 1498-1500.

Shapiro, F., Cahill, C., Malatantis, G. and Nayak, R. C. (1995). "Transmission electron microscopic demonstration of vimentin in rat osteoblast and osteocyte cell bodies and processes using the immunogold technique." Anat Rec 241(1): 39-48.

Shekaran, A. and Garcia, A. J. (2011). "Extracellular matrix-mimetic adhesive biomaterials for bone repair." J Biomed Mater Res A 96(1): 261-272.

Skalak, R. and Fox, C. F. (1988). Tissue engineering : proceedings of a workshop held at Granlibakken, Lake Tahoe, California, February 26-29, 1988. New York, Liss.

Slater, B. J., Kwan, M. D., Gupta, D. M., Panetta, N. J. and Longaker, M. T. (2008). "Mesenchymal cells for skeletal tissue engineering." Expert Opin Biol Ther 8(7): 885-893.

Spencer, G. J., McGrath, C. J. and Genever, P. G. (2007). "Current perspectives on NMDA-type glutamate signalling in bone." Int J Biochem Cell Biol 39(6): 1089-1104.

Stapleton, T. W., Ingram, J., Katta, J., Knight, R., Korossis, S., Fisher, J. and Ingham, E. (2008). "Development and characterization of an acellular porcine medial meniscus for use in tissue engineering." Tissue Eng Part A 14(4): 505-518.

Steinhausen, M., Endlich, K. and Wiegman, D. L. (1990). "Glomerular blood flow." Kidney Int 38(5): 769-784.

Stylios, G., Wan, T. and Giannoudis, P. (2007). "Present status and future potential of enhancing bone healing using nanotechnology." Injury 38 Suppl 1: S63-74.

Sukmana, I. (2012). "Microvascular guidance: a challenge to support the development of vascularised tissue engineering construct." ScientificWorldJournal 2012: 201352.

Tortora, G. J. and Derrickson, B. (2012). Principles of anatomy & physiology. Hoboken, NJ, Wiley.

Tortora, G. J. and Derrickson, B. (2012). The skeletal system: the axial skeleton. Principles of anatomy and physiology. L. Dougherty and S. Lister. Danvers, MA, John Wiley & Sons, Inc.: xxxiv,1222 p.

Tsigkou, O., Pomerantseva, I., Spencer, J. A., Redondo, P. A., Hart, A. R., O'Doherty, E., Lin, Y., Friedrich, C. C., Daheron, L., Lin, C. P., Sundback, C.

A., Vacanti, J. P. and Neville, C. (2010). "Engineered vascularized bone grafts." Proc Natl Acad Sci U S A 107(8): 3311-3316.

Uygun, B. E., Soto-Gutierrez, A., Yagi, H., Izamis, M. L., Guzzardi, M. A., Shulman, C., Milwid, J., Kobayashi, N., Tilles, A., Berthiaume, F., Hertl, M., Nahmias, Y., Yarmush, M. L. and Uygun, K. (2010). "Organ reengineering through development of a transplantable recellularized liver graft using decellularized liver matrix." Nat Med 16(7): 814-820.

Valentin, J. E., Freytes, D. O., Grasman, J. M., Pesyna, C., Freund, J., Gilbert, T. W. and Badylak, S. F. (2009). "Oxygen diffusivity of biologic and synthetic scaffold materials for tissue engineering." J Biomed Mater Res A 91(4): 1010-1017.

van der Plas, A., Aarden, E. M., Feijen, J. H., de Boer, A. H., Wiltink, A., Alblas, M. J., de Leij, L. and Nijweide, P. J. (1994). "Characteristics and properties of osteocytes in culture." J Bone Miner Res 9(11): 1697-1704.

van der Rest, M. and Garrone, R. (1991). "Collagen family of proteins." FASEB J 5(13): 2814-2823.

Wahl, D. A. and Czernuszka, J. T. (2006). "Collagen-hydroxyapatite composites for hard tissue repair." Eur Cell Mater 11: 43-56.

Wakitani, S., Goto, T., Pineda, S. J., Young, R. G., Mansour, J. M., Caplan, A. I. and Goldberg, V. M. (1994). "Mesenchymal cell-based repair of large, full-thickness defects of articular cartilage." J Bone Joint Surg Am 76(4): 579-592.

Waldrop, F. S., Puchtler, H., Meloan, S. N. and Younker, T. D. (1980). "Histochemical investigations of different types of collagen." Acta Histochem Suppl 21: 23-31.

Wijsman, J. H., Jonker, R. R., Keijzer, R., van de Velde, C. J., Cornelisse, C. J. and van Dierendonck, J. H. (1993). "A new method to detect apoptosis in paraffin sections: in situ end-labeling of fragmented DNA." J Histochem Cytochem 41(1): 7-12.

Wilshaw, S. P., Rooney, P., Berry, H., Kearney, J. N., Homer-Vanniasinkam, S., Fisher, J. and Ingham, E. (2011). "Development and Characterization of Acellular Allogeneic Arterial Matrices." Tissue Eng Part A.

Winquist, R. A. and Hansen, S. T., Jr. (1980). "Comminuted fractures of the femoral shaft treated by intramedullary nailing." Orthop Clin North Am 11(3): 633-648.

Xu, H., Wan, H., Sandor, M., Qi, S., Ervin, F., Harper, J. R., Silverman, R. P. and McQuillan, D. J. (2008). "Host response to human acellular dermal matrix transplantation in a primate model of abdominal wall repair." Tissue Eng Part A 14(12): 2009-2019.

Yaffe, D. and Saxel, O. (1977). "Serial passaging and differentiation of myogenic cells isolated from dystrophic mouse muscle." Nature 270(5639): 725-727.

Yang, B., Zhang, Y., Zhou, L., Sun, Z., Zheng, J., Chen, Y. and Dai, Y. (2010). "Development of a porcine bladder acellular matrix with well-preserved extracellular bioactive factors for tissue engineering." Tissue Eng Part C Methods 16(5): 1201-1211.

Yoo, J. U. and Johnstone, B. (1998). "The role of osteochondral progenitor cells in fracture repair." Clin Orthop Relat Res(355 Suppl): S73-81.

You, S., Kublin, C. L., Avidan, O., Miyasaki, D. and Zoukhri, D. (2011). "Isolation and propagation of mesenchymal stem cells from the lacrimal gland." Invest Ophthalmol Vis Sci 52(5): 2087-2094.

Yun, H. S., Kim, S. H., Khang, D., Choi, J., Kim, H. H. and Kang, M. (2011). "Biomimetic component coating on 3D scaffolds using high bioactivity of mesoporous bioactive ceramics." Int J Nanomedicine 6: 2521-2531.

Zhang, Y., He, Y., Bharadwaj, S., Hammam, N., Carnagey, K., Myers, R., Atala, A. and Van Dyke, M. (2009). "Tissue-specific extracellular matrix coatings for the promotion of cell proliferation and maintenance of cell phenotype." Biomaterials 30(23-24): 4021-4028.

Zhou, X., Zhang, Z., Feng, J. Q., Dusevich, V. M., Sinha, K., Zhang, H., Darnay, B. G. and de Crombrugghe, B. (2010). "Multiple functions of Osterix are required for bone growth and homeostasis in postnatal mice." Proc Natl Acad Sci U S A 107(29): 12919-12924.

Zimmermann, G. and Moghaddam, A. (2011). "Allograft bone matrix versus synthetic bone graft substitutes." Injury 42 Suppl 2: S16-21.

9 Acknowledgments

Finally, this thesis would not have been possible without the support of my family, my friends, and foremost Mihaela: thank you very much for your support, your understanding and continuous encouragement.